Thoracic Medicine

▌The Official Journal of

Taiwan Society of Pulmonary and Critical Care Medicine

Taiwan Society of Sleep Medicine

Taiwan Society for Respiratory Therapy
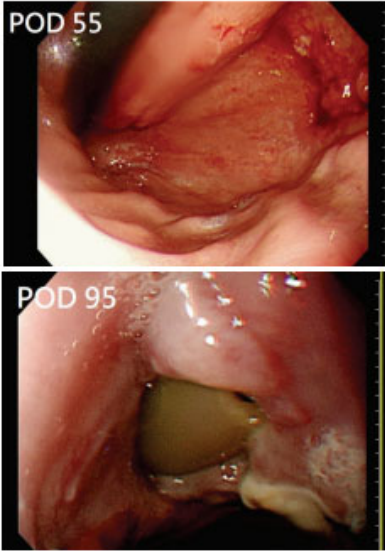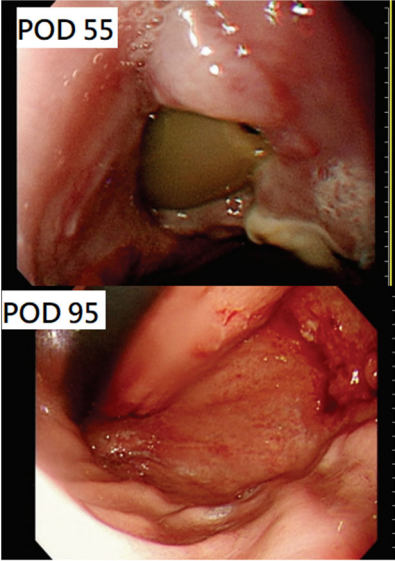
Taiwan Society of Tuberculosis and Lung Diseases

勘誤聲明

出版信息	2023 年第 38 卷第 3 期，頁碼為第 250-254 頁
論文標題	Salivary Bypass Stent and Intercostal Muscle Flap for Treatment of Cervical Esophageal Conduit Ischemia and Perforation
作者	Yu-Hsiang Wang, Cheau-Feng Lin
勘誤內容	**舊版：** 頁碼為第 252 頁 Fig.6.Esophagoscope, POD 55, revealed healing mucosa with 1 fistula formation at the gastric conduit. The chest tube was visible during the examination. Esophagoscope, POD 95, revealed healing mucosa with no fistula formation, but some stricture at the previous fistula side. **更正版：** 頁碼為第 252 頁 Fig.6.圖片 Esophagoscope, POD 55, revealed healing mucosa with 1 fistula formation at the gastric conduit. The chest tube was visible during the examination. Esophagoscope, POD 95, revealed healing mucosa with no fistula formation, but some stricture at the previous fistula side.

Thoracic Medicine

CONTENTS

Real-World Experience with Immunotherapy for Lung Cancer in a Tertiary Hospital in Central Taiwan

Hsu-Yuan Chen[1], Yi-Cheng Shen[1], Hung-Jen Chen[1], Chih-Yen Tu[1], Yu-Chao Lin[1,2], Te-Chun Hsia[1,3]

Introduction: Clinical trials have demonstrated the promising effects of immunotherapy in lung cancer treatment, but real-world data is scarce. The main aim of this study was to explore real-world experience with immunotherapy in treating lung cancer patients.

Methods: Eligibility criteria included a diagnosis of an advanced stage of lung cancer and having received immunotherapy from 2015 to 2018. The protocol was approved by the institutional review board of our institution. Medical records were reviewed retrospectively.

Results: A total of 39 patients (males, 69.2%; mean age, 59.8 years) were enrolled. Clinical characteristics included non-squamous cell carcinoma in 74.4% of patients, stage IV in 92.3%, and brain metastasis in 35.9%; 17.9% of patients were hepatitis B carriers, 7.7% had received previous radiotherapy, and 76.9% had received combined chemotherapy: 1st treatment line (20.5%), 2nd (23.1%), 3rd (20.5%), and >= 4th (35.9%), respectively. Mean time to treatment failure was 8.9 months. The patients with brain metastasis who had received late-line therapy (>= 4th) showed a longer time to treatment failure. Common side effects included dermatitis (12.8%), fatigue (12.8%) and fever (10.3%), and the severe side effect was dermatitis (n=1, 2.6%).

Conclusion: Real-world data reflect the conditions of patients with a clinical medical need. Our study included subgroups with late-line therapy or those with brain metastasis, and revealed that those 2 groups experienced a longer time to treatment failure. Physicians should not only be familiar with immunotherapy as first-line therapy, but also consider it as part of the treatment plan for patient populations that need medical care in our daily practice. *(Thorac Med 2023; 38: 177-186)*

Key words: Lung Cancer, immunotherapy

[1]Division of Pulmonary and Critical Care Medicine, Department of Internal Medicine, China Medical University Hospital, Taichung, Taiwan. [2]Graduate Institute of Clinical Medical Science, China Medical University, Taichung, Taiwan. [3]Department of Respiratory Therapy, China Medical University, Taichung, Taiwan
Address reprint requests to: Dr. Yu-Chao Lin, Department of Internal Medicine, China Medical University Hospital, No. 2, Yude Road, Taichung

Introduction

Cancer is the 2nd most common etiology of death worldwide, following cardiovascular events. Lung cancer-related cancer deaths are estimated to be 1.6 million per year, and lung cancer is the main etiology of all cancer mortality [1]. Non-small-cell lung cancer (NSCLC), especially adenocarcinoma and squamous cell carcinoma, accounted for 85% of all lung cancer cases in a study from Spain [2], and is always in an advanced unresectable tumor stage when diagnosed. However, targeted therapy improved the overall response rate and overall survival (OS) of patients with a genetic alteration like an epidermal growth factor receptor (EGFR) mutation, or an anaplastic lymphoma kinase (ALK) or ROS proto-oncogene 1 (ROS1) translocation. Metastatic lung cancer patients without common genetic alterations should receive standard platinum-based doublet chemotherapy. Although median OS with doublet cytotoxic chemotherapy has evolved from 8-10 months to 12-13 months when using a new less toxic regimen [3], the treatment result is still clinically unsatisfactory.

Tumor cells adopt several mechanisms during tumorigenesis and metastasis, including angiogenesis, and escape immune cell surveillance. One of the important features is the programmed cell death protein 1/programmed death-ligand 1 (PD-1/PD-L1) pathway [4], which induces immune tolerance. Cancer immunotherapy is a kind of therapy that focuses on the immune checkpoint and allows the immune system to resume its fight against cancer cells. Blocking the PD-1 and PD-L1 pathways with antibodies offers a chance to restore T cell-mediated antitumor immunity [5-6].

Clinically available regimens of immune checkpoint blockers (ICBs) for advanced NSCLC treatment in Taiwan are nivolumab, pembrolizumab and atezolizumab. Nivolumab and pembrolizumab are PD-1 inhibitors, and atezolizumab is a PD-L1 inhibitor. Pembrolizumab improved the OS of advanced NSCLC patients' compared to chemotherapy, in both a first-line and second-line setting [7-8]. Nivolumab [9-10] is approved for metastatic NSCLC with disease progression during or after platinum-based chemotherapy. Atezolizumab reduced mortality risk and improved progression-free survival (PFS) significantly as first-line treatment for advanced NSCLC [11].

Although many clinical trials have revealed that ICBs seemed to have a promising treatment effect on lung cancer patients, real-world data for immunotherapy is scarce. The aim of study was to understand real-world experience with immunotherapy, including the treatment pattern, immunotherapy effect on OS, and its safety in practice.

Methods

Patients and methods

Eligibility criteria for the enrolled patients included a histological diagnosis of lung cancer with advanced tumor stage IIIb to IV, and having received ICB medications (nivolumab, pembrolizumab, atezolizumab) from January, 2015 to December, 2018. Patients enrolled in clinical trials were excluded. The protocol was approved by the institutional review board (IRB) at China Medical University Hospital, a medical center located in central Taiwan. The study was retrospective in design and patients' informed consent was waived.

Data collection

Chart and medical records were reviewed retrospectively and clinical characteristics, treatment modalities and outcome characteristics were recorded. Clinical characteristics included age, gender, body mass index, smoking status, performance status, tumor histology subtype, tumor stage, brain metastasis, and presence of any driver mutations like an EGFR mutation or ALK rearrangement. The initial cancer diagnosis as a basis for receiving immunotherapy and the immunotherapy treatment course were recorded. Treatment modalities included dosing of immunotherapy, treatment lines of immunotherapy, and whether immunotherapy was received alone or in combination with radiotherapy or chemotherapy (platinum-based or non-platinum-based) or other regimens (tyrosine kinase inhibitor, anti-angiogenesis). Outcome characteristics included time-to-treatment failure (TTF) and adverse effects during treatment.

Definition

The time from the initial cancer diagnosis to receiving immunotherapy was defined as the time from the first lung cancer diagnosis to the initiation of immunotherapy treatment. TTF was defined as the time from initiation of immunotherapy to death or the last follow-up. Adverse effects were based on assessment by the treating physician and graded using the Common Terminology Criteria for Adverse Events (CTCAE), version 4.0.

Statistical analysis

Categorical variables are presented as the number of patients and percentages. All data were compiled and statistical analysis was done using SAS version 9.4 (SAS Institute Inc., Cary, NC). We presented means with standard deviations (SDs) for continuous variables and proportions for categorical variables.

Results

General characters of patients

We enrolled 51 patients and excluded 12 who had participated in a clinical trial. The remaining 39 patients with advanced NSCLC had received immunotherapy (nivolumab, pembrolirumab, atezolizumab) from January 2015 to December 2018 at China Medical University Hospital (Table 1). The mean age of the enrollees was 59.8 years (24.8-83.2) and males were predominant (n=27, 69.2%). The most common Eastern Cooperative Oncology Group (ECOG) performance status was 1 (n=22, 56.4%), followed by ECOG 0 (n=12, 30.8%). Seventy-four percent of all patients had adenocarcinoma (n=29), and 92.3% had stage IV disease (n=36). Fourteen patients had brain metastasis; 18 patients (46.1%) had an unknown PD-L1 status and 9 (23.1%) had PD-L1 expression 1-50%. Small numbers of patients presented with a driver gene mutation: 7 (18%) with an EGFR mutation and 2 (5.1%) with an ALK re-arrangement.

Treatment patterns and side effects

Of the 39 patients in this study, 22, 11, and 6 had received immunotherapy regimens with nivolumab, atezolizumab and pembrolizumab, respectively. Most patients (n=36, 92.3%) had not undergone radiotherapy before. The mean time from initial cancer diagnosis to receiving immunotherapy was 21.3 months. The mean length of immunotherapy was 5.8 months. Seventy-seven percent of patients (n=30) were

Table 1. Demographic Data of 39 Patients With Advanced NSCLC Who Received Immune Checkpoint Inhibitors

Variable	Total N (%)*
Age (y)	59.8 (24.8-83.2)
Gender:	
Male	27 (69.2)
Female	12 (30.8)
BMI[+]	23.9 (15.9-31.6)
ECOG PS[+]	
0	12 (30.8)
1	22 (56.4)
2	5 (12.8)
Smoking:	
Non-smoker	32 (82.0)
Ex- or current smoker	7 (18.0)
Cell type	
Squamous	10 (25.6)
Non-squamous	29 (74.4)
Staging	
Stage IIIB	3 (7.7)
Stage IV	36 (92.3)
Brain metastasis	
Yes	14 (35.9)
No	25 (64.1)
Hepatitis	
HBs Ag(+)	7
HCV Ab(+)	0
EGFR[+] mutation	
Positive	7 (18.0)
Negative	23 (59.0)
Unknown	9 (23.0)
PDL1[+] percentage	
<=1%	6 (15.4)
1-50%	9 (23.1)
>=50%	6 (15.4)
Unknown	18 (46.1)
ALK[+] rearrangement	
Positive	2 (5.1)
Negative	23 (59.0)
Known	14 (35.9)

*Data are presented as n (%) or mean range

+Acronyms: BMI = body mass index; ECOG PS = Eastern Cooperative Oncology Group performance status; EGFR= epidermal growth factor receptor; ALK = anaplastic lymphoma kinase; PD L1 = programmed death ligand 1

treated with combined chemotherapy, especially with a non-platinum-based regimen (n=22, 73.3%). Thirty-one patients (80%) received immunotherapy as at least more than second-line therapy, and 14 received it as more than fourth-line therapy. The mean TTF of all patients was 8.9 months (Table 2).

A total of 36 episodes of adverse effects were reported in 22 patients (56.4%). Dermatitis (n=5, 12.8%), fatigue (n=5, 12.8%) and fever (n=4, 10.3%) were the common side effects in the study, and their common severity was grade 1 or 2. Only 1 patient (2.6%) had a severe side effect with the presentation of dermatitis (Table 3).

Time to treatment failure (TTF)

The mean and median TTF of all patients were 8.9 and 5 months, respectively. Patients who were female, elderly (>70 y/o), and with a good performance status (ECOG 0-1), and who had a non-squamous histology and were never/former smokers, tended to have a longer TTF. A longer mean or median TTF was observed in the subgroups of those combined with chemotherapy or those who had brain metastasis. Different treatment lines also had different TTF. Patients with a late-line therapy (>= 4th line)

Table 2. Treatment Variables of 39 Patients With Advanced NSCLC who Received Immunotherapy

Variable	Total N (%)*
Immunotherapy regimen	
Nivolumab	22 (56.4)
Pembolizumab	6 (15.4)
Atezolizumab	11 (28.2)
Previous radiotherapy	
Yes	3 (7.7)
No	36 (92.3)
Combine chemotherapy	
Platinum-based	8 (20.5)
Other regimen[+]	22 (56.4)
No	9 (23.1)
Line of immunotherapy	
1st line	8 (20.5)
2nd line	9 (23.1)
3rd line	8 (20.5)
4th line	14 (35.9)
Time from initial cancer diagnosis to receiving immunotherapy (M)	21.3 (0.2-87.5)
Length of immunotherapy (M)	5.8 (0.5-31.0)
Time to treatment failure with immunotherapy (M)	8.9 (0.5-31.0)

*Data are presented as n (%) or mean range

+Other regimens: including non-platinum chemotherapy, anti-angiogenesis, tyrosine kinase inhibitor

Table 3. Treatment-related Adverse Effects of 39 NSCLC Patients

Side effects	Total N (%)
Side effects (Grade 1 or 2)	
Dermatitis	5 (12.8)
Fatigue	5 (12.8)
Fever	4 (10.3)
Vomiting	2 (5.1)
Hypothyroidism	1 (2.6)
Liver function impairment	1 (2.6)
Body ache	1 (2.6)
Chest tightness	1 (2.6)
Anemia	1 (2.6)
Allergy	1 (2.6)
Dyspnea	1 (2.6)
Vertigo	1 (2.6)
Pneumonitis	1 (2.6)
Severe side effect[*] (>=Grade 3)	1 (2.6)

*Dermatitis

tended to have longer TTF, followed by the 2nd line therapy subgroup. The subgroup with PD-L1 expression <1% (n=6) had the longest TTF (13.3M), followed by the unknown PD-L1 expression status subgroup (10.7M) (Table 4).

Discussion

This study excluded patients enrolled in clinical trials, and focused on real-world data of immunotherapy use in advanced NSCLC patients in central Taiwan. Lung cancer treatment has evolved from cytotoxic therapies to targeted therapy and immunotherapy, and responses are related to the factors of tumor genetic alternation or the status of PD-L1 expression. With more and more data available, immunotherapy has become the standard of care in lung cancer treatment. But with the strict patient selection criteria, only about 30% of NSCLC patients are eligible to participate in clinical trials [12]. The small patient population yields an evaluation of the treatment response that cannot necessarily be generalized to all lung cancer populations. Since some clinical variants exist, such as different patient populations, disease statuses or treatment lines of immunotherapy, the application of clinical trial data to daily practice presents an uncertain benefit. Therefore, it is important to explore the data of clinical practice, to further decrease the gap between the results of trials and daily practice in the real world.

Immunotherapy as second-line versus chemotherapy has demonstrated significantly longer PFS and OS. Median OS was about 10.4 to 13.8 months for NSCLC patients with different immunotherapy regimens [7, 10 ,13]. Immunotherapy as first-line treatment has also produced promising data, with median OS of about 19-22 months, and even up to 30 months in patients

Table 4. Median and Mean Time to Treatment Failure of Different Subgroups

Population	Median time to treatment failure (m) [95% CI]	Mean time to treatment failure (m) [95% CI]
Overall	5 [3.27-11.4]	8.9±8.9
Sex		
Male	3.97 [2.2-5.3]	7.3±8.8
Female	11.5 [3.7-20.2]	12.5±8.4
Age (years)		
≤70	4.43 [3.27-11.57]	8.9±8.7
>70	5.17 [0-17.3]	9.1±1.0
Smoking status		
Never/former smoker	5.23 [3.27-11.43]	9.2±9.0
Smoker	3.97 [0-19.63]	7.6±8.6
Histology		
Squamous	3.23 [0-11.37]	7.1±8.7
Non-squamous	5.3 [3.7-11.57]	9.5±9.0
ECOG* score		
0-1	5.62 [3.93-11.57]	9.3±9.4
2	1.13 [0.67-5.3]	8.7±8.8
Brain metastasis		
Metastasis	5.23 [2.53-11.57]	9.9±9.5
Non-metastasis	4.2 [2.5-16.73]	1.9±1.9
Combined chemotherapy		
Yes	5.08 [3.93-11.43]	10.2±11.6
Not	2.53 [0-24.47]	8.5±8.1
Treatment line		
1	3.4 [0-5]	3.9±3.3
2	6.07 [0.67-21.23]	10.1±9.3
3	3.60 [0.97-20.2]	8.8±10.6
>=4	11.2 [4.03-17.27]	11.1±9.4
PD L1*		
<1	10.07 [4.03-31.43]	13.3±10.3
1-50	3.27 [1.13-16.73]	6.2±7.7
>50	3.82 [0-5.3]	3.3±1.6
Unknown	8.4 [8.5-17.27]	10.7±9.6

*Acronyms: ECOG = Eastern Cooperative Oncology Group performance status; PD L1 = programmed death ligand 1

with PD-L1 expression >50% [8,11,14].

During the period of our study, the initial PD-L1 testing method utilized in our hospital was Daco 22C3. This led to the highest usage of nivolumab during the same time, owing to the compassionate treatment provided to the patients. We found that the time from initial cancer diagnosis to immunotherapy was 21.3 months. This reflected an improvement in lung cancer treatment, even in patients without an acquired oncogene mutation (like EGFR). However, longer patient survival means that the clinical physician has more challenges in treating patients with limited available tools. Therefore, familiar treatment tools like immunotherapy gain in importance for physicians. The shorter TTF that was observed with immunotherapy as first-line treatment might be due to insufficient follow-up time in this subgroup. Twenty-two patients (56.4%) in our group received immunotherapy as late-line therapy (>= 4th line), and the TTF was 11.3 months longer than in the other groups (Table 4). The longer TTF in patients who received late-line therapy and in older patients might be related to the relatively good performance of immunotherapy combined with chemotherapy.

In our study, patients who received combined chemotherapy (n=30, 77%) tended to have longer TTF than did those patients whose treatment regimens did not include chemotherapy. And 22 patients (22/30, 73%) who received a non-platinum-based regimen were due to receiving as second line therapy or above. There were significant outcome benefits for advanced NSCLC patients treated with immunotherapy combined with chemotherapy in the KEYNOTE-189 and IMpower 150 trials [11, 14]. The data from Keynote 024 showed significant PFS or OS when immunotherapy was single-

use in a special population with a higher PD-L1 expression [8].

The PD-L1 expression status seemed not to be correlated with TTF in our study. The groups of patients with longer TTF were the PD-L1 < 1% group, followed by those with an unknown PD-L1 expression status. There are some explanations for this phenomenon. First, the PD-L1 < 1% patient number was small (n=6, 15.4%) in our study. Second, there were no validated immunohistochemistry (IHC) assays based on different PD-L1 antibodies used in different studies, thus possibly varying the relationship between PD-L1 expression and different immunotherapy regimens. Third, we did not check PD-L1 expression routinely before immunotherapy was available clinically, which could contribute to the higher proportion of patients with unknown PD-L1 expression (n=18, 46.1%). In this study, most of the PD-L1 expression data was obtained at the time of initial diagnosis, and there was no routine request for PD-L1 data before the use of second or subsequent lines of immunotherapy. In addition, prior to Taiwan's National Health Insurance (NHI) covering the cost of immune checkpoint inhibitors, patients had to pay for immunotherapy out-of-pocket, or rely on compassionate therapy. This also influenced the willingness to re-biopsy. Therefore, the real distribution of PD-L1 expression and outcome correlations is unclear.

Five patients with ECOG 2 had a shorter TTF than patients with ECOG 0-1 in our data. Lin et al. reported that real-world data showed ECOG status was an independent predictor of PFS and OS, indicating that immunotherapy offers less benefit to patients with a poor ECOG status [15]. Factors contributing to the poor treatment response in those patients included not only poor physical status and energy level,

but also rapid disease progression.

Brain metastasis developed in 8-10% of all cancer patients, and in up to 50% of NSCLC patients (16, 17). Up to 1/3 of metastatic brain lesions might be the first site of failure during the treatment course, due to limited treatment options (18). Most studies excluded brain metastases due to concerns about central nervous system penetration and historically poor outcomes. The landmark KEYNOTE-189 and KEYNOTE-010 studies showed that the proportions of enrolled patients with brain metastasis varied from 10-20% (7, 14). In our study, the proportion of patients with brain metastasis was 35% (n=14), higher than that of clinical trials. This indicates that there is a need to attend to those patients with brain metastasis. We found that 64.3% of patients (n=9) with brain metastasis received immunotherapy as at least fourth-line therapy, and had longer median TTF than those with no brain metastasis (10.6 vs 4.5 months). Goldberg SB et al. reported a 33% intra-cranial response rate in 18 NSCLC patients (19), and suggested systemic immunotherapy might play a role in brain metastases. We think that the improved radiotherapy technique used for local control of brain lesions, combined with chemotherapy in most patients (n=11, 78.6%), yielded a better TTF for brain metastatic patients in our data. Multidisciplinary care and immunotherapy might be promising treatment options for those patients with brain metastasis.

However, there were some limitations in our study. First, there might be a selection bias in the retrospective data, and there was no standard treatment plan for different patients, so the study results may have been influenced by patient selection, which initially favored individuals who had already undergone first-line treatment, rather than selecting patients simultaneously. Second, the PD-L1 expression was not obtained for every patient, so correlating the relationship between PD-L1 expression and immunotherapy treatment response in our study would be difficult. Third, the patient population was small since immune checkpoint inhibitors were not covered by Taiwan's NHI until April 2019, patients may have been influenced by the economic burden and may have been less willing to receive ICBs. In addition, the follow-up time was not long enough in the subgroup with high PD-L1 expression receiving immunotherapy as first-line therapy. We acknowledge that time-to-treatment may not fully align with current treatment recommendations for immune checkpoint inhibitors due to a time-related bias. It is crucial to recognize the limitations of this approach, and results should be interpreted with caution.

Conclusion

Immunotherapy is playing a more and more important role in lung cancer treatment, and will be into the future. Longer patient survival and the lack of treatment choices presents the physician with more challenges in determining follow-up treatment in late-line therapy. This study presented real-world data and reflected the need for clinical medical care of patients, including those with late-line therapy or brain metastasis. Our data demonstrated a non-inferior TTF in the groups clinically. The proportions of side effects with immunotherapy were not high, and were manageable in our study. Physicians should not only be familiar with immunotherapy as first-line therapy but also consider it as part of the treatment plan for patient populations, with the existing medical demands in our daily practice.

References

1. Global Burden of Disease Cancer Collaboration. Global, Regional, and National Cancer Incidence, Mortality, Years of Life Lost, Years Lived With Disability, and Disability-Adjusted Life-Years for 29 Cancer Groups, 1990 to 2016: A Systematic Analysis for the Global Burden of Disease Study. JAMA Oncol 2018 Nov 1; 4(11): 1553-68.

2. Escuin JS. Lung cancer in Spain. Current epidemiology, survival and treatment. Arch Bronconeumol 2009; 45: 341-8.

3. Patel JD, Socinski MA, Garon EB *et al*. PointBreak: A randomized phase III study of pemetrexed plus carboplatin and bevacizumab followed by maintenance pemetrexed and bevacizumab versus paclitaxel plus carboplatin and bevacizumab followed by maintenance bevacizumab in patients with stage IIIB or IV nonsquamous non-small-cell lung cancer. J Clin Oncol 2013; 31: 4349-57.

4. Chinai JM, Janakiram M, Chen F, *et al*. New immunotherapies targeting the PD-1 pathway. Trends Pharmacol Sci 2015; 36: 587-95.

5. Topalian SL, Hodi FS, Brahmer JR, *et al*. Safety, activity, and immune correlates of anti-PD-1 antibody in cancer. N Engl J Med 2012; 366: 2443-54.

6. Herbst RS Soria J-C, Kowanetz M, *et al*. Predictive correlates of response to the anti-PD-L1 antibody MPDL3280A in cancer patients. Nature 2014; 515: 563-7.

7. Herbst RS, Baas P, Kim DW, *et al*. Pembrolizumab versus docetaxel for previously treated, PD-L1-positive, advanced non-small-cell lung cancer (KEYNOTE-010): a randomised controlled trial. Lancet 2016; 387: 1540-50.

8. Reck M, Rodriguez-Abreu D, Robinson AG, *et al*. Pembrolizumab versus chemotherapy for PD-L1-positive non-small-cell lung cancer. N Engl J Med 2016; 375: 1823-33.

9. Borghaei H, Paz-Ares L, Horn L, *et al*. Nivolumab versus docetaxel in advanced nonsquamous non-small-cell lung cancer. N Engl J Med 2015; 373: 1627-39.

10. Brahmer J, Reckamp KL, Bass P, *et al*. Nivolumab versus docetaxel in advanced squamous-cell non-small-cell lung cancer. N Engl J Med 2015; 373: 123-35.

11. Socinski MA, Jotte RM, Cappuzzo F, *et al*. IMpower150 Study Group. Atezolizumab for first-line treatment of metastatic nonsquamous NSCLC. N Engl J Med 2018; 378(24): 2288-301.

12. Yoo SH, Keam B, Kim M, *et al*. Generalization and representativeness of phase III immune checkpoint blockade trials in non-small cell lung cancer. Thorac Cancer 2018 Jun; 9(6): 736-44.

13. Rittmeyer A, Barlesi F, Waterkamp D, *et al*, for the OAK Study Group*. Atezolizumab versus docetaxel in patients with previously treated non-small-cell lung cancer (OAK): a phase 3, open-label, multicentre randomised controlled trial. Lancet 2017; 389: 255-65.

14. L. Gandhi, D. Rodríguez Abreu S, Gadgeel E, *et al*, for the KEYNOTE-189 Investigators*. Pembrolizumab plus chemotherapy in metastatic non–small-cell lung cancer. N Engl J Med 2018; 378: 2078-92.

15. Lin SY, Yang CY, Liao BC, *et al*. Tumor PD-L1 expression and clinical outcomes in advanced-stage non-small cell lung cancer patients treated with nivolumab or pembrolizumab: real-world data in Taiwan. J Cancer 2018 Apr 19; 9(10): 1813-20.

16. Barnholtz-Sloan JS, Sloan AE, Davis FG, *et al*. Incidence proportions of brain metastases in patients diagnosed (1973 to 2001) in the Metropolitan Detroit Cancer Surveillance System. J Clin Oncol 2004 Jul 15; 22(14): 2865-72.

17. Schouten LJ, Rutten J, Huveneers HA, *et al*. Incidence of brain metastases in a cohort of patients with carcinoma of the breast, colon, kidney, and lung and melanoma. Cancer 2002 May 15; 94(10): 2698-705.

18. Tamura T., Kurishima K., Nakazawa K., *et al*. Specific organ metastases and survival in metastatic non-small-cell lung cancer. Mol Clin Oncol 2015; 3(1): 217-21.

19. Goldberg SB, Gettinger SN, Mahajan A, *et al*. Pembrolizumab for patients with melanoma or non-small-cell lung cancer and untreated brain metastases: early analysis of a non-randomised, open-label, phase 2 trial. Lancet Oncol 2016 Jul; 17(7): 976-83.

Comparing the Real-World Efficacy of Erlotinib and Afatinib in Treating Advanced Lung Squamous Cell Carcinoma

I-Hung Lin[1], Yen-Hsiang Huang[1,2,3], Po-Hsin Lee[1,2,4,5], Kuo-Hsuan Hsu[6], Jeng-Sen Tseng[1,2,3,7], Tsung-Ying Yang[1,8]

Background and Aims: Erlotinib and afatinib are drugs of choice for patients with advanced squamous cell carcinoma (SqCC) of the lung. Here, we aimed to study the efficacy of erlotinib and afatinib in real-world practice.

Methods: We retrospectively screened lung SqCC patients who received erlotinib or afatinib between Jan 2009 and Aug 2021 in a hospital-based cohort. We excluded those patients who had received erlotinib or afatinib for less than 2 weeks, who had received chemotherapy combined with erlotinib or afatinib, or who had a mixed histology. Progression-free survival (PFS) was evaluated.

Results: A total of 167 patients were analyzed (140 in the erlotinib group, 23 in the afatinib group, and 4 who had been treated with both erlotinib and afatinib). In the erlotinib group, 76.4% of patients had received erlotinib as the third- or higher line of therapy, compared with 39.1% in the afatinib group (p=0.030). Disease control rates in the erlotinib and afatinib groups were 28.6% and 21.7%, respectively (p=0.021). The proportions of patients who had discontinued tyrosine kinase inhibitor treatment due to adverse events in the erlotinib and afatinib groups were 1.4% and 21.7%, respectively (p=0.001). There was no significant difference in PFS between the erlotinib and afatinib groups (median 2.4 months [95% CI, 2.0 to 2.7] vs 2.7 months [95% CI, 2.2 to 3.2]; p=0.833). All of the patients who had received afatinib with prior erlotinib treatment showed benefits from erlotinib treatment, and 3 of them experienced stable disease after afatinib use.

Conclusion: Either erlotinib or afatinib can be a treatment option in a real-world setting for advanced lung SqCC patients who have progressed after prior treatments. We found no difference in PFS between erlotinib and afatinib treatment. Afatinib may provide benefits to some patients showing resistance to prior erlotinib treatment. ***(Thorac Med 2023; 38: 187-198)***

Key words: EGFR-TKI, SqCC, erlotinib, afatinib, efficacy, progression-free survival, adverse event

[1]Division of Chest Medicine, Department of Internal Medicine, Taichung Veterans General Hospital, Taichung, Taiwan. [2]College of Medicine, National Yang Ming Chiao Tung University, Taipei, Taiwan. [3]Institute of Biomedical Sciences, National Chung Hsing University, Taichung, Taiwan. [4]Ph.D. Program in Translational Medicine, National Chung Hsing University. [5]Rong Hsing Research Center for Translational Medicine, National Chung Hsing University. [6]Division of Critical Care and Respiratory Therapy, Department of Internal Medicine, Taichung Veterans General Hospital, Taichung, Taiwan. [7]Department of Post-Baccalaureate Medicine, College of Medicine, National Chung Hsing University, Taichung, Taiwan. [8]Department of Life Sciences, National Chung Hsing University, Taichung, Taiwan
Address reprint requests to: Dr. Po-Hsin Lee, Division of Chest Medicine, Department of Internal Medicine, Taichung Veterans General Hospital, No.1650, Sect. 4, Taiwan Blvd., Taichung, 407 Taiwan

Introduction

Despite the availability of innovative screening modalities and treatment, lung cancer is still a major cause of malignancy-related mortality worldwide [1]. Adenocarcinoma is the most common subtype of non-small cell lung cancer (NSCLC), followed by squamous cell carcinoma (SqCC), which accounts for 29.4% of patients [2]. Unlike adenocarcinoma, which has more treatment options, including different types of epidermal growth factor receptor (EGFR) tyrosine-kinase inhibitors (TKIs), SqCC has a relatively limited number of treatment options. Aside from SqCC cases with limited kinds of EGFR mutations that can be treated with EGFR-TKIs, the first-line treatment recommendations for advanced SqCC without targetable molecular drivers depends on the status of the patient's programmed cell death ligand 1(PD-L1) expression. Despite the growing number of treatment options, such as immune checkpoint inhibitors (ICIs) [3-5] and chemotherapy [6] that have been accepted as first-line treatment for advanced SqCC, second-line treatment choices remain limited. In addition, the efficacy of second-line treatments seldom meets the expectation.

EGFR-TKIs are possible choices of second-line treatment for advanced SqCC, especially for those patients for whom ICIs or chemotherapy are unavailable or contraindicated, or who are intolerant. The LUX-Lung 8 study showed a significant survival benefit in patients undergoing second-line treatment with afatinib for SqCC, when compared with erlotinib [7]. The study results might be statistically significant, but they are not clinically significant due to the small differences in progression-free survival (PFS) between the 2 groups (2.4 vs. 1.9 months

in the afatinib group vs. the erlotinib group, respectively) and their overall survival (OS, 7.9 vs. 6.8 months in the afatinib group vs. the erlotinib group, respectively). Besides, afatinib also appears to have more frequent drug-related adverse events (93% vs. 81%), as well as grade 3 drug-related adverse events (25% vs. 16%) [7]. For the above reasons, the superiority of afatinib over erlotinib in treating advanced SqCC remains unclear.

Though the results of the LUX-Lung 8 study were not clinically significant, some of the patients with advanced SqCC showed benefits from EGFR-TKIs. The final analysis of the LUX-Lung 8 study revealed that ERBB family mutations were more commonly observed (50%) among patients showing long-term disease control with afatinib, compared to those without similar long-term disease control (19%) [8]. Apart from the ERBB family mutations, no other possible factors related to the efficacy of EGFR-TKIs have been reported. The expression status of PD-L1 is not only an important biomarker to consider when selecting which first-line treatment to use in patients with lung cancer, but it is also a predictor of some targeted therapies. A high PD-L1 expression in patients with EGFR-mutant lung adenocarcinoma may indicate a higher frequency of primary resistance to EGFR-TKIs [9,10]. In contrast, some mutations with positive PD-L1 are associated with a longer OS [11,12]. However, whether the expression of PD-L1 is associated with the efficacy of EGFR-TKIs in treating SqCC remains unknown.

The combined use of EGFR-TKIs and ICIs in EGFR-mutant NSCLC is known to increase treatment-related adverse events (trAEs).13 Nonetheless, whether first-line ICIs treatment followed by EGFR-TKIs also increases trAEs

remains unclear. This issue gains greater attention as ICIs are becoming first-line treatment choices in patients with advanced SqCC. Whether trAEs increase in the treatment scenario using first-line ICIs followed by EGFR-TKI as second-line or higher treatment in real-world settings remains unclear.

Here, we aimed to determine the differences in efficacy between different EGFR-TKIs in treating patients with a squamous histology. These patients already had undergone first-line treatment. We aimed also to explore the characteristics that might have led to the patient benefiting from EGFR-TKIs treatment, and to determine the possible influence of sequential treatments with ICIs and EGFR-TKIs on trAEs. Specifically, we studied real-world experience in treating advanced SqCC using afatinib or erlotinib.

Methods

This retrospective study was conducted at Taichung Veterans General Hospital, in Taichung, Taiwan. We screened out patients with newly diagnosed lung SqCC with histology during the period Jan 2011 to Dec 2020, and who had been treated with an EGFR-TKI (erlotinib or afatinib). We excluded those who had received an EGFR-TKI for less than 14 days, who had a mixed histology (combined SqCC and adenocarcinoma), who had concomitant EGFR-TKI and other anti-cancer treatments, who had been treated with EGFR-TKI at lung cancer stage I, II, or IIIA, and those who previously had been treated with gefitinib. Patients were followed up until December 31, 2021. All methods used in this study were approved by the Institutional Review Board of Taichung Vet-

erans General Hospital (IRB CF20175B), and procedures were performed in accordance with the Declaration of Helsinki and relevant guidelines and regulations.

The staging of lung cancer followed the American Joint Committee on Cancer (AJCC) staging system (8th edition) [14]. We adopted the definitions of unidimensional measurements proposed by Response Evaluation Criteria in Solid Tumors (RECIST, version 1.1) [15]. The chief outcome of this study was PFS with the use of EGFR-TKIs, which was defined as the time from the start of TKI treatment to the time of disease progression or death. Other outcomes included the disease control rate and trAEs.

To compare inter-group differences in categorical variables, Fisher's exact test and Pearson's chi-square test were used. Continuous variables were compared using the Mann–Whitney U test. PFS was estimated using the Kaplan–Meier method. Inter-group differences were assessed using the stratified log-rank test. Factors associated with PFS were assessed using the Cox proportional hazard model. The strength of association was presented as the hazard ratio (HR) and 95% confidence interval (CI). In this study, we used 2-tailed statistical tests, and significance was set at $P < 0.05$. All analyses were performed with the IBM SPSS Statistics package, version 23 (IBM Corporation, Armonk, NY).

We used propensity score matching (PSM) to explore the association between types of EGFR-TKI and PFS among the enrolled patients. The optimal nearest neighbor matching algorithm was used in PSM, and the caliper distance of the standard mean difference was set at 0.40. Statistical analyses were conducted with R (3.6.0), and the level of significance was 0.05.

Results

Study subjects and their characteristics relative to different EGFR-TKI treatments

The algorithm and categories of the study participants are illustrated in Figure 1. We included a total of 167 patients with stage IIIB or IV lung SqCC receiving erlotinib or afatinib; 140 of the 167 patients received erlotinib treatment, 23 received afatinib treatment, and the remaining 4 received both treatments. Characteristics of the study population are shown in Table 1. More patients in the erlotinib group had received an EGFR-TKI as third-line or higher treatment (76.4% vs. 39.1%, *p*=0.030). More patients in the afatinib group had received ICIs before EGFR-TKI treatment (21.7% vs. 6.4%, *p*=0.030). The disease control rate was higher in the erlotinib group (28.6% vs. 21.7%, *p*=0.021). More patients in the afatinib group discontinued their EGFR-TKI due to adverse events (21.7% vs. 1.4%, *p*=0.001).

Clinical outcomes of patients with lung SqCC receiving EGFR-TKIs

As shown in Table 2, risk factors for PFS as revealed by univariate analysis were the following: smoking history, ECOG performance status, and line of EGFR-TKI treatment. Different EGFR-TKI types had no impact on clinical outcomes. In multivariable analysis, ECOG performance status and line of EGFR-TKI treatment were independent risk factors. The median PFS was 2.7 months (95% CI, 2.2–3.2) for the afatinib group, and 2.4 months (95% CI, 2.0–2.7) for the erlotinib group (*p*=0.833) (Figure 2A). There was no significant difference in PFS of patients with lung SqCC between those receiving afatinib and erlotinib (*p*=0.833).

Sub-group analysis based on the line of EGFR-TKI treatment and the EGFR-TKI type

In patients who received an EGFR-TKI as their second-line treatment, ECOG performance status and TKI type were identified as inde-
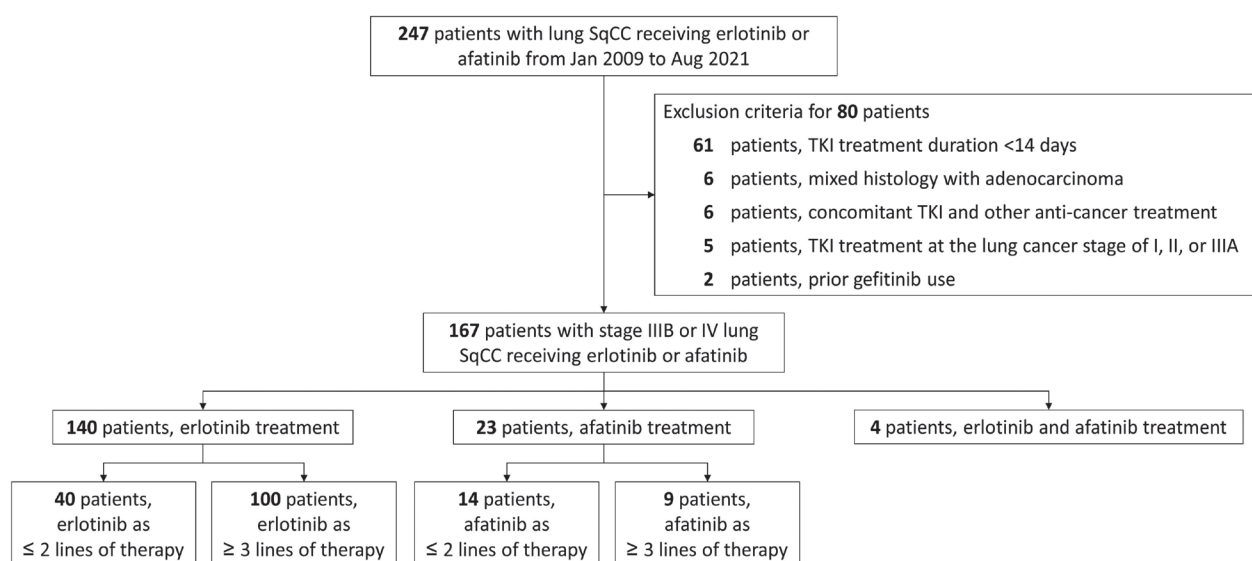
Fig. 1. Algorithm for enrollment of the study participants. SqCC, squamous cell carcinoma; TKI, tyrosine kinase inhibitor.

Table 1. Characteristics of Patients with Stage IIIB or IV Lung Squamous Cell Carcinoma Receiving Erlotinib or Afatinib

	Total, N=163	Erlotinib, N=140	Afatinib, N=23	p value
Age	67.0 (60.2–74.5)	67.1 (61.8 – 74.5)	63.4 (53.8 – 72.4)	0.151
Gender				0.391
Male	132 (81.0%)	115 (82.1%)	17 (73.9%)	
Female	31 (19.0%)	25 (17.9%)	6 (26.1%)	
Smoking				0.200
Never	43 (26.4%)	34 (24.3%)	9 (39.1%)	
Ever	120 (73.6%)	106 (75.7%)	14 (60.9%)*	
ECOG PS before TKI				0.312
1	78 (47.9%)	63 (45.0%)	15 (65.2%)	
2	38 (23.3%)	35 (25.0%)	3 (13.0%)	
3	33 (20.2%)	29 (20.7%)	4 (17.4%)	
4	14 (8.6%)	13 (9.3%)	1 (4.3%)	
Initial stage				0.242
III	54 (33.1%)	49 (35.0%)	5 (21.7%)	
IV	109 (66.9%)	91 (65.0%)	18 (78.3%)	
Line of treatment				0.030
<=2	47 (28.8%)	33 (23.6%)	14 (60.9%)	
>=3	116 (71.2%)	107 (76.4%)	9 (39.1%)	
Prior ICI				0.030
No	149 (91.4%)	131 (93.6%)	18 (78.3%)	
Yes	14 (98.6%)	9 (6.4%)	5 (21.7%)	
PD-first-line treatment				<0.001
<1%	13 (8.0%)	6 (4.3%)	7 (30.4%)	
1-49%	17 (10.4%)	8 (5.7%)	9 (39.1%)	
>=50%	5 (3.1%)	2 (1.4%)	3 (13.0%)	
N/A	128 (78.5%)	124 (88.6%)	4 (17.4%)	
EGFR				<0.001
Wild-type	11 (6.7%)	7 (5.0%)	4 (17.4%)	
Mutation	4 (2.5%)	1 (0.7%)	3 (13.0%)	
N/A	148 (90.8%)	132 (94.3%)	16 (69.6%)	
Brain metastasis before TKI				0.253
No	132 (81.0%)	111 (79.3%)	21 (91.3%)	
Yes	31 (19.0%)	29 (20.7%)	2 (8.7%)	
Response				
Disease control	45 (27.6%)	40 (28.6%)	5 (21.7%)	0.021
Partial response	19 (11.7%)	17 (12.1%)	2 (8.7%)	0.027
Stable disease	26 (16.0%)	23 (16.4%)	3 (13.0%)	
Progressive disease	103 (63.2%)	91 (65.0%)	12 (52.2%)	
Not evaluable	15 (9.2%)	9 (6.4%)	6 (26.1%)*	
DC TKI due to trAEs				0.001
Yes	7 (4.3%)	2 (1.4%)	5 (21.7%)	
No	156 (95.7%)	138 (98.6%)	18 (78.3%)	

TKI, tyrosine kinase inhibitor; ICI, immune checkpoint inhibitor; N/A, not available; DC, discontinue; trAEs, treatment-related adverse events; PS, performance status; PD, progressive disease. *In the afatinib group, 6 patients were unevaluable for their response to TKI. One of these patients was lost to follow-up, and the other 5 discontinued TKI due to adverse events. Since afatinib has a higher proportion of adverse effects than erlotinib, the treatment response of a higher proportion of cases in the afatinib group could not be evaluated.

Table 2. Univariate and Multivariable Analysis for Progression-free Survival in Patients with lung Squamous Cell Carcinoma Receiving Tyrosine kinase Inhibitor Treatment

Variable	Univariate HR (95% CI)	*p* value	Multivariable HR (95% CI)	*p* value
Age	0.996 (0.983–1.010)	0.616	0.992 (0.977–1.007)	0.307
Sex				
Male	Reference		Reference	
Female	0.686 (0.444–1.060)	0.089	1.262 (0.643–2.477)	0.499
Smoking history				
Never-smoker	Reference		Reference	
Smoker	2.127 (1.411–3.208)	<0.001	1.924 (0.997–3.714)	0.051
ECOG PS				
1	Reference		Reference	
2	1.547 (1.019–2.348)	0.040	1.499 (0.972–2.311)	0.067
3	1.300 (0.834–2.025)	0.246	1.305 (0.815–2.090)	0.268
4	4.425 (2.345–8.348)	<0.001	4.081 (2.121–7.852)	<0.001
Line of TKI treatment				
<=2	Reference		Reference	
>=3	1.934 (1.279–2.924)	0.002	1.568 (1.005–2.448)	0.048
TKI type				
Erlotinib	Reference			
Afatinib	0.944 (0.551–1.619)	0.835		
Prior ICI				
No	Reference			
Yes	1.348 (0.682–2.666)	0.391		
Initial stage				
III	Reference			
IV	1.046 (0.738–1.484)	0.800		
Brain metastasis before TKI				
No	Reference			
Yes	0.857 (0.563–1.305)	0.472		

TKI, tyrosine kinase inhibitor; ICI, immune checkpoint inhibitor; PS, performance status

pendent prognostic factors for PFS using the multivariable Cox proportional hazard model (Supplementary Table 1). For patients receiving afatinib and erlotinib as second-line treatment, the median PFS was 2.4 (95% CI, 1.8–3.0) vs. 3.2 (95% CI, 1.9–4.5) months (log rank *p*=0.039), respectively (Supplementary Figure 1A).

The prognostic results for PFS in patients who received EGFR-TKI as their third-line or higher treatment were not identical. In the multivariable Cox proportional hazard model, ECOG performance status and TKI type were identified as prognostic factors for PFS (Supplementary Table 2). However, the prognosis in the afatinib group seemed to be better. For patients receiving afatinib and erlotinib as second-line treatment, the median PFS was 4.2 (95% CI, 1.3–7.1) vs. 2.4 (95% CI, 2.0–2.7) months (log rank *p*=0.039), respectively (Supplementary
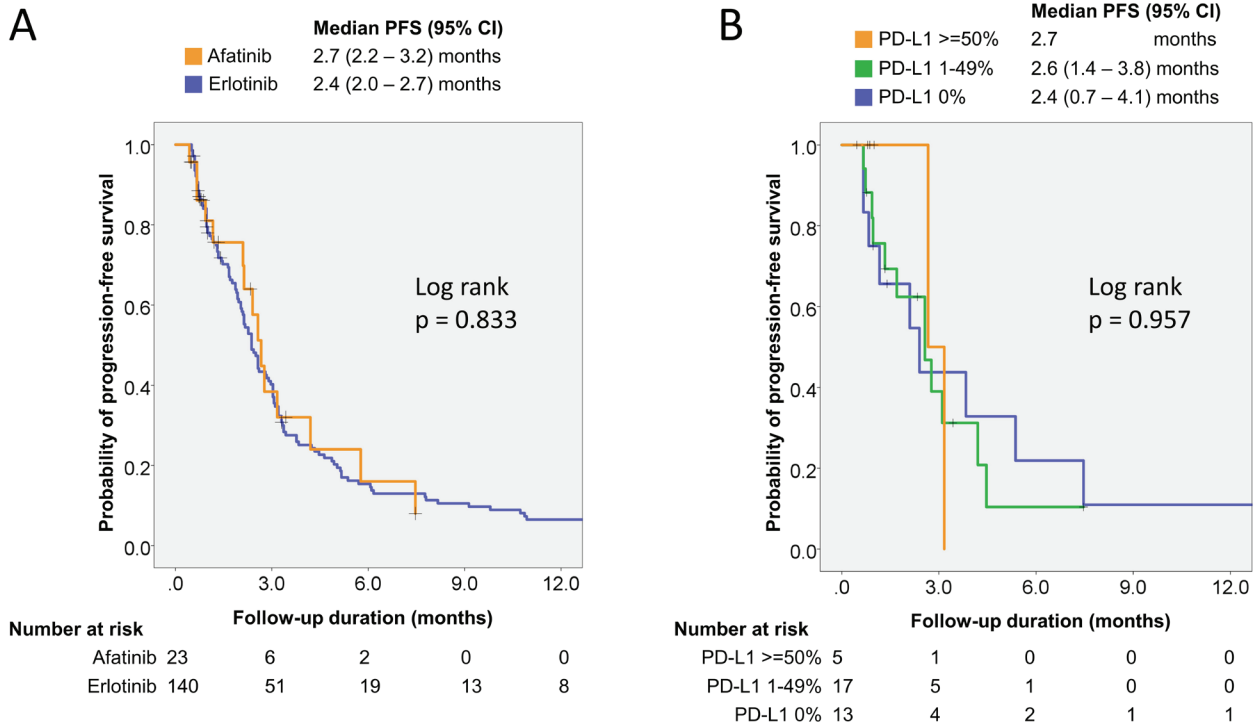
Fig. 2. (A) PFS measured from the start of TKI treatment to disease progression or death based on TKI types. (B) PFS based on PD-L1 status

Figure 2B).

Furthermore, we performed sub-group analysis based on the EGFR-TKI type to investigate the prognostic factors. We found that the line of EGFR-TKI treatment was an independent risk factor only in the erlotinib group (Supplementary Table 3), and not in the afatinib group (Supplementary Table 4).

Characteristics and clinical outcomes of the propensity score-matched population

A total of 17 patient pairs from the original cohort were propensity-score matched, and the demographic and clinical characteristics were matched between groups (Supplementary Table 5). As shown in Supplementary Figure 2, there was no significant difference in the PFS of lung SqCC patients between those receiving afatinib and those receiving erlotinib (*p*=0.66).

Clinical outcomes based on PD-L1 expression status

Among 35 patients with available PD-L1 data, the PD-L1 expression in 5 patients was >=50%, in 17 patients was 1-49%, and in 13 patients was <1% (Table 1). The median PFS was 2.7 months for patients with PD-L1 >=50%, 2.6 months (95% CI, 1.4–3.8) for patients with PD-L1 1-49%, and 2.4 months (95% CI, 0.7–4.1) for patients with PD-L1 <1% (Figure 2B). There was no significant difference in PFS across patients with different PD-L1 expressions (*p*=0.957).

Patients who received both erlotinib and afatinib

Four patients with lung SqCC received both erlotinib and afatinib. All of them first re-

Table 3. Clinical Data and Outcomes of Patients Receiving Erlotinib Treatment Before Afatinib Use

Patient number	No. 1	No. 2	No. 3	No. 4
Sex	Male	Female	Male	Female
Age	56.7	51.0	74.4	68.6
Smoking status	Smoker	Never-smoker	Smoker	Never-smoker
Initial stage	IV	IV	IV	III
Prior erlotinib treatment				
Erlotinib response	PR	SD	SD	PR
Erlotinib PFS (month)	14.7	22.2	24.3	23.3
Treatment after erlotinib failure	Chemotherapy	Chemotherapy	Afatinib	Chemotherapy
Later afatinib treatment				
ECOG PS before afatinib	1	1	2	1
Brain metastasis before afatinib	No	No	No	Yes
Afatinib PFS (month)	7.9	3.9	34.7	4.9
Afatinib response	SD	PD	SD	SD

PFS, progression-free survival; PR, partial response; SD, stable disease; PD, progressive disease; PS, performance status. The EGFR and PD with first-line treatment status of the 4 patients were not available.

Table 4. Clinical data of Patients with lung Squamous Cell Carcinoma Discontinuing TKI Treatment Due to Adverse Events

Patient number	No. 5	No. 6	No. 7	No. 8	No. 9	No. 10	No. 11
Sex	Male	Female	Male	Male	Male	Male	Male
Age	78	71	62	59	75	68	70
PD-L1 status	N/A	N/A	0%	1-49%	1-49%	>=50%	N/A
EGFR status	N/A	Wild-type	N/A	N/A	N/A	Mutated	Wild-type
Prior ICI	No	No	No	No	No	Yes[$]	No
TKI type	Erlotinib	Erlotinib	Afatinib	Afatinib	Afatinib	Afatinib	Afatinib
TKI dose	150 mg	150 mg	30 mg	40 mg	40 mg	40 mg	40 mg
Line of TKI treatment	2	3	3	2	2	2	3
TKI duration (months)	0.6	3.3[*]	0.5	2.3	1.3	0.9	0.5
trAEs							
Diarrhea	Yes						Yes
Rash or acne			Yes[#]			Yes[@]	
Stomatitis			Yes				Yes
Paronychia					Yes		
Others		Fever		Pneumonitis			

TKI, tyrosine kinase inhibitor; N/A, not available; ICI, immune checkpoint inhibitor; trAEs, treatment-related adverse events. $Pembrolizumab for 2 doses 1 month before afatinib treatment. *Poor drug adherence during the TKI treatment course. #Patient presented with folliculitis. @Patient presented with a drug eruption.

ceived erlotinib, followed by afatinib treatment. Their clinical data and outcomes are shown in Table 3. Two patients achieved a partial response after erlotinib treatment, and the other 2 had stable disease. The PFS with erlotinib use among these 4 patients was longer than the median PFS in our study. Three of the patients received chemotherapy treatment after erlotinib failure, and the fourth patient received afatinib immediately after disease progression with erlotinib. Three of the patients achieved stable disease after afatinib treatment.

Treatment-related adverse events with TKIs

Clinical data of lung SqCC patients discontinuing EGFR-TKI treatment due to trAEs are shown in Table 4. Two patients in the erlotinib group and 5 in the afatinib group discontinued EGFR-TKI treatment due to trAEs. For those discontinuing erlotinib due to trAEs, the dose they had received was 150 mg. The trAEs were severe diarrhea and recurrent fever. None of the patients that received erlotinib after prior ICIs treatment had discontinued EGFR-TKI due to trAEs. The dose of afatinib in those patients discontinuing treatment due to trAEs was 40 mg in 4 patients, and 30 mg in 1 patient. They discontinued afatinib due to diarrhea, skin toxicity, paronychia, and pneumonitis. Five patients received ICIs prior to afatinib and 1 of them discontinued EGFR-TKI treatment due to trAEs.

Discussion

Although both erlotinib and afatinib are approved to treat patients with advanced lung SqCC, the real-world efficacy of these EGFR-TKIs remains unclear. In this study, we found that in treating patients with advanced lung SqCC, there is no difference between erlotinib and afatinib with regard to PFS. The patient's PD-L1 status also did not influence the efficacy of the EGFR-TKIs. More patients discontinued afatinib due to adverse events than did those receiving erlotinib. For some patients with acquired resistance to prior erlotinib treatment, afatinib may still provide benefits. Our results in a real-world setting showed that both erlotinib and afatinib were treatment choices for patients with advanced lung SqCC following progression after first-line treatment.

The benefits of EGFR-TKIs in treating lung SqCC have been reported in several studies. In the Br.21 trial, erlotinib improved PFS and OS in patients with lung SqCC, compared with placebo (HR 0.61, $p<0.001$) [16]. The randomized-controlled TAILOR and DELTA trials were conducted to compare the efficacy of erlotinib against pretreated standard second-line docetaxel chemotherapy in patients with advanced NSCLC [13,17]. In the DELTA study, docetaxel appeared superior to erlotinib in terms of PFS for patients with non-adenocarcinoma histology, based on subgroup analysis [13]. However, the TAILOR study reported docetaxel had no significant advantage over erlotinib with regard to PFS and OS in the SqCC subgroup [17]. Furthermore, in a meta-analysis comparing the efficacy of EGFR-TKIs and chemotherapy as second-line treatment for patients with NSCLC, EGFR-TKIs showed better tolerability and an OS that was comparable with chemotherapy regardless of the EGFR mutation status [18].

Based on these findings, the randomized-controlled LUX-Lung 8 study, comparing the efficacy of second-line treatment with afatinib or erlotinib in patients with advanced lung SqCC, was subsequently conducted. In that study, afatinib was found to have a better PFS

(2.4 vs. 1.9 months, HR 0.82, *p*=0.0427) and OS (7.9 vs. 6.8 months, HR 0.81, *p*=0.0077) [7]. A retrospective study also compared the effectiveness of second-line afatinib versus chemotherapy for patients with lung SqCC, and found that afatinib provided patients with a better PFS (4.7 vs. 2.6 months, HR 0.53, *p*=0.013) and comparable OS (16.0 vs. 12.3 months, HR 0.65, *p*=0.112) [19]. However, the real-world effectiveness of erlotinib and afatinib remained unclear, and EGFR-TKIs were typically applied as second-line treatment in most of the above studies. In our present study, we found no difference between erlotinib and afatinib treatment regarding PFS among patients with advanced lung SqCC. The discrepancy in results between our study and the LUX-Lung 8 study could be partly explained by the difference in ethnic populations in the 2 studies, less of a smoking history in the study population, more patients receiving EGFR-TKIs as third- or greater line of treatment, more patients with an ECOG performance status of 2 or higher in our study, and differences in response to prior chemotherapy or ICIs between the 2 studies.

Consistent with the LUX-Lung 8 study, adverse events leading to discontinuation of EGFR-TKIs in our cohort included diarrhea, skin toxicity, stomatitis, and paronychia [7]. In previous reports, the combined use of EGFR-TKIs and ICIs in EGFR-mutant NSCLC patients raised concerns about more trAEs. A meta-analysis reported that trAEs are more common in combined treatment (EGFR-TKI and ICIs) than in EGFR-TKI monotherapy in treating EGFR-mutant NSCLC patients (skin toxicity: odds ratio [OR] 1.19, p=0.012; gastrointestinal tract toxicity: OR 1.04, *p*=0.790, interstitial lung disease: OR 1.28, *p*=0.001) [20]. Nowadays, the introduction of ICIs in the treatment of lung

SqCC has become a promising choice for selected patients [21]. Are more trAEs a concern for first-line ICIs treatment followed by EGFR-TKIs? In our cohort, only 1 of 14 patients that received ICIs before EGFR-TKI discontinued the EGFR-TKI due to adverse events. Further studies are warranted to evaluate the adverse events in combined or sequential use of EGFR-TKI and ICIs.

Four patients in our study received afatinib with prior erlotinib treatment, and afatinib provided benefit to 3 of them. Patients No. 1 and No. 4 achieved a partial response after erlotinib treatment, and their PFS with erlotinib was better than the median PFS in our study. They received chemotherapy after developing erlotinib resistance, and afatinib was used after chemotherapy failure. They experienced stable disease after afatinib treatment. In a retrospective cohort study, 14 patients that had responded to prior erlotinib were re-treated with erlotinib after progression to chemotherapy. Twelve patients (86%) achieved disease control after re-treatment with erlotinib [22]. The above-mentioned phenomena may be explained by a regained TKI sensitivity following the drug holiday. On the other hand, patient No. 3 responded differently. He developed disease progression after erlotinib treatment. Afatinib was prescribed, and he then achieved stable disease. This implied that for those patients with acquired resistance to prior erlotinib treatment, afatinib may still be of benefit.

The expression status of PD-L1 in lung cancer patients is an important biomarker for selecting the appropriate first-line treatment. PD-L1 status can also be a predictor for some targeted therapies. Patients with EGFR-mutant lung adenocarcinoma with a high PD-L1 expression are likely to have a greater chance of

developing primary resistance to EGFR-TKIs [9,10]. With regard to ALK fusion, a non-V3a/b subtype plus positive PD-L1 are associated a longer OS [11]. Besides, in patients with ROS-1 rearrangement taking crizotinib, a trend toward longer OS was noted in patients with strong PD-L1 expression [12]. In our study, with the limited case number, we found no significant impact of PD-L1 expression on the outcomes of lung SqCC patients receiving EGFR-TKIs.

Several limitations of this study are acknowledged. First, the retrospective nature of the study and the limited number of SqCC patients receiving EGFR-TKI. Second, more patients received afatinib than erlotinib as second-line treatment. These factors may be related to the existing regulations of National Health Insurance reimbursement in Taiwan. Third, the PD-L1 expression and EGFR status were not evaluated in all of our patients. These limitations may lead to a bias in evaluating treatment outcomes and contribute to the discrepancy in the analysis of prognostic factors between different lines of EGFR-TKI treatment and EGFR-TKI types in this study. Fourth, trAEs were not comprehensively recorded for most of our patients. The trAEs were only evaluated and recorded for those patients discontinuing EGFR-TKI treatment. Therefore, we cannot safely conclude that patients receiving afatinib had experienced more trAEs than those receiving erlotinib. Our present results should therefore be interpreted with caution, and further prospective studies are warranted to validate these findings.

Conclusion

We found no significant difference in PFS in patients with advanced lung SqCC treated with erlotinib or with afatinib. More patients receiving afatinib discontinued treatment due to adverse events than did those receiving erlotinib. For patients with acquired resistance to prior erlotinib treatment, afatinib may provide benefits to a selected group. In a real-world setting, both erlotinib and afatinib can be options in treating advanced lung SqCC patients who have progressed after prior treatments.

Acknowledgement

References

1. Sung H, Ferlay J, Siegel RL, *et al*. Global Cancer Statistics 2020: GLOBOCAN Estimates of Incidence and Mortality Worldwide for 36 Cancers in 185 Countries. CA Cancer J Clin 2021; 71(3): 209-49. DOI: 10.3322/caac.21660.

2. Ganti AK, Klein AB, Cotarla I, *et al*. Update of incidence, prevalence, survival, and initial treatment in patients with non-small cell lung cancer in the US. JAMA Oncol 2021; 7(12): 1824-32. DOI: 10.1001/jamaoncol.2021.4932.

3. Mok TSK, Wu YL, Kudaba I, *et al*. Pembrolizumab versus chemotherapy for previously untreated, PD-L1-expressing, locally advanced or metastatic non-small-cell lung cancer (KEYNOTE-042): a randomised, open-label, controlled, phase 3 trial. Lancet 2019; 393(10183): 1819-30. DOI: 10.1016/S0140-6736(18)32409-7.

4. Jassem J, de Marinis F, Giaccone G, *et al*. Updated overall survival analysis from IMpower110: atezolizumab versus platinum-based chemotherapy in treatment-naive programmed death-ligand 1-selected NSCLC. J Thorac Oncol 2021; 16(11): 1872-82. DOI: 10.1016/j.jtho.2021.06.019.

5. Hellmann MD, Paz-Ares L, Bernabe Caro R, *et al*. Nivolumab plus ipilimumab in advanced non-small-cell lung cancer. N Engl J Med 2019; 381(21): 2020-31. DOI: 10.1056/NEJMoa1910231.

6. Fossella F, Pereira JR, von Pawel J, *et al*. Randomized, multinational, phase III study of docetaxel plus platinum combinations versus vinorelbine plus cisplatin for advanced non-small-cell lung cancer: the TAX 326 study group. J Clin Oncol 2003; 21(16): 3016-24. DOI: 10.1200/JCO.2003.12.046.

7. Soria J-C, Felip E, Cobo M, *et al*. Afatinib versus erlotinib as second-line treatment of patients with advanced squamous cell carcinoma of the lung (LUX-Lung 8): an open-label randomised controlled phase 3 trial. Lancet Oncol 2015; 16(8): 897-907.

8. Goss GD, Cobo M, Lu S, *et al*. Afatinib versus erlotinib as second-line treatment of patients with advanced squamous cell carcinoma of the lung: Final analysis of the randomised phase 3 LUX-Lung 8 trial. EClinicalMedicine (Lancet) 2021; 37: 100940. DOI: 10.1016/j.eclinm.2021.100940.

9. Hsu K-H, Huang Y-H, Tseng J-S, *et al*. High PD-L1 expression correlates with primary resistance to EGFR-TKIs in treatment naïve advanced EGFR-mutant lung adenocarcinoma patients. Lung Cancer 2019; 127: 37-43.

10. Hsu K-H, Tseng J-S, Yang T-Y, *et al*. PD-L1 strong expressions affect the clinical outcomes of osimertinib in treatment naïve advanced EGFR-mutant non-small cell lung cancer patients. Sci Rep 2022; 12(1): 1-10.

11. Chang G-C, Yang T-Y, Chen K-C, *et al*. ALK variants, PD-L1 expression, and their association with outcomes in ALK-positive NSCLC patients. Sci Rep 2020; 10(1): 1-9.

12. Chu C-H, Huang Y-H, Lee P-H, *et al*. Various impacts of driver mutations on the PD-L1 expression of NSCLC. PLoS One 2022; 17(8): e0273207.

13. Kawaguchi T, Ando M, Asami K, *et al*. Randomized phase III trial of erlotinib versus docetaxel as second- or third-line therapy in patients with advanced non–small-cell lung cancer: Docetaxel and Erlotinib Lung Cancer Trial (DELTA). J Clin Oncol 2014; 32(18): 1902-8.

14. Goldstraw P, Chansky K, Crowley J, *et al*. The IASLC lung cancer staging project: proposals for revision of the TNM stage groupings in the forthcoming (eighth) edition of the TNM classification for lung cancer. J Thorac Oncol 2016; 11(1): 39-51.

15. Eisenhauer EA, Therasse P, Bogaerts J, *et al*. New response evaluation criteria in solid tumours: revised RECIST guideline (version 1.1). Eur J Cancer 2009; 45(2): 228-47.

16. Wheatley-Price P, Ding K, Seymour L, *et al*. Erlotinib for advanced non–small-cell lung cancer in the elderly: an analysis of the National Cancer Institute of Canada Clinical Trials Group Study BR. 21. J Clin Oncol 2008; 26(14): 2350-7.

17. Garassino MC, Martelli O, Broggini M, *et al*. Erlotinib versus docetaxel as second-line treatment of patients with advanced non-small-cell lung cancer and wild-type EGFR tumours (TAILOR): a randomised controlled trial. Lancet Oncol 2013; 14(10): 981-8.

18. Li N, Yang L, Ou W, *et al*. Meta-analysis of EGFR tyrosine kinase inhibitors compared with chemotherapy as second-line treatment in pretreated advanced non-small cell lung cancer. PLoS One 2014; 9(7): e102777.

19. Chen Y-Y, Chang S-C, Chang C-Y, *et al*. Real-world effectiveness of second-line afatinib versus chemotherapy for the treatment of advanced lung squamous cell carcinoma in immunotherapy-naïve patients. BMC Cancer 2021; 21(1): 1-9.

20. Chan DW-K, Choi HC-W, Lee VH-F. Treatment-related adverse events of combination EGFR tyrosine kinase inhibitor and immune checkpoint inhibitor in EGFR-mutant advanced non-small cell lung cancer: a systematic review and meta-analysis. Cancers 2022; 14(9): 2157.

21. Yuan H, Liu J, Zhang J. The current landscape of immune checkpoint blockade in metastatic lung squamous cell carcinoma. Molecules 2021; 26(5): 1392.

22. Becker A, Crombag L, Heideman D, *et al*. Retreatment with erlotinib: regain of TKI sensitivity following a drug holiday for patients with NSCLC who initially responded to EGFR-TKI treatment. Eur J Cancer 2011; 47(17): 2603-6.

Afatinib As Potential Treatment for NRG1 Fusion-Driven Non-Small Cell Lung Cancer: A Case Report

Chi-Hao Wu[1], Ching-Han Lai[1], Xin-Min Liao[1]

Driver mutations and tyrosine kinase inhibitors play pivotal roles in the treatment of advanced stage non-small cell lung cancer. Besides the common mutations, such as in EGFR, ALK, ROS1, and BRAF, there are some other mutations that are also worth targeting. With the development of next-generation sequencing technology and new drugs, an increasing number of mutations can now be targeted to improve the prognosis of non-small cell lung cancer. One of these uncommon mutations, neuregulin 1 (NRG1) fusion, has rarely been reported. Here, we reported a case of lung adenocarcinoma with this rare mutation -- NRG1 fusion -- that successfully responded to the drug afatinib. *(Thorac Med 2023; 38: 199-204)*

Key words: NRG1 fusion, non-small cell lung cancer, afatinib, ErbB family, RNA-based next-generation sequencing

Introduction

Oncogenic driver mutations and clinically available signaling pathway inhibitors have had a significant impact on non-small cell lung cancer (NSCLC) patient management. Currently, targeted therapies are mainly focused on a few driver mutations, such as EGFR, ALK, ROS1 and BRAF. Although oncogenic gene fusions involving an NRG1 alteration are rare, they have been recently described as a new target in patients with advanced or metastatic NSCLC. Here, we describe a patient with stage IV lung adenocarcinoma harboring NRG1 gene fusions that had a durable response to the irreversible pan-ErbB inhibitor, afatinib.

Case Report

A 67-year-old man with a history of hypertension and type 2 diabetes mellitus presented to our hospital with epigastric pain that he had experienced for 2 months. He was a retired teacher. He used to smoke socially when he was young, and he usually consumed 60-100 ml of Kaoliang (sorghum) liquor every week. He reported that he had been exposed to pulmonary tuberculosis many years ago; however, the

[1]Division of Pulmonary Medicine, Department of Internal Medicine, National Cheng Kung University Hospital, Tainan
Address reprint requests to: Dr. Xin-Min Liao, No. 138, Shengli Road, North District, Tainan City 704, Taiwan

chest radiograph during the following 3 years did not reveal a specific lung lesion. He had lost approximately 2-3 kg of weight in the 3 months prior to his initial presentation to our hospital.

Upon arrival at our hospital, a survey of the patient's gastrointestinal system, including abdominal ultrasonography and esophagogastroduodenoscopy, was unremarkable. However, chest radiography revealed a lung mass in the left lower lobe (LLL). Furthermore, chest computed tomography (CT) revealed a suspected LLL lung cancer with right lung metastasis and mediastinal lymphadenopathy. CT-guided biopsies proved this to be a lung invasive mucinous adenocarcinoma without EGFR and ROS1 mutations, or ALK fusion. Immunostaining of PDL1 displayed less than 1%. There was no evidence of brain or bone metastases, and the initial stage was diagnosed as T1cN3M1a, stage IV.

The patient received chemotherapy with pemetrexed plus cisplatin from October 2018 to January 2019, followed by maintenance chemotherapy with pemetrexed until May 2019. He had no severe adverse events during this period, and the best response documented by chest CT during first-line treatment was stable disease. Nevertheless, the follow-up chest CT on 21 May 2019 showed lung cancer with progression and new bone metastasis at L3. CT-guided re-biopsy of the LLL tumor was performed in June 2019, and the collected tissue was sent for RNA-based next-generation sequencing (NGS) (ACTDrug®+), which yielded a CD74-NRG1 mutation.

The patient received second-line chemotherapy with Taxotere from early July 2019, while awaiting the NGS report; however, the follow-up chest CT in October still showed lung cancer with progression (Figure 1A). Therefore,
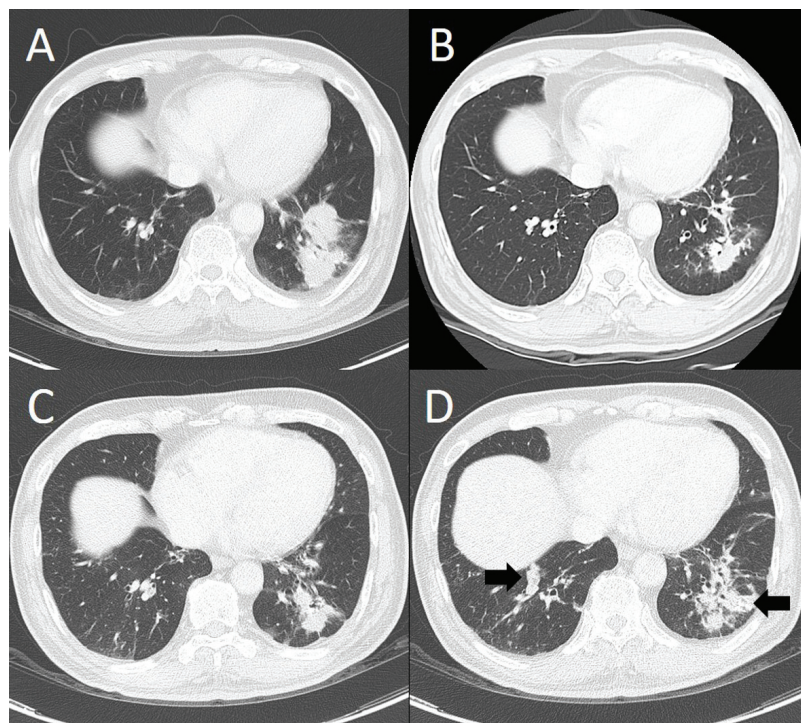

Fig. 1. Chest CT image showing the primary tumor at the left lower lobe before (A), after 3 months (B), and after 21 months (C and D) of afatinib treatment.

afatinib was administered to target the CD74-NRG1 mutation as a third-line therapy in mid-October 2019. Follow-up chest CT scan on 8 January 2020 showed obvious shrinkage of the lung cancer (Figure 1B), and partial regression was considered. On 27 July 2021, the LLL residual tumor target and right lower lobe metastatic tumor showed an increase in size (Figure 1C and 1D). Therefore, progressive disease was considered, and afatinib treatment was discontinued after a total of 21 months. The patient is still alive, as of this writing, and on treatment.

Discussion

Several extracellular ligands can bind to the ErbB protein family, which subsequently influences the intracellular process. These ligands can be divided into 2 groups: those that bind to ErbB1/ErbB4 receptors or to ErbB3/ErbB4 receptors. Neuregulins, which are composed of NRG1–4, are the ligands that bind ErbB3/ErbB4. NRG1 possesses an epidermal growth factor (EGF)-like domain on the cell surface. As NRG1 is proteolytically cleaved and released into the cytoplasm, it is primarily involved in a broad spectrum of cellular processes, and is not limited to neural development [1]. Upon binding of NRG1, the receptors form either heterodimers or homodimers; this occurs preferentially with the ErbB2 receptor, resulting in the activation of downstream intracellular pathways, including PI3K-AKT and MAPK [2]. Overexpression of NRG1 on the cell surface, but not over-secretion, plays an important role in cell proliferation and oncogenesis [3]. Furthermore, CD74-NRG1 fusion has been shown to confer cancer stem cell (CSC)-like properties, including sphericalization, in immature progenitor-like cells [4].

The NRG1 mutation was first reported in 2014, when Fernandez-Cuesta et al. identified CD74-NRG1 fusions in invasive mucinous adenocarcinoma [3]. In addition to CD74, at least 17 other fusion partners, including SLC3A2, SDC4, RBPMS, and WRN, were subsequently discovered. In an analysis of 21,858 tumor specimens that underwent anchored multiplex polymerase chain reaction for targeted RNA sequencing, NRG1 fusion prevalence was found to be 0.2%. Of these, CD74 was the most common partner (29%), followed by ATP1B1 (10%), SDC4 (7%), and RBPMS (5%) [5].

NGS is an advanced technique used in the detection of gene mutations. However, in a large analysis of 17,485 solid tumors, NRG1 fusion was under-detected via DNA NGS [6]. Targeted RNA sequencing could compensate for this defect, possibly because of the complexity and diversity of fusion architecture and the large intronic regions characteristic of NRG1 [7]. Thus, RNA sequencing is more reliable and sensitive for NRG1 fusion detection than DNA NGS. To date, immunohistochemistry (IHC) and fluorescence in situ hybridization (FISH) techniques have been the primary methods used to detect oncogenic mutations. FISH has been successfully used as the primary method to identify NRG1þ NSCLC; however, the specific fusion partners are unknown in many NRG1 FISH-positive cases [8-9]. Fernandez-Cuesta and colleagues reported that phospho-HER3 (p-ERBB3) IHC had a sensitivity of 100% and a specificity of 97.5% among 245 lung adenocarcinoma samples [3]. A screening approach for p-ERBB3 IHC, followed by RNA sequencing, may be an optimal and cost-effective approach to identify rare fusion cases [10].

Overall, NRG1 fusion is an extremely rare driver mutation in NSCLC. Several studies

have shown that the incidence of NRG1 fusion is approximately 0.14–0.3% [5, 6]. In terms of tumor pathohistology, invasive mucinous adenocarcinoma (IMA) is the most common subtype that harbors NRG1 fusion (61%), followed by non-specific adenocarcinoma (29%), and squamous cell carcinoma (6%) [11]. NRG1 fusion is mutually exclusive of KRAS, which is a common mutation in IMA [5, 6]. The reported cases tended to be female (66%) and non-smokers (30%), whereas smokers were not as highly reported (58%) [12]. Most of the work on NRG1 fusion was done in East Asia; therefore, it was thought to be prone to occur among the Asian population. However, a recent evaluation of 85 Caucasian lung cancer patients revealed NRG1 rearrangements in 31% of patients with IMA, indicating that NRG1 is a shared driver mutation in both Asian and Caucasian ethnicities [13].

As NRG1 is the ligand for the ErbB family, monoclonal antibodies and tyrosine kinase inhibitors have potential for future treatment. Afatinib suppressed ErbB2, ErbB3, and extracellular signal-regulated kinase phosphorylation, indicating the downregulation of ErbB signaling in a preclinical model [12]. Another pan-ErbB kinase inhibitor, tarloxotinib, also demonstrated efficacy in cell lines and patient-derived xenografts in a preclinical study [14]. Zenocutuzumab, a monoclonal antibody for ErbB2 and ErbB3, has shown antitumor activity against NRG1 fusion-positive cancers [15]. In a review of NSCLC with NRG1 fusions, afatinib was the most commonly administered drug, in 7 of 11 patients treated [7]. In another case series of metastatic NRG1 fusion-positive tumors treated with afatinib, the duration of the treatment response of NRG1 fusion-positive NSCLC ranged from 1.2 months to more than

27 months, while progression-free survival after afatinib treatment ranged from 3 to more than 36 months in non-lung cancer subjects [16]. We summarized the data from published case reports that described responses to afatinib in patients with solid tumors harboring NRG1 fusions in Table 1 [6, 16-21].

In addition, a patient who was treated with the anti-ErbB3 molecule GSK2849330 (no longer in development) developed progressive disease after a partial response lasting 19 months [6]. Also, the monoclonal antibodies lumretuzumab and zenocutuzumab showed a duration of response ranging from 4 months to more than 7 months, although most treatment courses are still ongoing [15, 22].

The prognosis of NRG1 fusion in IMAs remains unclear. In a study evaluating a series of 59 patients with IMA, patients with NRG1 fusions had poorer overall survival than those without NRG1 fusions (median 51.9 months vs. not reached; P = 0.019) [9]. In contrast, another study showed that there was no prognostic difference between patients with or without NRG1 fusions [23].

Our patient had characteristics similar to those of the reported NRG1 fusion cases. The pathological cell type was IMA and was free from common mutations, including EGFR, ALK and ROS-1. He had the most commonly found fusion, CD74- NRG1, and the treatment response was longer than 12 months, which is above the average of reported cases. However, further investigation is needed to understand this rare mutation, including the core mechanism of NRG1 fusion development and the responses of different NRG1 fusion subtypes to different target therapies, so as to provide potentially better treatment for patients.

Table 1. Published Cases of Ppatients with Metastatic NRG1 Fusion-Driven Solid Tumors Who Were Treated with Afatinib

Age, gender	Cancer cell type	Prior treatments	Best tumor response	Time to treatment failure (months)	Reference
Cases of lung cancer					
42 y/o, male	Nonmucinous adenocarcinoma	Chemotherapy	Partial response	12	[18]
62 y/o, male	Mucinous adenocarcinoma	Surgery	Durable response	10	[18]
43 y/o, female	Nonmucinous adenocarcinoma	Chemotherapy, NOTCH inhibitor	Partial response	12	[20]
62 y/o, female	Invasive mucinous adenocarcinoma	Chemotherapy	Partial response	6.5	[17]
81 y/o, male	Invasive mucinous adenocarcinoma	Surgery	Stable disease	3	[6]
56 y/o, female	Invasive mucinous adenocarcinoma	Chemotherapy, surgery, radiotherapy, immunotherapy	Progressive disease		[6]
51 y/o, male	Invasive mucinous adenocarcinoma	Chemotherapy, surgery, radiotherapy	Progressive disease		[6]
56 y/o, female	Nonmucinous adenocarcinoma	Surgery, chemotherapy, EGFR tyrosine kinase inhibitor, radiotherapy	Partial response	24	[16]
62 y/o, female	Nonmucinous adenocarcinoma	Chemotherapy, immunotherapy	Partial response	Ongoing after 27 months	[16]
68 y/o, male	Invasive nonmucinous adenocarcinoma	Surgery, chemotherapy, immunotherapy	Stable disease	4	[16]
43 y/o, female	Invasive mucinous adenocarcinoma	Chemotherapy, immunotherapy	Partial response	>18	[16]
34 y/o, female	Invasive mucinous adenocarcinoma	Surgery, chemotherapy	Partial response	5, then 6 months	[16]
Cases other than lung cancer					
38 y/o, female	Cholangiocarcinoma	Chemotherapy, surgery	Response	8	[20]
59 y/o, male	Pancreatic ductal adenocarcinoma	Chemotherapy	Partial response	5.5	[21]
54 y/o, male	Pancreatic ductal adenocarcinoma	Chemotherapy	Partial response	Ongoing after 5 months	[21]
30 y/o, female	Pancreatic ductal adenocarcinoma	Chemotherapy	Partial response	3	[19]
NA, female	Low-grade serous ovarian cancer	NA	Stable disease	>36	[24]
69 y/o, male	Colorectal cancer	Surgery, chemotherapy	Stable disease	16	[16]

References

1. Willem M. Proteolytic processing of neuregulin-1. Brain Res Bull 2016; 126(Pt 2): 178-82.

2. Fernandez-Cuesta L, Thomas RK. Molecular pathways: targeting NRG1 fusions in lung cancer. Clin Cancer Res 2015; 21(9): 1989-94.

3. Fernandez-Cuesta L, Plenker D, Osada H, *et al*. CD74-NRG1 fusions in lung adenocarcinoma. Cancer Discov 2014; 4(4): 415-22.

4. Murayama T, Nakaoku T, Enari M, *et al*. Oncogenic fusion gene CD74-NRG1 confers cancer stem cell-like properties in lung cancer through a IGF2 autocrine/paracrine circuit. Cancer Res 2016; 76(4): 974-83.

5. Jonna S, Feldman RA, Swensen J, *et al*. Detection of NRG1 gene fusions in solid tumors. Clin Cancer Res 2019; 25(16): 4966-72.

6. Drilon A, Somwar R, Mangatt BP, et al. Response to ERBB3-directed targeted therapy in NRG1-rearranged cancers. Cancer Discov 2018; 8(6): 686-95.

7. Laskin J, Liu SV, Tolba K, *et al*. NRG1 fusion-driven tumors: biology, detection, and the therapeutic role of afatinib and other ErbB-targeting agents. Ann Oncol 2020; 31(12): 1693-703.

8. Duruisseaux M, McLeer-Florin A, Antoine M, *et al*. NRG1 fusion in a French cohort of invasive mucinous lung adenocarcinoma. Cancer Med 2016; 5(12): 3579-85.

9. Shin DH, Lee D, Hong DW, *et al*. Oncogenic function and clinical implications of SLC3A2-NRG1 fusion in invasive mucinous adenocarcinoma of the lung. Oncotarget 2016; 7(43): 69450-65.

10. Nagasaka M, Ou SI. Neuregulin 1 fusion-positive NSCLC. J Thorac Oncol 2019; 14(8): 1354-9.

11. Cha YJ, Shim HS. Biology of invasive mucinous adenocarcinoma of the lung. Transl Lung Cancer Res 2017; 6(5): 508-12.

12. Nakaoku T, Tsuta K, Ichikawa H, *et al*. Druggable oncogene fusions in invasive mucinous lung adenocarcinoma. Clin Cancer Res 2014; 20(12): 3087-93.

13. Trombetta D, Graziano P, Scarpa A, *et al*. Frequent NRG1 fusions in Caucasian pulmonary mucinous adenocarcinoma predicted by Phospho-ErbB3 expression. Oncotarget 2018; 9(11): 9661-71.

14. Estrada-Bernal A, Le AT, Doak AE, *et al*. Tarloxotinib is a hypoxia-activated pan-HER kinase inhibitor active against a broad range of HER-family oncogenes. Clin Cancer Res 2021; 27(5): 1463-75.

15. Schram AM, Odintsov I, Espinosa-Cotton M, *et al*. Zenocutuzumab, a HER2xHER3 bispecific antibody, is effective therapy for tumors driven by NRG1 gene rearrangements. Cancer Discov 2022.

16. Cadranel J, Liu SV, Duruisseaux M, *et al*. Therapeutic potential of afatinib in NRG1 fusion-driven solid rumors: a case series. Oncologist 2021; 26(1): 7-16.

17. Cheema PK, Doherty M, Tsao MS. A case of invasive mucinous pulmonary adenocarcinoma with a CD74-NRG1 fusion protein targeted with afatinib. J Thorac Oncol 2017; 12(12):e200-e2.

18. Gay ND, Wang Y, Beadling C, *et al*. Durable response to afatinib in lung adenocarcinoma harboring NRG1 gene fusions. J Thorac Oncol 2017; 12(8): e107-e10.

19. Heining C, Horak P, Uhrig S, *et al*. NRG1 fusions in KRAS wild-type pancreatic cancer. Cancer Discov 2018; 8(9):1087-95.

20. Jones MR, Lim H, Shen Y, *et al*. Successful targeting of the NRG1 pathway indicates novel treatment strategy for metastatic cancer. Ann Oncol 2017; 28(12): 3092-7.

21. Jones MR, Williamson LM, Topham JT, *et al*. NRG1 gene fusions are recurrent, clinically actionable gene rearrangements in KRAS wild-type pancreatic ductal adenocarcinoma. Clin Cancer Res 2019; 25(15): 4674-81.

22. Kim HS, Han JY, Shin DH, *et al*. EGFR and HER3 signaling blockade in invasive mucinous lung adenocarcinoma harboring an NRG1 fusion. Lung Cancer 2018; 124: 71-5.

23. Shim HS, Kenudson M, Zheng Z, *et al*. Unique genetic and survival characteristics of invasive mucinous adenocarcinoma of the lung. J Thorac Oncol 2015; 10(8): 1156-62.

24. Murumägi A. Ungureanu D. Khan S. *et al*. Clinical implementation of precision systems oncology in the treatment of ovarian cancer based on ex-vivo drug testing and molecular profiling. Cancer Res 2019; 79 (Abstract 2945).

Chest Wall Tuberculosis Mimicking Parasitic Infection: A Case Report

You-Lung Chang[1], Chien-Hong Chou[1]

Tuberculosis has long been known as the "great mimicker" because of its ever-changing presentation. Here, we reported the case of a young Filipino with asthma who initially presented with intermittent right upper quadrant abdominal pain. Further laboratory studies revealed high serum eosinophilia and eosinophil-predominant pleural effusion, which almost misled us to the diagnosis of parasitic infection, based on parasite findings in the stool. The definite diagnosis of chest wall tuberculosis was made based on the results of computed tomography and surgical procedure of the chest wall. **(Thorac Med 2023; 38: 205-208)**

Key words: mycobacterium, eosinophilia, pleural effusion, parasite, eosinophilic granulomatosis with polyangiitis

Introduction

Tuberculosis (TB) has long been known as the "great mimicker" because of its many different manifestations. In the radiographic examination, TB may mimic common bacterial pneumonia or malignancy [1]. In the clinical exam, TB may mimic rheumatologic disease or parasite infection [2]. Here, we report the case of an asthmatic young Filipino presenting with high serum eosinophilia and eosinophil-predominant pleural effusion, which almost misled us to the diagnosis of parasitic infection or eosinophilic granulomatosis with polyangiitis (EGPA), based on his history of asthma, the high percentage of eosinophils (>50%) in the pleural effusion, and the parasite finding in the stool.

Case report

A 23-year-old Filipino, who had a medical history of mild asthma since childhood, with 1-2 exacerbations per year and occasional use of a metered dose inhaler, came to Taiwan about 1 year ago. During the last 6 months, he suffered from intermittent sharp right upper quadrant abdominal pain and tenderness, radiating to the right back, with a score of 7-8 out of 10 on deep breathing. The pain was relieved if he attempted shallow breathing, and had worsened in most recent 3 months. He denied fever,

cough, dyspnea, nausea, vomiting, or diarrhea.

The abdominal echography performed in the outpatient department revealed moderate right pleural effusion. Physical examination showed decreased breathing sounds in the right lung, but no local tenderness. Laboratory serum data showed the following: total protein 6.5 g/dL, lactate dehydrogenase (LDH) 593 U/L, white blood cells (WBC) 10.74 k/μL, neutrophils 50.3%, eosinophils 20.8%, absolute eosinophil count 2233/μL, and IgE 991 IU/ml. A subsequent pleural effusion study revealed a yellow cloudy appearance with the following biochemical findings: protein 6486 mg/dL, LDH 593 U/L, WBC 10500/μk, lymphocytes 12%, eosinophils 81%, and adenosine deaminase 16U/L, but a negative acid-fast stain and TB culture. In view of the high serum eosinophilia, eosinophil-predominant pleural effusion and asthma, parasitic infection or EGPA was highly suspected after systemic review. Tracing back his medical history, he sometimes walked barefoot in daily life, had a pet dog 7 years ago and had eaten undercooked beef for the last 1 year. In addition, he was a homosexual. EGPA was tentatively excluded because only asthma and eosinophilia met the diagnostic criteria. Subsequent investigations were unrevealing, including negative results for the following: sputum TB polymerase chain reaction (PCR), parasitic ova in the pleural effusion, serum HIV screen, and rheumatologic profile (ANA, anti-ENA, c-ANCA, p-ANCA).

A later stool egg concentration examination revealed Blastocystis hominis. However, after use of metronidazole at 250 mg tid po for 10 days, followed by 750 mg tid po for 7 days, the follow-up pleural effusion study still showed a high percentage of eosinophil counts (protein 6260 mg/dL, WBC 5020/μk, lymphocytes 14%,
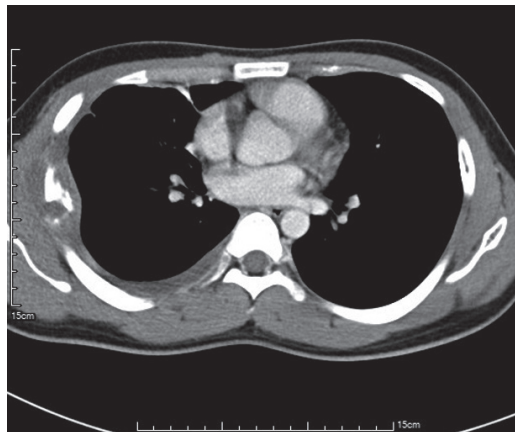
Fig. 1. fluid accumulation or soft tissue lesion with destruction and erosion of the 6th and 7th ribs in the right 5th-7th intercostal space

eosinophils 74%), despite recovery of serum eosinophilia (serum eosinophils 6.3%, absolute counts 593 per microliter) and that pleural biopsy revealed merely fibrosis.

Finally, chest computed tomography (CT) disclosed fluid accumulation or soft tissue lesion with destruction and erosion of the 6th and 7th ribs in the right 5th-7th intercostal space (Figure 1). The patient underwent chest wall debridement and partial rib resection with uniportal video-assisted thoracic surgery decortications. Pathology showed a positive TB PCR and granulomatous inflammation with some acid-fast bacilli from the chest wall and pleura specimen. After 2 months of anti-TB medication treatment with a HERZ regimen (a fixed-dose combination regimen with isoniazid, rifampicin, ethambutol and pyrazinamide), the follow-up chest radiograph revealed no further pleural effusion, and laboratory studies showed no more eosinophilia (serum eosinophil 2.8%, absolute counts 152 per microliter).

Discussion

Chest wall TB is a rare presentation, ac-

counting for only 1 to 2 percent of all cases of TB [3]. TB is also an uncommon cause of eosinophilic pleural effusion (EPE) [4]. Here, we presented a case with chest wall TB manifesting EPE. EPE is de-fined as pleural effusion with greater than 10% eosinophil counts, and it accounts for 5-16% of exudative pleural effusions [5]. EPE is associated with many diseases, such as malignancies, infections (e.g., bacteria, fungi or parasites), autoimmune diseases, pulmonary embolism, drug reactions, chest trauma, and many others [6]. Serum eo-sinophilia is found in up to 75% of patients with EPE [5].

EGPA was suspected in this case because the patient had a history of asthma, pe-ripheral blood eosinophilia and a high percentage of eosinophils in the pleural effu-sion, but was ruled out, because a late onset and difficulty in treating asthma were the characteristics of EGPA [7-8]. TB-induced EPE was not initially suspected because the most common cause of secondary eosinophilia is parasitic infection, and parasitic effusion usually has a high percentage of eosinophil counts [9-10]. Tong et al. report-ed that the mean eosinophil and lymphocyte proportions in parasitic pleural effusions were significantly higher and lower, respectively, than that of TB pleural effusions, at 78.13% ± 21.60% and 7.27% ± 5.61%. Hwang *et al*. also found that most patients with paragonimiasis-related pleural effusions had low levels of lymphocytes (<50%) and significantly more eosinophils (>10%) in their pleural effusions [9, 11].

However, low ADA levels in the pleural effusion misled us to the possible diag-nosis of parasitic infection. According a meta-analysis published in 2019, the sensi-tivity, specificity and diagnostic odds ratio of ADA to TB pleural effusion were 0.92 (95% CI: 0.90–0.93), 0.90 (95% CI: 0.88–0.91) and 97.42 (95% CI:

74.90–126.72), respectively [12]. High ADA levels are considered to be a sensitive and specific marker for diagnosing TB pleural effusion, but can also be found in pneumonia, em-pyema, and neoplasm [13-14]. ADA2, the isoenzyme of ADA, and the ratio of ADA1/ADAp may improve performance in sensitivity and specificity (100% and 92–97%), but the additional laboratory process is rather difficult and expensive [15].

Asymptomatic Blastocystis hominis infection with hypereosinophilia has been reported in Taiwan, but treatment was not suggested in most medical literature [16-17]. We treated the patient with metronidazole, because initially there was no evi-dence of an etiology of eosinophilia other than Blastocystis hominis. Recovery from serum eosinophilia under treatment with metronidazole may be explained in part by its effect on TB under anaerobic conditions [18].

In conclusion, TB is so far the "great mimicker", and we should not rule out the possibility of TB infection until there is clear evidence of parasitic or other etiolo-gies.

References

1. Prapruttam D, Hedgire SS, Mani SE, *et al*. Tuberculosis-the great mimicker. Semin Ultrasound CT MR 2014; 35(3): 195-214.
2. Franco-Paredes C, Diaz-Borjon A, Senger MA, *et al*. The ever-expanding association between rheumatologic diseases and tuberculosis. Am J Med 2006; 119(6): 470-7.
3. Grover SB, Jain M, Dumeer S, *et al*. Chest wall tuberculosis - A clinical and imaging experience. Indian J Radiol Imaging 2011; 21(01): 28-3.
4. Oba Y, Abu-Salah T. The prevalence and diagnostic significance of eosinophilic pleural effusions: a meta-analysis and systematic review. Respiration 2012; 83(3): 198-208.
5. Kalomenidis I, Light RW. Eosinophilic pleural effusions.

Current Opin Pulm Med 2003; 9(4): 254-60.

6. Krenke R, Nasilowski J, Korczynski K, *et al*. Incidence and aetiology of eosinophilic pleural effusion. Eur Respir J 2009; 34(5): 1111-7.

7. D'Cruz DP, Barnes NC, Lockwood CM. Difficult asthma or Churg-Strauss syndrome? BMJ 1999; 318(7182): 475-6.

8. Hirasaki S, Kamei T, Iwasaki Y, *et al*. Churg-Strauss Syndrome with pleural involvement. Intern Med 2000; 39(11): 976-8.

9. Tong S, Zhu Y, Wan C. Distinguishing tuberculosis pleural effusion from parasitic pleural effusion using pleural fluid characteristics: A case control study. Medicine (Baltimore) 2019; 98(5): e14238.

10. Tefferi A, Patnaik MM, Pardanani A. Eosinophilia: secondary, clonal and idiopathic. Brit J Haematol 2006; 133(5): 468-492.

11. Hwang KE, Song HY, Jung JW, *et al*. Pleural fluid characteristics of pleuropulmonary paragonimiasis masquerading as pleural tuberculosis. Korean J Intern Med 2015; 30(1): 56-61.

12. Aggarwal AN, Agarwal R, Sehgal IS, *et al*. Adenosine deaminase for diagnosis of tuberculous pleural effusion: A systematic review and meta-analysis. PLoS One 2019; 14(3): e0213728.

13. Pettersson T, Ojala K, Weber TH. Adenosine deaminase in the diagnosis of pleural effusions. Acta Med Scand 1984; 215(4): 299-304.

14. Liang QL, Shi HZ, Wang K, *et al*. Diagnostic accuracy of adenosine deaminase in tuberculous pleurisy: A meta-analysis. Respir Med 2008; 102(5): 744-754.

15. Jimenez Castro D, Diaz Nuevo G, Perez-Rodriguez E, *et al*. Diagnostic value of adenosine deaminase in nontuberculous lymphocytic pleural effusions. Eur Respir J 2003; 21(2): 220-4.

16. Coyle CM, Varughese J, Weiss LM, *et al*. Blastocystis: to treat or not to treat…. Clin Infect Dis 2011; 54(1): 105-110.

17. Kuo HY, Chiang DH, Wang CC, *et al*. Clinical significance of Blastocystis hominis: experience from a medical center in northern Taiwan. J Microbiol Immunol Infect 2008; 41(3): 222-6.

18. Alsaad N, Wilffert B, van Altena R, *et al*. Potential antimicrobial agents for the treatment of multidrug-resistant tuberculosis. Eur Respir J 2014; 43(3): 884-97.

Immune Checkpoint Inhibitors-Related Interstitial Lung Disease Presenting as Usual Interstitial Pneumonia in a Patient with Small-Cell Lung Cancer: A Case Report and Literature Review

Hsiao-Chin Shen[1], Chi-Lu Chiang[1]

Immune checkpoint inhibitors (ICIs) such as programmed death (PD) 1 and PD ligand 1 inhibitors have proved to be effective in the treatment of advanced lung cancer. However, ICIs can also stimulate the immune system, resulting in immune-related adverse events (irAEs). ICI-induced pneumonitis, which is an irAE in the lung, displays a wide range of imaging features, including usual interstitial pneumonia (UIP), although this is relatively rare. The treatment for symptomatic ICI-induced pneumonitis involves stopping ICIs and administering systemic steroids. If the initial symptoms do not improve, a titrated steroid dose and additional immunosuppression can be considered. In this study, we reported the case of a patient with advanced small-cell lung cancer who received ICIs. This patient developed pneumonitis presenting an UIP pattern after a few courses of ICIs. She was successfully treated with steroid pulse therapy and mycophenolate mofetil. We described the imaging characteristics, and discussed the management strategies for this adverse event in patients with lung cancer treated with ICIs. *(Thorac Med 2023; 38: 209-216)*

Key words: immune-related adverse events, pneumonitis, usual interstitial pneumonia

Introduction

Treatment for advanced lung cancer has evolved to include chemotherapy, targeted therapy, and immune checkpoint inhibitors (ICIs) for selected patients in the first-line setting [1]. ICIs enhance antitumor activities, but they can also stimulate the immune system, resulting in immune-related adverse events (irAEs), such as pneumonitis [2]. Pulmonary irAEs can be sche-matically divided into ICI-induced pneumonitis and sarcoidosis-like reactions. ICI-induced pneumonitis may display a wide range of imaging features, which are not classifiable as any specific pattern in some cases. The most frequent imaging pattern of ICI-induced pneumonitis is organizing pneumonia (OP) [3]. Usual interstitial pneumonia (UIP) is a relatively rare imaging pattern of ICI-induced pneumonitis. We herein report the case of a patient with ICI-

[1]Department of Chest Medicine, Taipei Veterans General Hospital, Taipei, Taiwan
Address reprint requests to: Dr. Chi-Lu, Chiang, Department of Chest Medicine, Taipei Veterans General Hospital 201, Section 2, Shih-Pai Road, Taipei, 112, Taiwan

induced pneumonitis presenting UIP. Clinical and radiographic improvements were noted after treatment with corticosteroid and mycophenolate mofetil (MMF).

Case Description

A 63-year-old female patient received a diagnosis of extensive-stage small-cell lung cancer (ES-SCLC) in April 2020. The clinical staging was IVB (cT4N3M1c) with multiple liver metastases. The initial chest computed tomography (CT) in April 2020 (Figure 1) revealed a mass lesion at the right lower lobe as the primary lung cancer, without ground-glass opacities (GGOs), reticulation, traction bronchiectasis, or other imaging features of interstitial lung disease. The patient had never smoked and had no history of exposure-evoked chronic hypersensitivity pneumonitis or familial or chronic drug-induced pneumonitis. This indicated that pre-existing idiopathic pulmonary fibrosis was unlikely.

The patient had participated in a clinical trial and received chemotherapy combined with atezolizumab as first-line treatment beginning in May 2020. After 4 cycles of chemotherapy combined with atezolizumab and 4 cycles of maintenance atezolizumab, the patient complained of intermittent shortness of breath and desaturation, and chest CT revealed a decrease in the size of the primary and liver metastatic tumors, but an increase in subpleural interlobular septa thickening in the lungs. Grade II ICI-induced pneumonitis was diagnosed (severity of pneumonitis was defined according to the Common Terminology Criteria for Adverse Events, version 4.0), and treatment with methylprednisolone at 8 mg/day was begun in September 2020 (Figure 1). The patient had no symptoms
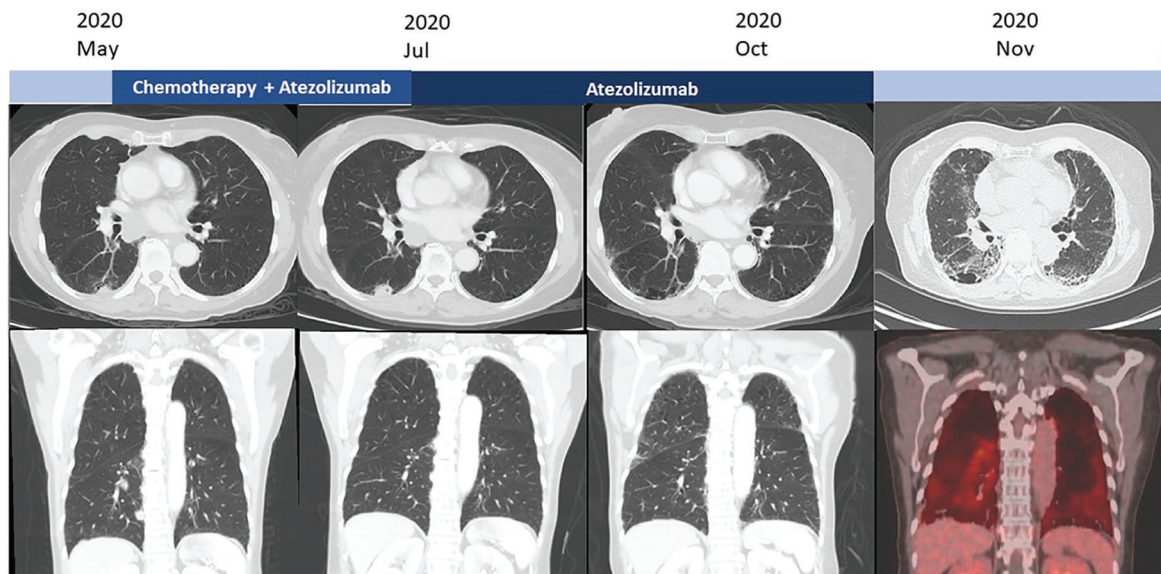
Fig. 1. Chest computed tomography (CT) images.
The patient underwent a clinical trial with atezolizumab plus chemotherapy. She was diagnosed with atezolizumab-induced pneumonitis after 4 months, identified by the presence of subpleural reticulation on the CT scan. Methylprednisolone was then prescribed in September 2020. The CT scan images were taken at the time of the cancer diagnosis, during atezolizumab treatment, at the atezolizumab-induced pneumonitis diagnosis, and during the deterioration of pneumonitis, respectively.

Table 1. The patient's Pulmonary Function Tests

	2020/3 (Baseline)	2020/09 (Atezolizumab)	2020/12 (Pneumonitis)	2021/01 (After steroid +MMF)
FVC (% prediction)	2.43 (95)	1.85 (74)	1.64 (65)	1.75 (70)
FEV1 (% prediction)	1.52 (75)	1.53 (77)	1.4 (70)	1.5 (76)
FEV1/FVC (%)	81	82	85.46	86
DLco (% prediction)		38	19	

Pulmonary function tests were performed at the baseline of cancer diagnosis, during atezolizumab treatment, at the pneumonitis diagnosis, and after steroid combined with MMF treatment, respectively. FVC, forced vital capacity; FEV1, forced expiratory volume in 1 second; DLco, diffusion capacity of carbon monoxide.

related to connective tissue disease and was serologically negative for all auto-antibodies. A pulmonary function test revealed a reduction in gas exchange and restrictive ventilatory impairment (Table 1).

Atezolizumab therapy was restarted after clinical improvement was seen in the respiratory symptoms and with steroid tapering. However, after 2 cycles of atezolizumab, the patient developed progressive dyspnea on exertion. She became oxygen-dependent, requiring 4-5 L of oxygen through a nasal cannula at all times.

In November 2020, we performed whole body positron emission tomography, which re-vealed diffuse interlobar septal thickening with infiltrative fluorodeoxyglucose uptake, which was more prominent in the bilateral lower lungs. Moreover, we noted subpleural reticula-tion with peripheral traction bronchiectasis and bilateral lower lung honeycombing, compatible with a UIP pattern (Figure 2). Based on the diagnosis of grade III ICI-induced pneumonitis, we prescribed empirical antibiotic therapy with levofloxacin and administered steroid pulse therapy (methylprednisolone 500 mg/day for 3 days). The steroid was tapered after pulse therapy (methylprednisolone 62.5 mg/day for 2 days, followed by 31.25 mg/day for 3 days, and
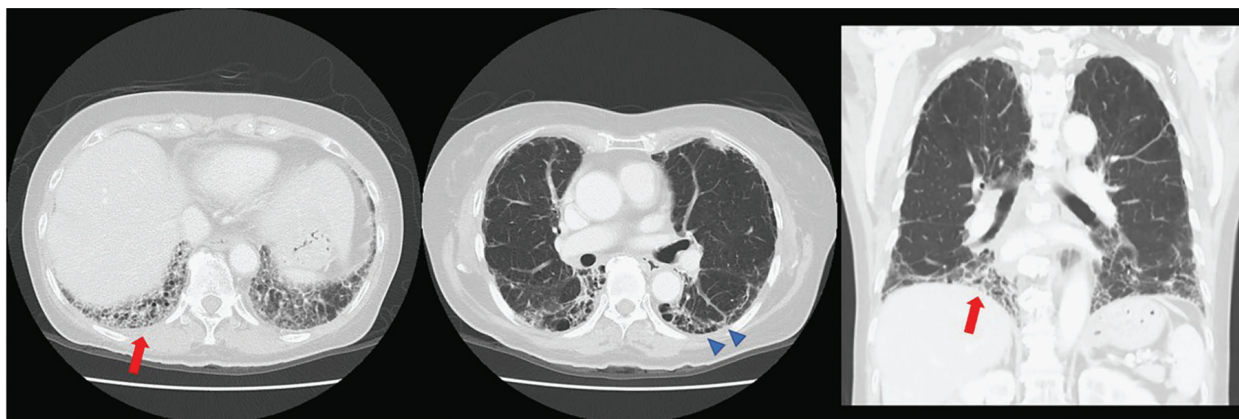
Fig. 2. Chest computed tomography performed 8 months after the first atezolizumab administration.
The interstitial abnormality exhibited reticulation with peripheral traction bronchiectasis (blue arrowheads). Honeycomb lesions appeared in the lower lobe (red arrow).
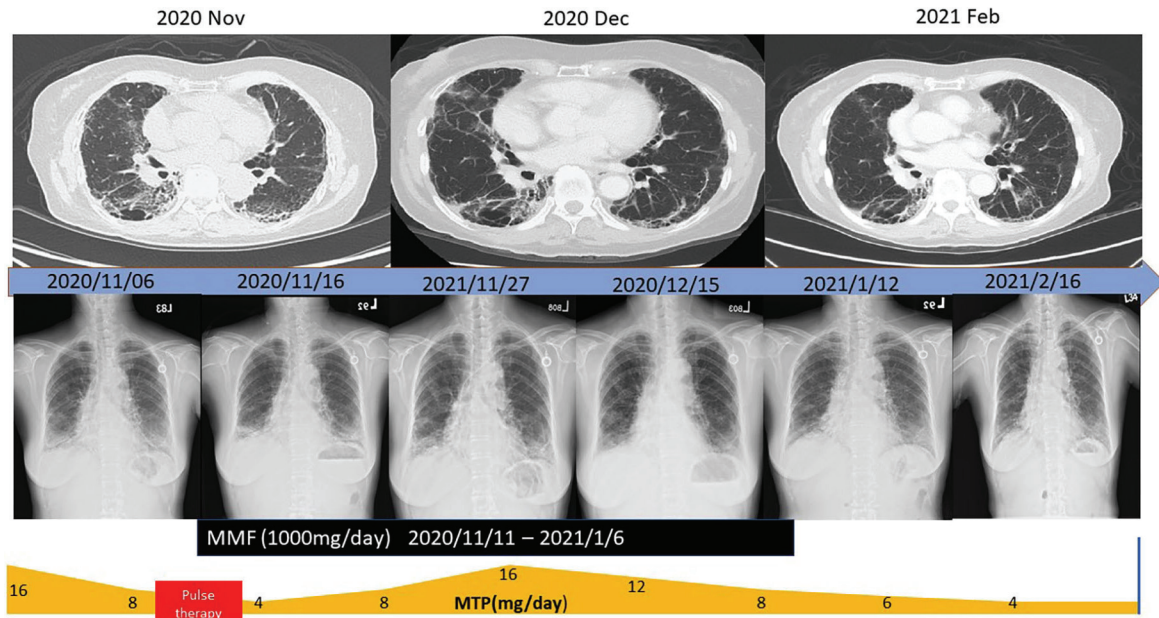
Fig. 3. Treatment course and representative clinical image after the deterioration of atezolizumab-induced pneumonitis.
Steroid pulse therapy (methylprednisolone 500 mg/day for 3 days) and mycophenolate mofetil (MMF) were administered to treat the pneumonitis deterioration. Chest CT revealed improvements in pneumonitis after pulse therapy and MMF. Chest radiographs were taken before pulse therapy, after pulse therapy, and after MMF therapy, respectively

then 8 mg/day).

However, because of an inadequate clinical response to steroid pulse therapy, we administered MMF (1000 mg/day) 2 days after pulse steroid therapy. After 2 weeks, the patient no longer required oxygen support, and a chest CT in December 2020 revealed improvements in the pneumonitis (Figure 3). In addition to the clinical and radiological improvements, a follow-up pulmonary function test in January 2021 revealed a slight improvement in the forced vital capacity (Table 1). Based on the stability of the clinical symptoms and on chest radiograph results, we stopped the MMF treatment in January 2021, retaining oral corticosteroid (methylprednisolone 4 mg/day). However, the patient developed tumor progression in May 2021.

Discussion

ICIs such as programmed death (PD) 1 and PD ligand 1 inhibitors have proved to be effective and have become the standard of care in the treatment of lung cancer [2]. Atezolizumab, a PD ligand 1 inhibitor, in combination with chemotherapy can prolong survival in patients with ES-SCLC. ICI-induced pneumonitis is reported to be one of the most common pulmonary-related irAEs, with an incidence of approximately 1%-5% [2]. The higher incidence of pneumonitis among patients with non–small-cell lung cancer receiving immunotherapy might be due to these patients being more prone to drug-related toxic effects on the lung. This would be exacerbated by a history of smoking, damaged underlying lung parenchyma, chronic obstructive pulmonary disease (COPD), and pulmonary fibrosis [2, 4-6]. An existing or large tumor burden in the lung and combination therapy may also be risk factors for ICI-induced pneumonitis

[2], and a prospective study revealed a poor performance status as another potential risk factor for this condition [7].

Radiologic diagnosis of ICI-induced pneumonitis is challenging because of the lack of typical imaging findings. ICI-induced pneumonitis may display a wide range of imaging features, rather than a specific pattern. Moreover, ICI-induced pneumonitis is a dynamic process, and evolves over time. The presence of underlying abnormalities, such as COPD or tumoral spread, may make the identification of ICI-induced pneumonitis-related features even more difficult [3, 8-10]. The main radiologic patterns of presentation are summarized in Table 2 [11]. The most frequent imaging pattern of ICI-induced pneumonitis is OP; other main patterns of ICI-induced pneumonitis are nonspecific interstitial pneumonia (NSIP), hypersensitivity pneumonitis, acute interstitial pneumonitis or diffuse alveolar damage, a"tree in bud" appearance, and isolated pulmonary nodules or mass-like lesions. Finally, imaging findings do not always meet the criteria of a specific pattern, such as with diffuse or patchy GGOs, which can be categorized as an unclassifiable pattern [11]. In the present case, ICI-induced pneumonitis was indicated by the presence of a subpleural reticular shadow with traction bronchiectasis and honeycombing predominantly in the lower lobes, which is comparable to a UIP pattern based on recently developed criteria [12], as reported in other cases [13-14]. In these case reports and in our case, the ICI-induced pneumonitis with UIP image patterns had similar clinical characteristics, and the pulmonary function test findings identified ICI-induced pneumonitis with other common patterns, such as OP or NSIP.

Progressive cancer lesions and infection are frequent complications that may develop in patients with lung cancer. Thus, a chest CT scan with contrast should be performed to eliminate differential diagnoses and provide evidence for ICI-induced pneumonitis. Moreover, bronchoscopy with bronchoalveolar lavage, with or

Table 2. Imaging Feature Findings of the Most Frequent Radiologic Patterns of Immune Checkpoint Inhibitors-Induced Pneumonitis

Radiologic Pattern	Imaging Features
OP	Patchy alveolar consolidations and/or GGOs
NSIP	Bilateral GGOS with reticulations
HP	Bilateral GGOs, centrilobular micronodules, and patchy hypo-attenuated lobules
AIP/DAD	Diffuse GGOs with alveolar consolidation in the dependent parenchyma
Bronchiolitis	Centrilobular micronodules with a tree-in-bud appearance and bronchial wall thickening
Pulmonary nodules or mass-like lesions	Solitary nodule or mass
Unclassifiable pattern	Abnormalities with no typical aspect/distribution or isolated features
Sarcoidosis-like	Symmetrical bilateral hilar and mediastinal enlargement, bilateral micronodules in a peri-lymphatic distribution

AIP/DAD, acute interstitial pneumonitis/diffuse alveolar damage; GGOs, ground-glass opacities; HP, hypersensitivity pneumonitis; ICI, immune checkpoint inhibitor; NSIP, nonspecific interstitial pneumonia; OP, organizing pneumonia. Reference: J Thorac Oncol 2021 Sep; 16(9): 1449-1460.

without biopsies, can help exclude the presence of infections or tumor progression and can provide evidence of immune-related pneumonitis; for example, a high percentage of lymphocytes may reveal the presence of lymphocytic alveolitis [10, 15]. The treatment for ICI-induced pneumonitis differs between symptomatic and asymptomatic patients. Several oncology-related associations have issued recommendations for the management of pulmonary irAEs (Table 3) [16]. For asymptomatic ICI-induced pneumonitis, ICI might be continued with careful

Table 3. Management of Pneumonitis in Patients Treated with Immune Checkpoint Inhibitors (ICI) According to the American Society of Clinical Oncology (ASCO) and European Society for Medical Oncology (ESMO)

	ESMO [18]	ASCO [19]
Grade 1		
ICI management	Consider delay of treatment	Hold ICI
Treatment of pneumonitis	No specific treatment	No specific treatment
Patient monitoring	Monitor symptoms every 2-3 days	Clinically monitor patients weekly, and 1 chest CT scan to be repeated in 3-4 weeks
Drug re-challenge	No specified recommendation	Yes, if radiographic evidence of improvement or resolution
Grade 2		
ICI management	Hold ICI	Hold ICI
Treatment of pneumonitis	Prednisone 1-2 mg/kg/day orally and taper over 6 weeks	Prednisone 1-2 mg/kg/day orally and taper over 4-6 weeks
Patient monitoring	Bronchoalveolar lavage: optional. Monitor symptoms daily, repeat chest radiography weekly, lung function tests including TLCO	Bronchoscopy with bronchial aspiration: optional Monitor every 3 days with history, physical examination and pulse oximetry, consider chest radiograph
Drug re-challenge	No specified recommendation	Yes, if resolution to grade ≤1
Grade 3/4		
ICI management	Discontinue ICI	Discontinue ICI
Treatment of pneumonitis	• Empirical antibiotics • (Methyl)prednisolone i.v. 2-4 mg/kg/day; taper corticosteroids ≥8 weeks. • If no improvement after 48 h, add infliximab 5 mg/kg or MMF	• Empirical antibiotics • (Methyl)prednisolone i.v. 1-2 mg/kg/day; taper corticosteroids over 4-6 weeks. • If no improvement after 48 h, may add infliximab 5 mg/kg or MMF 1 g twice a day or i.v. immunoglobulins for 5 days or cyclophosphamide
Patient monitoring	Bronchoalveolar lavage: optional. Hospitalization	Bronchoalveolar lavage: recommended. Hospitalization
Drug re-challenge	No specified recommendation	No

ICI, immune checkpoint inhibitors; CT, computed tomography; TLCO, transfer factor of the lung for carbon monoxide; i.v., intravenous; MMF, mycophenolate mofetil.

monitoring. If symptoms appear, ICI should be interrupted, and treatment with corticosteroids should be started in the absence of documented pulmonary infection. A higher dose of methylprednisolone (e.g., 1000 mg) can be considered for patients with acute respiratory failure. In clinical trials, 70%-100% of cases of ICI-induced pneumonitis have been resolved with appropriate treatment, with a time to resolution of 3-6 weeks [17]. In the absence of improvements within 2 days, the use of an immunosuppressive drug, such as infliximab, MMF, cyclophosphamide, or intravenous immunoglobulins, might be considered [18, 19]. In our case, grade III ICI-induced pneumonitis was resolved after corticosteroid therapy combined with an immunosuppressive agent (i.e., MMF).

Some studies have found that patients who experience irAEs may have a better treatment response [20, 21]. In general, rechallenge with ICI after irAEs and while recovering is feasible [20], but some fatalities have been reported [22]. Rechallenge with ICI therapies after the occurrence of ICI-related pneumonitis may be considered. The European Society for Medical Oncology (ESMO) [18] and the American Society of Clinical Oncology (ASCO) [19] both recommend that drug rechallenge can remain an option in patients with low-grade pneumonitis (Table 3).

Conclusion

We reported a rare case of ICI-induced pneumonitis presenting a UIP pattern. The clinical characteristics and pulmonary function test findings were similar to those of other cases of ICI-induced pneumonitis. Similar to other types of symptomatic ICI-induced pneumonitis, ICI-induced UIP is treated with systemic steroids. If a course of steroids does not reduce the severity of initial symptoms, additional immunosuppressants such as MMF should be considered without delay.

References

1. Wang M, Herbst RS, Boshoff C. Toward personalized treatment approaches for non-small-cell lung cancer. Nat Med 2021; 27(8): 1345-56.
2. Nishino M, Giobbie-Hurder A, Hatabu H, *et al*. Incidence of programmed cell death 1 inhibitor-related pneumonitis in patients with advanced cancer: a systematic review and meta-analysis. JAMA Oncol 2016; 2(12): 1607-16.
3. Nishino M, Ramaiya NH, Awad MM, *et al*. PD-1 inhibitor-related pneumonitis in advanced cancer patients: radiographic patterns and clinical course. Clin Cancer Res 2016; 22(24): 6051-60.
4. Toh CK, Wong EH, Lim WT, *et al*. The impact of smoking status on the behavior and survival outcome of patients with advanced non-small cell lung cancer: a retrospective analysis. Chest 2004; 126(6): 1750-6.
5. Bouros D, Hatzakis K, Labrakis H, *et al*. Association of malignancy with diseases causing interstitial pulmonary changes. Chest 2002; 121(4): 1278-89.
6. Coussens LM, Werb Z. Inflammation and cancer. Nature 2002; 420(6917): 860-7.
7. Okada N, Matsuoka R, Sakurada T, *et al*. Risk factors of immune checkpoint inhibitor-related interstitial lung disease in patients with lung cancer: a single-institution retrospective study. Sci Rep 2020; 10(1): 13773.
8. Dromain C, Beigelman C, Pozzessere C, *et al*. Imaging of tumour response to immunotherapy. Eur Radiol Exp 2020; 4(1): 2.
9. Naidoo J, Wang X, Woo KM, *et al*. Pneumonitis in patients treated with anti-programmed death-1/programmed death ligand 1 therapy. J Clin Oncol 2017; 35(7): 709-17.
10. Delaunay M, Cadranel J, Lusque A, *et al*. Immune-checkpoint inhibitors associated with interstitial lung disease in cancer patients. Eur Respir J 2017; 50(2).
11. Pozzessere C, Lazor R, Jumeau R, *et al*. Imaging features of pulmonary immune-related adverse events. J Thorac Oncol 2021; 16(9): 1449-60.

12. Raghu G, Remy-Jardin M, Myers JL, *et al*. Diagnosis of idiopathic pulmonary fibrosis. An official ATS/ERS/JRS/ALAT clinical practice guideline. Am J Respir Crit Care Med 2018; 198(5): e44-e68.

13. Abbas W, Rao RR, Gupta VG, *et al*. Immunotherapy-induced interstitial lung disease: Cases report. South Asian J Cancer 2019; 8(2): 79.

14. Yamakawa H, Oba T, Ohta H, *et al*. Nintedanib allows retreatment with atezolizumab of combined non-small cell lung cancer/idiopathic pulmonary fibrosis after atezolizumab-induced pneumonitis: a case report. BMC Pulm Med 2019; 19(1): 156.

15. Barjaktarevic IZ, Qadir N, Suri A, *et al*. Organizing pneumonia as a side effect of ipilimumab treatment of melanoma. Chest 2013; 143(3): 858-61.

16. Cadranel J, Canellas A, Matton L, *et al*. Pulmonary complications of immune checkpoint inhibitors in patients with nonsmall cell lung cancer. Eur Respir Rev 2019; 28(153).

17. Borghaei H, Paz-Ares L, Horn L, *et al*. Nivolumab versus docetaxel in advanced nonsquamous non-small-cell lung cancer. N Engl J Med 2015; 373(17): 1627-39.

18. Haanen J, Carbonnel F, Robert C, *et al*. Management of toxicities from immunotherapy: ESMO Clinical Practice Guidelines for diagnosis, treatment and follow-up. Ann Oncol 2018; 29(Suppl 4): iv264-iv266.

19. Brahmer JR, Lachetti C, Schneider BJ, *et al*. Management of immune-related adverse events in patients treated with immune checkpoint inhibitor therapy: American Society of Clinical Oncology clinical practice guideline. J Clin Oncol 2018; 36(17): 1714-68.

20. Fujii T, Colen RR, Bilen MA, *et al*. Incidence of immune-related adverse events and its association with treatment outcomes: the MD Anderson Cancer Center experience. Invest New Drugs 2018; 36(4): 638-46.

21. Attia P, Phan GQ, Maker AV, *et al*. Autoimmunity correlates with tumor regression in patients with metastatic melanoma treated with anti-cytotoxic T-lymphocyte antigen-4. J Clin Oncol 2005; 23(25): 6043-53.

22. Pollack MH, Betof A, Dearden H, *et al*. Safety of resuming anti-PD-1 in patients with immune-related adverse events (irAEs) during combined anti-CTLA-4 and anti-PD1 in metastatic melanoma. Ann Oncol 2018; 29(1): 250-255.

Recurrent Solitary Fibrous Tumor of the Pleura after Surgical Resection in a 62-year-old Male

Yang-Han Lin[1], Jiunn-Min Shieh[1]

Solitary fibrous tumor (SFT) is a rare neoplasm derived from mesenchymal tissue. The pleura is the most common site of SFT, and the diagnosis is based on the pathologic study of a tissue specimen. The standard management of SFT is surgical excision, although the risk of local recurrence and metastasis after surgery has been frequently noted. We reported a male patient who was a heavy smoker and had chronic cough symptoms for 20 years. Right lower lung tumor was incidentally found during a hospital visit. The biopsy result confirmed the diagnosis of SFT, and the patient underwent tumor excision. Two episodes of local recurrence of SFT were noted, 1 at 6 years and 1 at 9 years, respectively, after the first surgery. Surgical tumor resection was performed at each recurrent episode. *(Thorac Med 2023; 38: 217-221)*

Key words: solitary fibrous tumor, surgical resection, local recurrence

Introduction

Solitary fibrous tumor (SFT) is a rare neoplasm derived from mesenchymal tissue. According to a review article from the United States, SFT accounts for only about 2% of soft tissue tumors [1]. The possible sites of SFT include the thoracic cavity, peritoneal cavity, central nervous system, and deep soft tissue [1]. The pleura is the most common site of SFT, but the frequency (2.8 per 100,000 individuals) is still lower than that of other pleural tumors [2]. Pleural SFT can cause pulmonary symptoms such as cough, shortness of breath, and chest pain. Paraneoplastic syndrome is also found in patients with SFT. But most patients are asymptomatic, and the tumors are incidentally found by chest radiography during hospital visits [2, 3]. Surgical resection is the standard management of localized SFT. Most SFT are stable after complete resection, with a 5-year survival rate up to 84%, but there is still a risk of recurrent disease [4]. Those cases may need repeated surgery or adjuvant radiation therapy. We report the case of a male patient with an intra-thoracic SFT with recurrence, even after complete tumor resection.

[1]Division of Chest Medicine, Department of Internal Medicine, Chi Mei Medical Center, Tainan, Taiwan
Address reprint requests to: Dr. Jiunn-Min Shieh, Division of Chest Medicine, Department of Internal Medicine, Chi Mei Medical Center, Tainan, Taiwan; No.901 Zhonghua Road, Yong-Kang District, Tainan City 71004, Taiwan (R.O.C.)
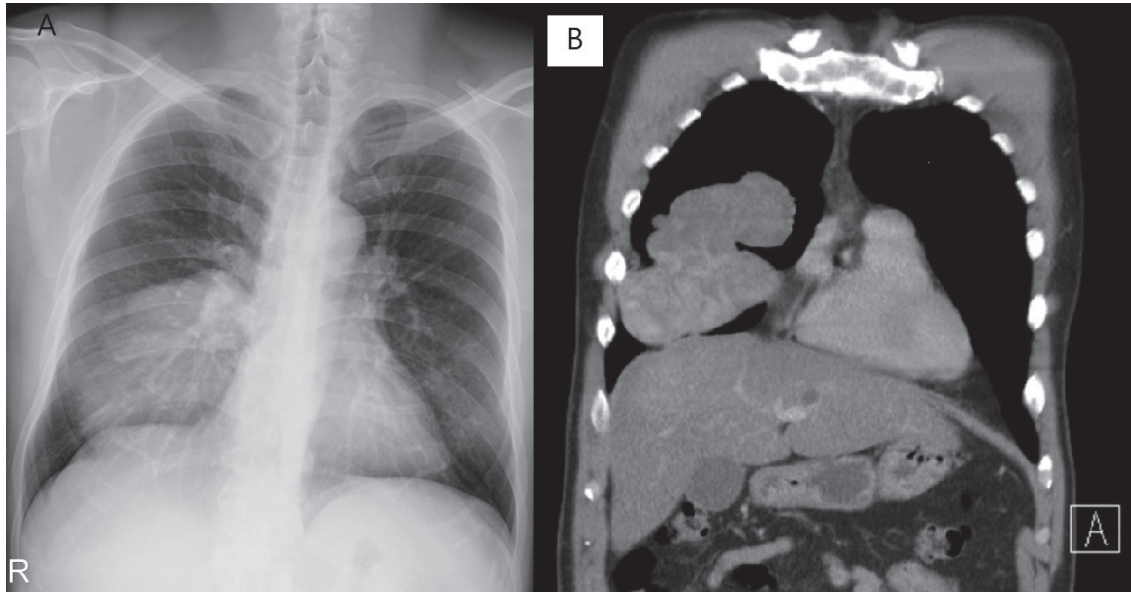
Fig. 1. (A) Initial chest radiography showed right lower lung field consolidation. (B) A chest computed tomography coronal view revealed a huge lobulated mass with right middle lobe and right chest wall involvement.

Case Report

This 62-year-old male had a smoking history of about 1 pack per day for 25 years. He presented with chronic cough with scanty sputum for 20 years. Right middle lung field consolidation was incidentally found by chest radiography during a health examination (Figure 1A). A chest computed tomography (CT) scan revealed a lobulated mass lesion about 12.2 x 5.6 x 11.5 cm in the right lower lung region, with involvement of the right middle lobe and right chest wall (Figure 1B). CT-guided biopsy was arranged for tissue diagnosis. In the histopathologic report of the biopsy, immunohistochemical staining revealed the tumor cells were positive for CD34, CD99, and BCL-2; therefore, SFT was suspected. A huge lobulated tumor with an irregular surface and hypervascularity was found in the right anterior lateral chest wall during the thoracotomy. The tumor also involved the right 5th and 6th ribs and partial

Fig. 2. Surgical resection of the right chest wall tumor. The specimen showed an irregular and hypervascular surface.

right middle lobe. Resection of the chest wall tumor and wedge resection of the right middle lobe were performed (Figure 2).

No evidence of recurrence was noted until 6 years later. Right lower lung region nodular opacity was found by plain film radiography of the chest (Figure 3A). A chest CT scan revealed a tumor lesion at the right anterior lower lung region (6.6 x 1.6 x 5.6 cm) (Figure 3B). Under the impression of a recurrent SFT, the patient
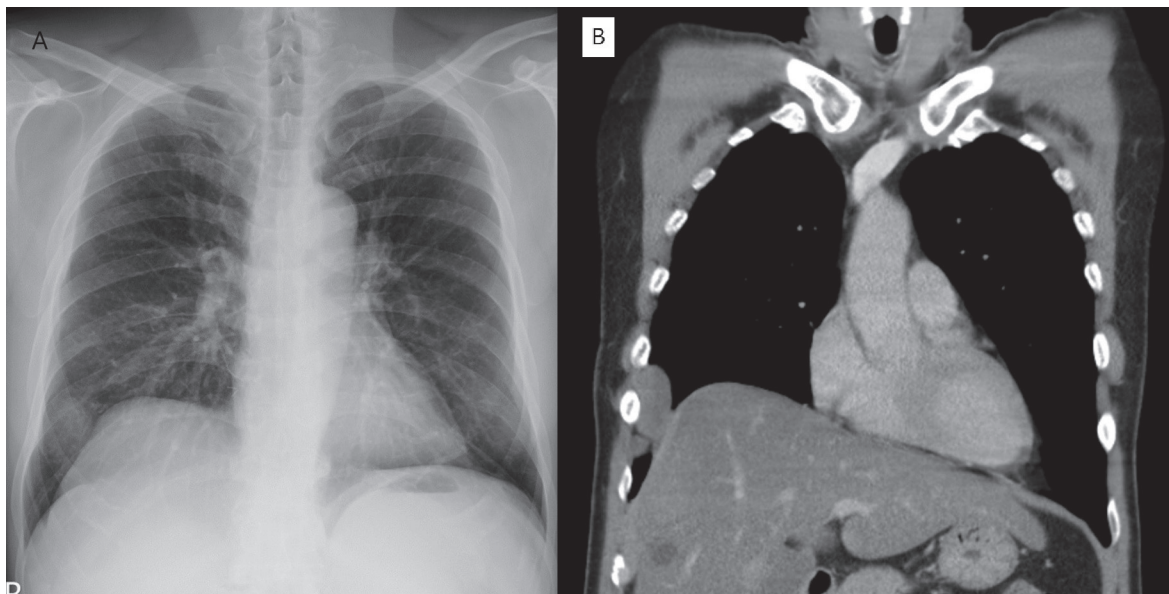
Fig. 3. (A) Six years after surgical resection, chest radiography revealed a nodular opacity at the right lower lung field. (B) A chest computed tomography coronal view showed a tumor lesion at the right anterior lower lung region. Recurrent solitary fibrous tumor of the pleura was suspected.

underwent video-assisted thoracic surgery. A 6 x 6 cm lobulated tumor with chest wall invasion was found at the right pleural base, and tumor-wide excision was performed. The pathologic report revealed positive immunostaining for CD34 and STAT6, which confirmed the diagnosis of recurrent SFT (Figure 4). However, a second local recurrence was noted 3 years later. Chest CT scan once again showed a right chest wall tumor, and he was referred to the surgeon for a third surgical intervention (Figure 5). Right lower chest wall tumor with central necrosis was found intraoperatively. The patient underwent tumor resection and reconstruction of the chest wall. Locally recurrent SFT was confirmed again by pathologic study (Figure 6).

Fig. 4. (A) Hematoxylin and eosin stain of the tumor (40X). (B) Hematoxylin and eosin stain of the tumor (400X) showed pleomorphic cells mixed with collagen in a haphazard arrangement. (C) Tumor cells showed positive immunostaining for CD34. (D) Tumor cells showed positive immunostaining for STAT6.

Discussion

SFT of the pleura seldom cause clinical symptoms, and asymptomatic tumors are de-tected by routine radiograph. Once the tumor lesion is suspected by chest X-ray, CT can pro-vide a clear image of its size and localization.
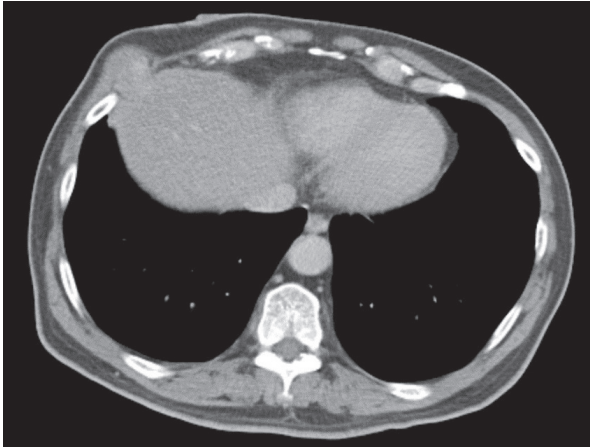
Fig. 5. Three years after the second surgery, a chest computed tomography axial view found a right chest wall tumor adjacent to the previous surgical site.
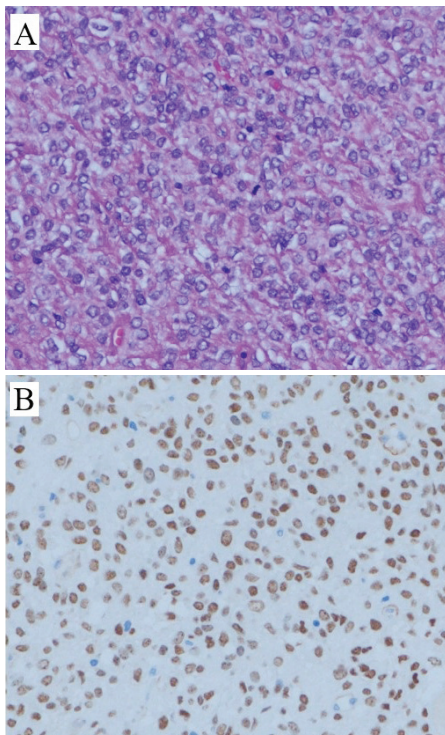

Fig. 6. (A) Hematoxylin and eosin stain of tumor cells (400X) showed a patternless arrangement and some mitotic cells. (B) Tumor cells were positive for immunostaining of STAT6.

SFT presents as a homogeneous, well-defined, lobular mass that adheres to the pleura. As a large tumor, it may compress adjacent structures and cause atelectasis or displacement of bronchi and vessels [5]. Diagnosis of SFT requires biopsy to identify typical morphologic and immunostaining features. Morphologic features may include variably pleomorphic spindle cells with collagen and a patternless arrangement. In our case, immunostaining showed positive for CD99, CD34, and BCL-2. Nuclear staining of STAT6 has high specificity in SFT. STAT6 staining can be used to differentiate SFT from other soft tissue tumors [1, 4, 6].

Surgical resection is a standard treatment and is widely applied with SFT of the pleura. The 5-year local recurrence rate and metastatic rate after surgical resection were 29% and 34%, respectively, in a multicenter study [4]. Features such as older age ($\geq$ 55 years), hypercellularity, increased mitosis (mitotic figures $\geq$ 4/10 high-power fields), presence of tumor necrosis, and tumor size greater than 10 cm were correlated with a higher recurrence rate. Of the above risk factors, tumor size greater than 10 cm has the highest hazard ratio of recurrence [6-8].

Our patient experienced 2 episodes of local recurrence in 9 years of follow-up. The pathology report of the first surgery showed the number of mitotic figures was 2/10 high-power fields, and no hypercellularity or tumor necrosis was observed. We suggested that the large tumor size may account for the local recurrence. Even if surgical resection is considered at first, there are still some patients who are inoperable or without clear surgical margins. Medical treatment can be used as first-line or adjuvant therapy in those patients.

Pazopanib is an inhibitor of vascular endothelial growth factor receptors. In a phase II trial, pazopanib was prescribed for patients with unresectable and metastatic SFT; 58% (18 of 31) of the patients had a partial response.

Median progression-free survival and median overall survival were 9.8 months and 49.8 months, respectively. These results showed the therapeutic effect of pazopanib on advanced SFT [9]. Chemotherapy can be considered in locally advanced SFT, but the results are less effective. A retrospective study reviewed the response to conventional chemotherapy in 21 cases of unresectable SFT. Doxorubicin-based or gemcitabine-based regimens were prescribed in most cases. No complete or partial response was reported in this study [10]. Radiation therapy may play a role in the management of SFT. Favorable results with local control were reported in single management of metastatic tumors, or adjuvant therapy in cases with unsafe surgical margins [11, 12]. However, the clinical evidence for chemotherapy and radiation therapy in SFT of the pleura is still controversial due to limited case numbers in clinical studies.

Conclusion

SFT of the pleura is usually asymptomatic. Complete surgical resection with an adequate excision margin is the preferred management. Histopathologic features can estimate risk of recurrence and metastasis after surgery. There is no definite role for medical treatment, such as radiation therapy, chemotherapy, or targeted therapy. But for those patients who are not able to undergo surgery, medical treatment may be another option for disease control.

References

1. Davanzo B, Emerson RE, Lisy M, *et al*. Solitary fibrous tumor. Transl Gastroenterol Hepatol 2018 Nov 21; 3: 94.
2. Chick JF, Chauhan NR, Madan R. Solitary fibrous tumors of the thorax: nomenclature, epidemiology, radiologic and pathologic findings, differential diagnoses, and management. AJR Am J Roentgenol 2013; 200(3): W238-48.
3. Lu C, Ji Y, Shan F, *et al*. Solitary fibrous tumor of the pleura: an analysis of 13 cases. World J Surg 2008; 32(8): 1663-8.
4. van Houdt WJ, Westerveld CMA, Vrijenhoek JEP, *et al*. Prognosis of solitary fibrous tumors: a multicenter study. Ann Surg Oncol 2013; 20(13): 4090-5.
5. Luciano C, Francesco A, Giovanni V, et al. CT signs, patterns and differential diagnosis of solitary fibrous tumors of the pleura. J Thorac Dis 2010; 2(1): 21-5.
6. Demicco EG, Park MS, Araujo DM, *et al*. Solitary fibrous tumor: a clinicopathological study of 110 cases and proposed risk assessment model. Mod Pathol 2012; 25(9): 1298-306.
7. Gold JS, Antonescu CR, Hajdu C, *et al*. Clinicopathologic correlates of solitary fibrous tumors. Cancer 2002; 94(4): 1057-68.
8. Tapias LF, Mino-Kenudson M, Lee H, *et al*. Risk factor analysis for the recurrence of resected solitary fibrous tumours of the pleura: a 33-year experience and proposal for a scoring system. Eur J Cardiothorac Surg 2013; 44(1): 111-7.
9. Martin-Broto J, Cruz J, Penel N, *et al*. Pazopanib for treatment of typical solitary fibrous tumours: a multicentre, single-arm, phase 2 trial. Lancet Oncol 2020; 21(3): 456-66.
10. Park MS, Ravi V, Conley A, *et al*. The role of chemotherapy in advanced solitary fibrous tumors: a retrospective analysis. Clin Sarcoma Res 2013; 3(1): 7.
11. Haas RL, Walraven I, Lecointe-Artzner E, *et al*. Radiation therapy as sole management for solitary fibrous tumors (SFT): a retrospective study from the Global SFT Initiative in collaboration with the Sarcoma Patients EuroNet. Int J Radiat Oncol Biol Phys 2018; 101(5): 1226-33.
12. Bishop AJ, Zagars GK, Demicco EG, *et al*. Soft tissue solitary fibrous tumor: combined surgery and radiation therapy results in excellent local control. Am J Clin Oncol 2018; 41(1): 81-85.

Late-Onset Rrespiratory Failure in Organophosphate poisoning

Wei-Hung Chang[1], Chi-Feng Huang[1]

Organophosphate poisoning is not uncommon in Taiwan. We encountered a patient with organophosphate poisoning who initially showed non-specific symptoms, a late-onset intermediate syndrome presenting with abrupt respiratory failure following acute cholinergic crisis, and improvement in the condition after appropriate treatment with pralidoxime and atropine. Based on toxic studies present in the literature, organophosphate poisoning has a high mortality rate if the treatment is inappropriate or underestimated. *(Thorac Med 2023; 38: 222-227)*

Key words: organophosphate poisoning (OP), intermediate syndrome (IMS), late-onset respiratory failure

Introduction

Organophosphate (OP) pesticides are widely used in agriculture. OP poisoning is not uncommon in suicidal patients in Taiwan, because these pesticides are readily available in the marketplace. A patient can be recognized as having possible OP poisoning by typical cholinergic signs, including increased secretions (bronchorrhea, salivation, tearing, or sweating), bradycardia, vomiting, and increased gastrointestinal motility (diarrhea or cramping), miosis, muscle fasciculation, and even coma resulting from severe exposure. Herein, we report a case of OP poisoning, with the intent that clinicians will become more aware of this potentially fatal condition. [1].

Case Report

A 47-year-old man who was an outdoor worker ingested pesticide (fenitrothion) 1 h after arguing with his family and was immediately brought to the emergency department (ED). Diaphoresis and muscle weakness were observed by the ED physicians. OP poisoning could not be ruled out because the patient reported pesticide ingestion at unknown amounts.

---

[1]Department of Internal Medicine, MacKay Memorial Hospital, Taperi City, Taiwan
Address reprint requests to: Dr. Chi-Feng Huang, Division of Chest Medicine, Department of Internal Medicine, Chi Mei Medical Center, Tainan, Taiwan; No.901 Zhonghua Road, Yong-Kang District, Tainan City 71004, Taiwan (R.O.C.)

Atropine 1 mg and pralidoxime 500 mg were quickly administered. All of the patient's clothes were removed. Intubation was not performed because of an absence of shortness of breath and mucus secretion. The patient showed us the empty bottle of fenitrothion that he had ingested. For the patient's safety, after primary management in the ED, he was transferred to the intensive care unit (ICU) for further management.

Initial levels of serum acetylcholinesterase were 1284 U/L (normal range: 4500-13320 U/L). Other laboratory test results showed no abnormality, no leukocytosis, and no electrolyte imbalance. In the ICU, the continuous infusion doses of pralidoxime were titrated because the patient had no symptom of acute cholinergic crisis. On the 3rd day of hospitalization, the patient's condition stabilized, and he was transferred to the original ward. On the evening of the 3rd day, sudden-onset symptoms of action tremors and pharyngeal weakness, pooling of secretions, and weakness of proximal limb muscles were observed. Intubation was performed, and he was transferred back to the ICU. This time, CXR revealed right lower lobe infiltration and increased leukocytosis, but no left shift. We then administered levofloxacin for suspected aspiration pneumonia.

Post-intubation, the patient showed no signs of systemic inflammatory response syndrome or hypothermia; however, persistent increases in secretion and diarrhea were observed. Owing to suspected OP intoxication Type II (intermediate syndrome), we administered atropine bolus injections frequently, based on his symptoms. The dose of atropine was decreased based on his symptoms of secretion and diarrhea. Ventilator support was continued until the 16th day of hospitalization, and weaning was successful

this time. Atropine infusion was discontinued on the 19th day of hospitalization, due to his stable condition. The patient was transferred to an ordinary ward on the 20th day of hospitalization, and discharged the next day.

Discussion

Neuromuscular weakness resulting from OP poisoning is divided into 3 types: (a) type I paralysis-muscle weakness occurring within the first day of admission associated with cholinergic signs; (b) type II paralysis or intermediate syndrome (IMS)-delayed muscle weakness occurring after the acute cholinergic phase of OP poisoning; (c) type III paralysis-polyneuropathy occurring 2-3 weeks after OP poisoning.

Type I symptoms include SLUDGE/BBB (salivation, lacrimation, urination, defecation, diaphoresis, gastric emesis, bronchorrhea, bronchospasm, and bradycardia). The ECG might show heart block, there might be QTc prolongation, and most patients were incubated, due to the symptom(s) presented. Type 2 (IMS) occurs between 24 and 96 h after resolution of the acute cholinergic crisis, and might present in 10-40% of patients. The symptom persists for 14-20 days (with adequate supportive care, such as ventilator support), and recovery usually occurs without sequelae. Few patients had Type 3 poisoning (OP-induced delayed polyneuropathy [OPIDP]), flaccid weakness of the lower extremities, and a high-stepping gait associated with bilateral foot drop. Recovery usually occurs within 6-12 months.

OP poisoning is diagnosed according to the history of ingestion of the poison, the characteristic clinical features, clinical improvement after atropine/oxime administration, and inhibition of cholinesterase activity. We measure cholinester-

ase for patient outcome clinically, and RBC/true cholinesterase is more accurately measured than serum/pseudocholinesterase. A 50% reduction in normal values of RBC cholinesterase diagnosed by persistent low levels is a predictor of IMS OP poisoning, and is useful in monitoring the clinical course of the illness. Persistent low levels are a predictor of IMS; levels 20% lower than the normal range may predict the onset of IMS [2]. If RBC cholinesterase is not available in the hospital, we may try an electro-neuro-myogram; 30-Hz rapid nerve stimulation-decremental responses correlate best with clinical weakness [3]. The most useful diagnostic test is the IMS. Other prognostic value tests include hyperglycemia (transient hyperglycemia and glycosuria are often seen in acute OP poisoning) [4]. The patient may show neutrophilic leukocytosis. ECG changes (QTc prolongation) indicate a poor prognosis in OP poisoning [5]. Metabolic acidosis develops in patients with OP poisoning, more commonly with hypotension [6]. Raised amylase levels correlate with severity and the presence of shock in acute OP poisoning [7].

The following are the steps to manage OP poisoning, according to previous literature. First, assess and record the 15-point Glasgow Coma Scale. Then, follow up with the pulse rate, blood pressure, and auscultation. If hypoxia is observed, intubation should be performed. Administer atropine to reduce bronchorrhea [8]. If we are not sure of the poisoning, we can try the atropine test (inject 0.6-1 mg atropine intravenously (IV): if pulse rate goes up by 25 per min or skin flushing develops, mild or no toxicity for OP exists). We should also decontaminate patients, remove all clothing, and wash with soap and water (ocular decontamination should be performed with water only). Gastro-

intestinal decontamination decreases absorption by 42% at 20 min and 16% at 60 min [9]. This should be considered only if the patient is incubated or conscious, and willing to cooperate. It is not beneficial otherwise, and rather increases chances of aspiration pneumonia and death. Induced emesis is contraindicated [10].

There is no evidence that suggests that patients with pesticide poisoning benefit from activated charcoal. We can use atropine subsequently to target endpoints of atropinization (clear chest, SBP >80 mmHg, heart rate >80/min, dry axillae, pupils no longer pinpoint, bowel sounds [[just-only??]] present), to reverse cholinergic features, and to improve cardiac and respiratory functions. According to the Journal of Medical Toxicology (2012), atropine infusion greatly reduced mortality compared to standard treatment with boluses of atropine (22.2% vs. 8%). The following steps should be taken: administer 1.8-3.0 mg of atropine IV and repeat the dose of atropine every 5 min, doubling the dose each time till atropinization occurs. Subsequently, administer 10-20% of the dose of atropine required for atropinization every hour by IV infusion, and a pralidoxime 1-2 g IV (30 mg/kg) bolus followed by an 8 mg/kg/h infusion. If atropine toxicity occurs (absent bowel sounds + fever + confusion), discontinue infusion for 60 min, then re-start infusion at 80% once the patient's?? temperature lowers and the patient calms down. Most patients do not need >3-5 mg/h of atropine infusion. The dose of atropine can be reduced by 20% every 4 h once the patient is stable. Pralidoxime will not be effective in very severe (large dose) cases of poisoning. Treatment with oximes should be initiated as early as possible; however, the treatment will not play a role if started after 48 h. The therapeutic end point is when reactivation

and increments in SChE levels occur; infusion continues until the patient is symptom free or until extubation [11].

Other medications such as benzodiazepines have caused sedation in well-ventilated patients, leading to control of seizures. Diazepam reduces neural damage and prevents respiratory failure (animal studies). Administering MgSO4 (4 g) IV on the first day after admission decreases the hospitalization period and mortality. It blocks calcium channels and reduces acetylcholine release from the presynapses, and also reduces CNS overstimulation via NMDA receptor activation. Clonidine inhibits the presynap-
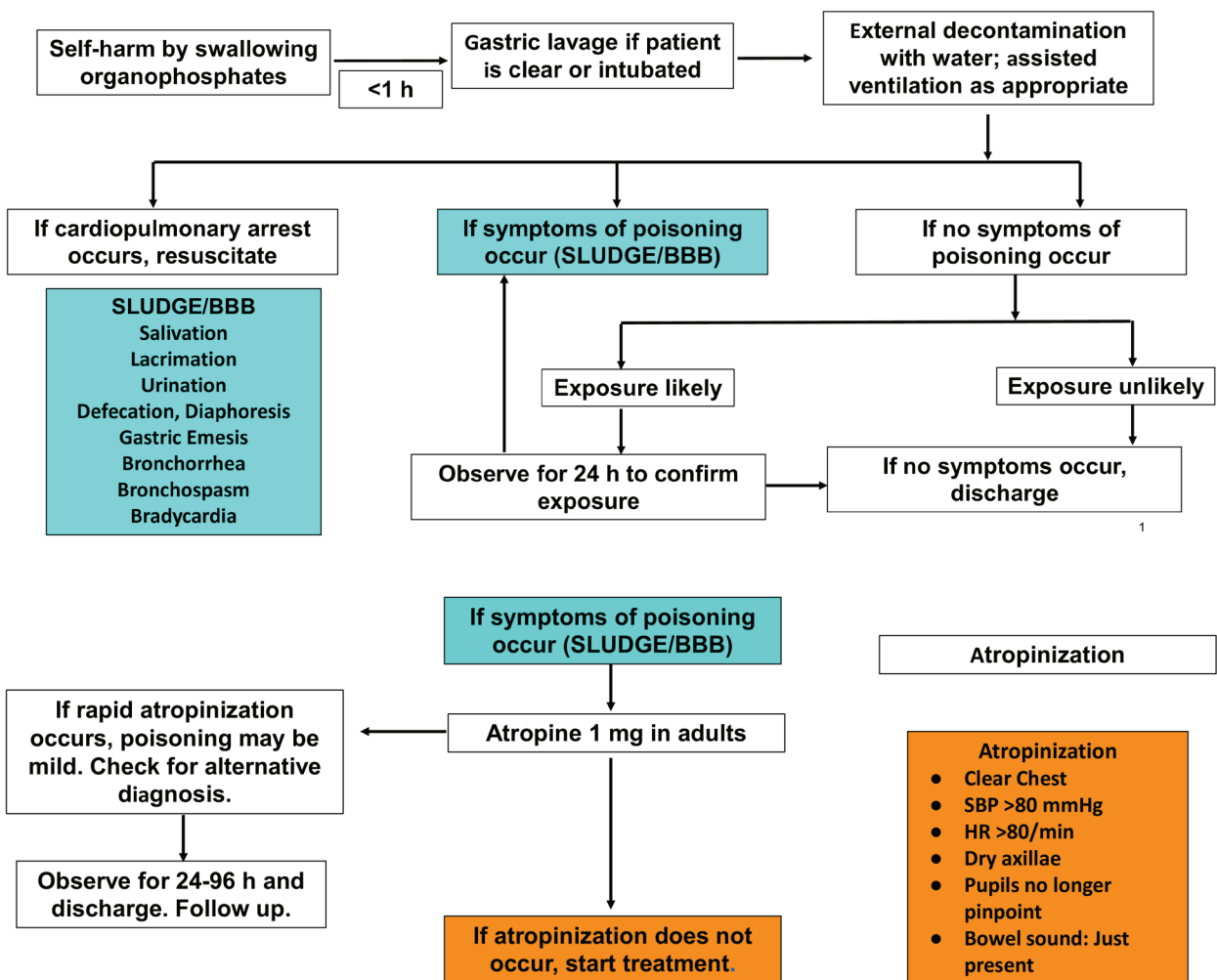
Fig. 1. Legend: Follow the treatment protocol as soon as possible to address the high mortality rate occurring due to inappropriate or underestimated treatment. Abbreviation: heart rate (HR), systolic blood pressure (SBP), intermediate syndrome (IMS)

If atropinization does not occur, start treatment.

Administer 1.8-3.0 mg of atropine through IV and repeat the dose of atropine every 5 min by doubling the dose each time till atropinization occurs. Subsequently, administer 10-20% of the dose of atropine required for atropinization every hour by IV infusion, with pralidoxime 1-2 g IV (30 mg/kg) bolus followed by 8 mg/kg/h infusion.

Check cholinesterase level, 50% reduction in normal values: diagnostic

Early enteral feeding Alkalinization MgSO$_4$ (4 g) IV on first day Benzodiazepines

If IMS totally symptomatic, ventilator support required if respiratory muscle paralysis occurs

Continue atropine + pralidoxime until symptoms improve and cholinesterase activity recovers

Atropine toxicity = Absent bowel sounds + fever + confusion. Stop infusion for 60 min if toxicity is noted Re-start infusion at 80%, once the temperature is reduced and the patient calms down.

Observe for 12-24 h without atropine for late signs of toxicity.

Once the patient is stable, reduce the atropine dose by 20% every 4 h.

Fig. 1. Legend: Follow the treatment protocol as soon as possible to address the high mortality rate occurring due to inappropriate or underestimated treatment. Abbreviation: heart rate (HR), systolic blood pressure (SBP), intermediate syndrome (IMS)
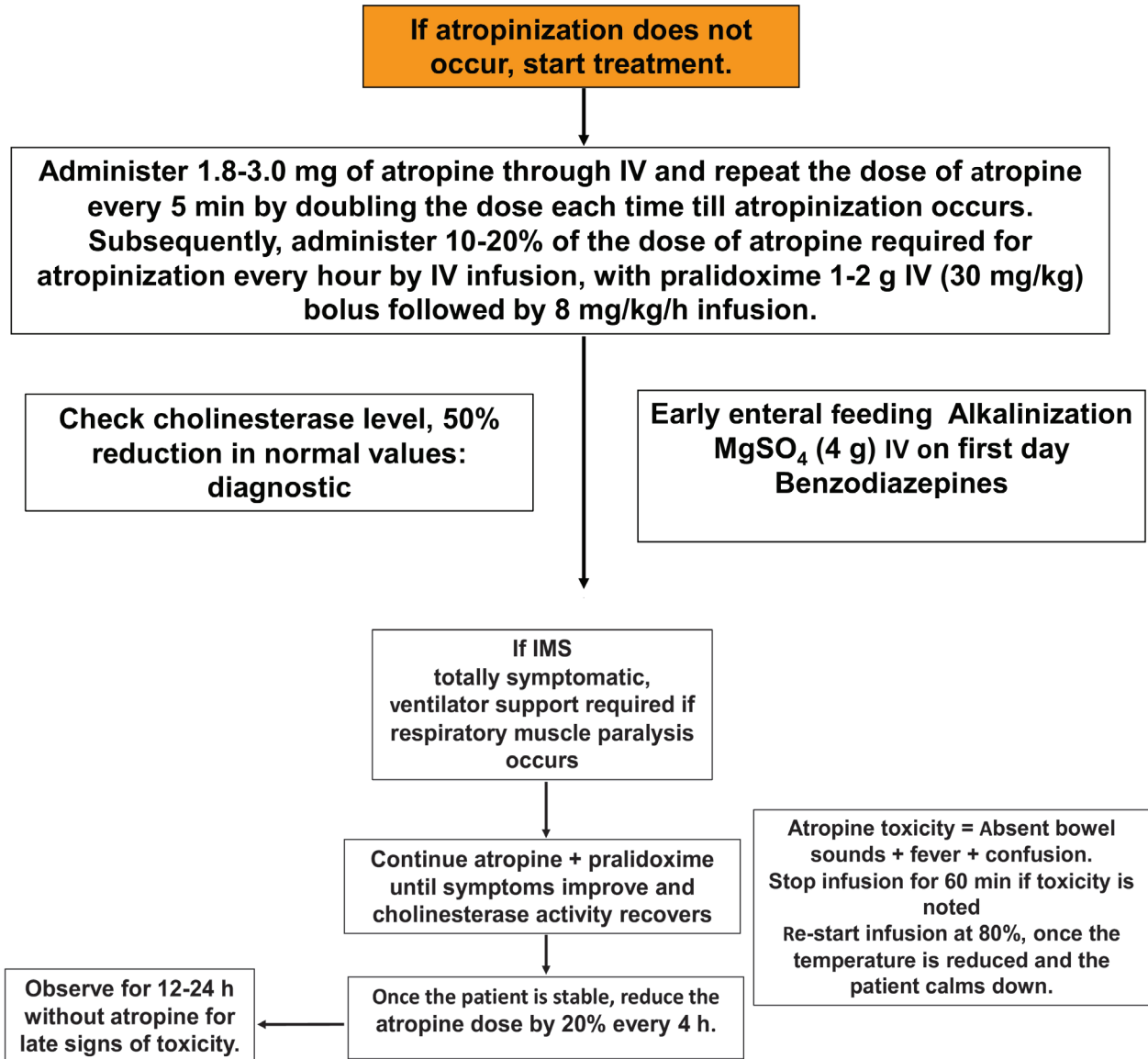
tic release of acetylcholine, which decreases the cholinergic neurons, and has synergistic interaction with atropine. Animal studies have shown a benefit in combining clonidine with atropine; however, the effect on humans is unknown. If the patient has IMS, he or she is totally symptomatic. Ventilator support is required if respiratory muscle paralysis occurs. Hypothermia may also be a sign of OP poisoning [12].

Treatments such as early enteral feeds are associated with improved outcomes in critically ill patients, because they prevent enterohepatic circulation [13]. Butyrylcholinesterase present in fresh frozen plasma (FFP) sequesters free poison in the blood and removes it from circulation (current evidence is not strong enough to reach a clear conclusion regarding the bioscavenger role of FFP). Finally, we can use standard therapy plus corticosteroids for OPIDP.

We have summarized the past year's goals of treatment in Figure 1. We sincerely suggest following the treatment protocol as soon as possible to address the high mortality rate occurring due to inappropriate or underestimated treatment.

Conclusion

Although the patient had no symptoms of acute cholinergic crisis, he should be routinely followed up with RBC cholinesterase tests to diagnose and monitor the clinical course of the illness to be aware of IMS. If the level of RBC cholinesterase is low, atropine plus pralidoxime administration should be discontinued until symptomatic improvement and recovery of cholinesterase activity occurs.

References

1. Huang YT, Lai PC, Su CY, *et al*. Intermediate syndrome after organophosphate ingestion. Tzu Chi Med J 2007; 19: 159-63.
2. Tajune J, Robert J. Organophosphoric poisoning. Ann Emerg Med 1987; 16: 193.
3. Senanayake N, Karalliedde L. Neurotoxic effects of OP insecticides: an intermediate syndrome. NEJM 1987; 316: 761-63.
4. Namba T, Nolte CT, Jackrel J, *et al*. Poisoning due to organophosphate insecticides. Acute and chronic manifestations. Am J Med 1971; 50: 475-92.
5. Shadnia S, Okazi A, Akhlaghi N, *et al*. Prognostic value of long QTc interval in acute and severe OP poisoning. J Med Toxicol 2009; 5(4).
6. Prakash O. Low pH predicts mortality in OPP and carbamates. JAPI 2002; 50: 857.
7. Lin CL, Yang CT, Pan KY, *et al*. Most common intoxication in nephrology ward organophosphate poisoning. Ren Fail 2004; 26: 349-54.
8. Erdman AR. Insecticides. In: Dart RC, Caravati EM, McGuigan MA, *et al*, eds. Medical Toxicology, 3rd edn. Philadelphia: Lippincott Williams & Wilkins, 2004: 1475-96.
9. Eddleston M, Haggalla S, Reginald K, *et al*. The hazards of gastric lavage for intentional self-poisoning in a resource poor location. Clin Toxicol 2007; 45: 136-43.
10. Eddleston M, Juszczak E, Buckley NA, *et al*. Randomised controlled trial of routine single or multiple dose superactivated charcoal in a region with high mortality. Clin Toxicol 2005; 43: 442-43.
11. J Med Toxicol. (2012) 8:108-117 DOI 10.1mms131s1-012-0214-6
12. Moffatt A, Mohammed F, Eddleston M, *et al*. Hypothermia and fever after organophosphorus poisoning in humans—a prospective case series. J Med Toxicol 2010; 6: 379-85.
13. Eddleston M, Haggalla S, Reginald K, *et al*. The hazards of gastric lavage for intentional self-poisoning in a resource poor location. Clin Toxicol 2007; 45(2): 136-43.

Foreign Body Inhalation-Related Pulmonary Actinomycosis Diagnosed by Transbronchial Lung Biopsy: A Case Report

Wen-Jui Chang[1,2], Chen-Yiu Hung[1,2], Shu-Min Lin[1,2]

Pulmonary actinomycosis is a rare disease related to aspiration of oral secretion or other objects such as a foreign body. The diagnosis of this disease is very difficult to confirm. We reported a 67-year-old Taiwanese man with pulmonary actinomycosis diagnosed by the pathology study of transbronchial lung biopsy specimens. Foreign body inhalation, which was later revealed to be animal bone-related, was determined during the examination. Although he had been under inadequate antibiotic treatment, the patient developed no deterioration of symptoms and chest radiography, which could be related to known variations in the treatment duration for pulmonary actinomycosis from case to case, or the fact that the infection focus had already been removed. *(Thorac Med 2023; 38: 228-235)*

Key words: pulmonary actinomycosis, foreign body, transbronchial lung biopsy, Grocott-Gomori methenamine-silver nitrate stain

Introduction

Pulmonary actinomycosis is a rare and slowly progressive disease caused by the aspiration of a usually harmless colonization of *Actinomyces* from the oral cavity or gastrointestinal tract [1, 2]. The disease is difficult to diagnose owing to the non-specific symptoms, radiological traits that mimic malignancy or other thoracic disease, inability to grow in an anaerobic culture if the specimen is not well processed, and the high false negative rate with biopsies [1].

Pulmonary actinomycosis contributes to about 15% of actinomycosis cases, and might involve the facial-cervical area, abdominal and pelvic cavity, skin, or the central nervous system [2]. The diagnosis is often delayed, and confirmed after surgical resection [1]. A long duration of antibiotic treatment is usually needed for this disease, although the efficacy and length of the treatment course could vary from case to case [3]. Pulmonary actinomycosis is a disease that requires careful observation and evaluation for both diagnosis and therapy.

[1]Department of Thoracic Medicine, Chang Gung Memorial Hospital, Taipei, Taiwan, [2]College of Medicine, Chang Gung University, Taoyuan, Taiwan
Address reprint requests to: Dr. Jiunn-Min Shieh, Division of Chest Medicine, Department of Internal Medicine, Chi Mei Medical Center, Tainan, Taiwan; No.901 Zhonghua Road, Yong-Kang District, Tainan City 71004, Taiwan (R.O.C.)

Case Report

A 67-year-old Taiwanese non-diabetic male presented to an emergency department in Tucheng Dist., New Taipei City, Taiwan, with the complaint of shortness of breath for 1 day. The patient's dyspnea was accompanied with fever, up to 37.9°C, and cough with purulent yellow sputum. He had no nausea, vomiting, headache, chest tightness, abdominal pain, or generalized edema.

His past medical history included chronic obstructive pulmonary disease, group C (with an exacerbation history ≥ 2 times or ≥ 1 time that led to hospital admission, as well as Modified Medical Research Council Dyspnea Scale 0-1, or Chronic Obstructive Pulmonary Disease Assessment Test < 10), which had been diagnosed for about 3 years and was under control with inhaled tiotropium. He also had anaplastic anemia, for which he underwent hematopoietic stem cell transplantation (HSCT) previously at another hospital in Taipei City. However, the patient had not been taking a regular immunosuppressant agent. The pulmonary function test confirmed severe airway obstruction, with forced expiratory volume in 1 second (FEV1) of 1.09 liter, and FEV1 divided by forced vital capacity (FVC) was 58.34%, without significant response to a bronchodilator. He had quit smoking for 5 years and had no history of alcohol or medication misuse. The patient had undergone no recent surgery of the face and neck, nor dental procedures. He had no trackable clinical condition related to travel, occupation, or contact and clustering history.

On admission to our ward, the patient was alert and oriented. His body temperature was 36.3°C, respiratory rate, 18/min, blood pressure, 143/84 mmHg, pulse rate, 114/min, and his oxyhemoglobin saturation by pulse oximetry was 97% under nasal cannula 3 L/min. Physical examination revealed bilateral symmetric expansion during respiration and bilateral basal crackles.

Laboratory evaluation showed leukocytosis with a white blood cell (WBC) count of 16.8 x 10^3 /uL, with a predominant segment count of 88% and eosinophil count of 0%. The patient's hemoglobin was 15.3 g/dL, and platelets were 196 x 10^3 /uL. His liver and renal function was normal, and his electrolytes were within normal range. His C-reactive protein (CRP) was 54.5 mg/L, while the normal range should be lower than 5 mg/dL in our hospital.

Chest radiography plain film (CXR) on his third day of admission showed slightly increased consolidation at the right lower lung (Figure 1). Under the impression of community-acquired pneumonia (CAP), the patient was treated with levofloxacin 750 mg daily for
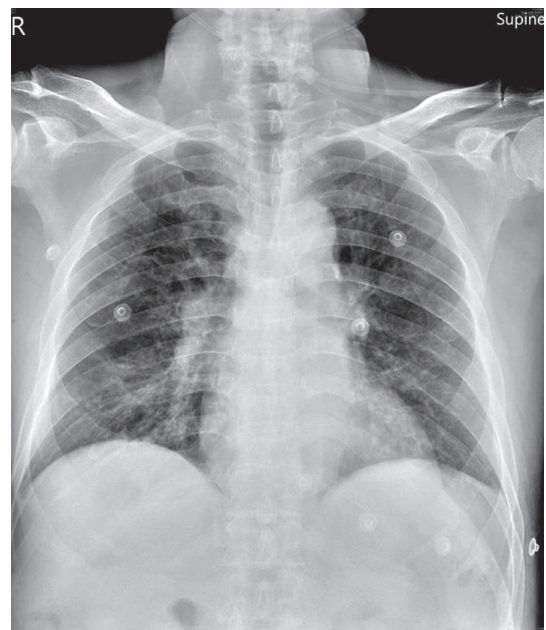

Fig. 1. CXR of the patient with pulmonary actinomycosis. Increased right lower lung consolidation was found.
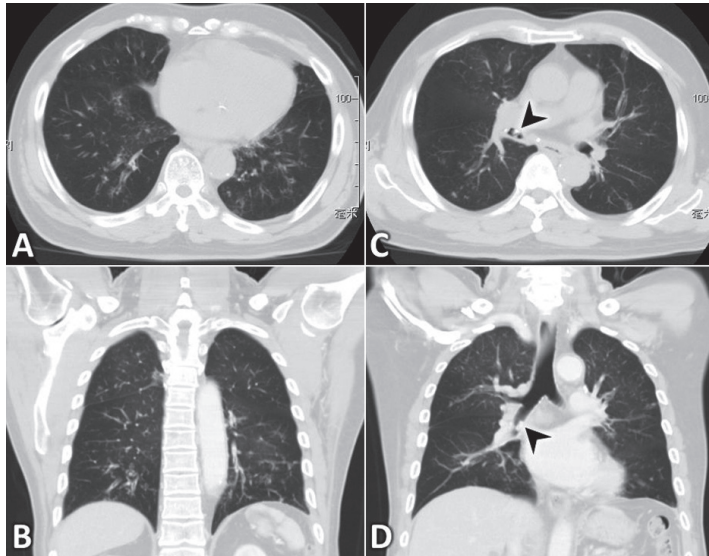
Fig. 2. Computed tomography scan of the patient revealed (A)(B) a tree-in-bud pattern (marked with white arrowheads) with centrilobular nodules with a linear branching pattern at the bilateral lower lobes, and (C)(D) an endobronchial hyperdense lesion (marked with black arrowheads) in the lower part of the right main bronchus.

5 days. The 3 sets of blood culture revealed no growth of bacteria, and the sputum culture showed mixed flora. Urine analysis showed no pyuria or proteinuria. The patient was discharged from the hospital once the dyspnea had been relieved.

Further studies, including chest high resolution computed tomography (HRCT) and bronchoscopy, were arranged at the outpatient clinic due to delayed resolution of the pneumonia with cough symptoms and consolidation on the CXR, to rule out other diseases such as malignancy. Chest HRCT revealed an endobronchial lesion in the lower part of the right main bronchus (9.5 x 6 x 4 mm) (Figure 2-C, D). A tree-in-bud pattern with centrilobular nodules with a linear branching pattern could be seen at the bilateral lower lobe (Figure 2-A, B). There was no evidence of pulmonary malignancy.

Bronchoscopy was performed and revealed a bone-like hard foreign body with a dark brown and black color at the orifice of the right middle bronchus; it was later removed with forceps. Endobronchial granulation-like tissue, with a white color and elevated necrotic pattern (Figure 3), was also found near the area where the foreign body was located; the lesion was
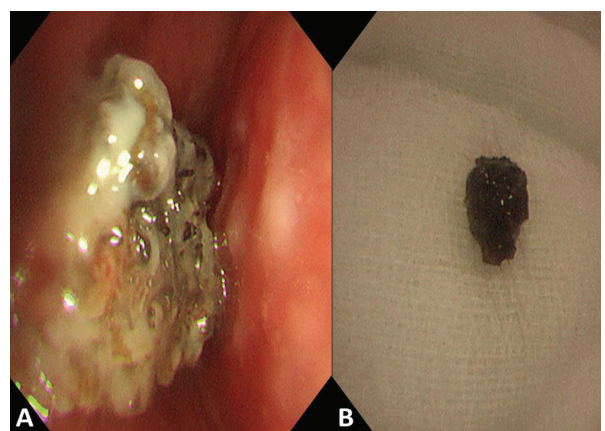

Fig. 3. Bronchoscopy of the patient revealed (A) a bone-like hard foreign body with a dark brown and black color at the right middle bronchus, with the surrounding endobronchial mucosa presented in a white, elevated necrotic pattern. (B) The foreign body was removed by forceps and placed on a piece of gauze.

biopsied trans-bronchially. Transbronchial lung biopsy (TBLB) was also performed for the lung parenchyma via the right middle bronchus, under endobronchial ultrasound. Bronchial washing was performed at the right middle bronchus and later revealed no growth of bacteria or fungus.

The histopathology slides indicated bronchial tissue with chronic inflammation. The endobronchial lesion was revealed to be due to an animal bone covered by sulfur granules, under hematoxylin and eosin (HE) stain. The sulfur granules were observed mostly around the endobronchial mucosa. Bone fragments were also found in the endobronchial tissue. Sulfur granules with a deep magenta color (Figure 4-C) could be seen surrounding the pink bone fragments (Figure 4-B) and infiltrating into the endothelial tissue of the bronchus (Figure 4-A). Under Grocott-Gomori methenamine-silver nitrate (GMS) stain, filamentous bacteria were revealed (Figure 5). These bacteria were mainly located in the endobronchial mucosa. There was no observable alveolar tissue on the same slide. Actinomycosis was thus diagnosed. Antimicrobial therapy with oral amoxycillin 875 mg and clavulanate potassium 125 mg twice daily was initiated and maintained for 21 days. Treatment was discontinued due to very poor compliance and the patient's refusal.

Discussion

We reported a patient with pulmonary actinomycosis who initially presented with CAP. He was later confirmed to have actinomycosis in association with foreign body inhalation after TBLB revealed the growth of filamentous bacteria with sulfur granules. The patient was treated with a suitable antibiotic, but with an
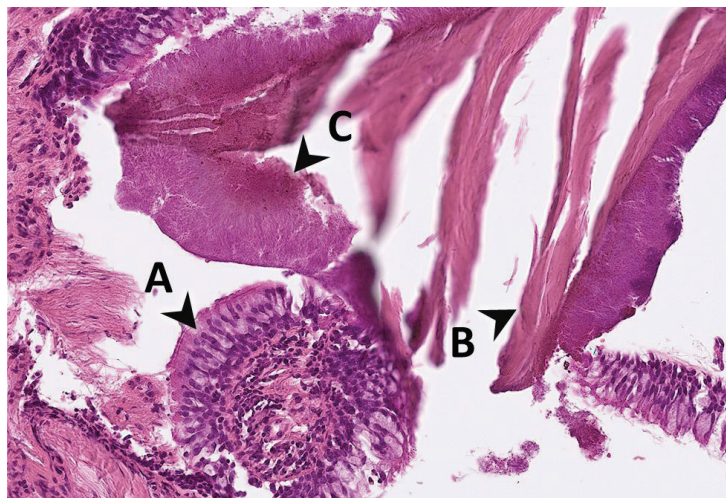

Fig. 4. Transbronchial lung biopsy specimen under HE stain (40X) revealed (A) a normal bronchial epithelium, (B) pink bone fragments of the foreign body, and (C) sulfur granules with a deep magenta color. HE: hematoxylin and eosin.
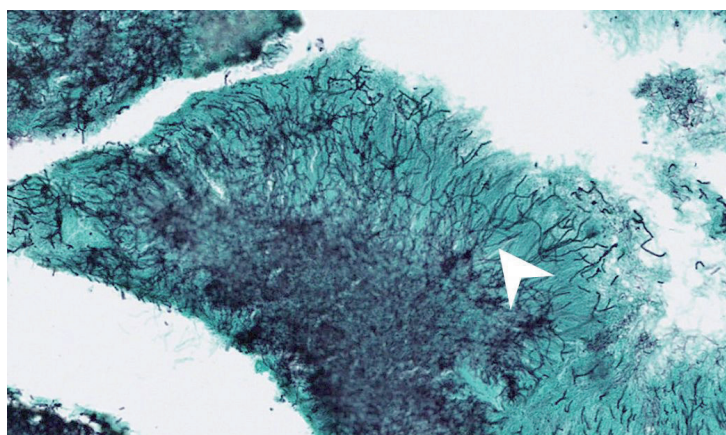

Fig. 5. Under GMS stain (120X), filamentous bacteria (Actinomyces) can be seen. GMS: Grocott-Gomori methenamine-silver nitrate.

inadequate treatment duration.

Actinomyces is a Gram-positive anaerobic bacterium. It was misclassified as fungi more than a century ago, owing to the filamentous appearance and slow progression of related diseases [1, 4, 5]. Actinomycosis was reported to involve various organs, but pulmonary actino-

mycosis amounted to just 15% of these diseases [1-2].

Patients of all ages were reported to have had pulmonary actinomycosis, with an increased prevalence in males aged 30 to 50 years old [6-8]. *Actinomyces* might be carried by saliva or other material from the digestive tract or oral cavity into the lower airway, causing further pulmonary infection [1]. The disease progresses slowly, resulting in acute and chronic inflammation of the lung parenchyma, which gradually develops into focal necrosis, fibrosis, cavitation [9], or even pleural effusion and empyema [1]. A few risk factors, such poor oral hygiene [10], dental diseases [10], conditions that lead to a higher chance of aspiration, such as alcoholism [11], underlying lung diseases such as bronchiectasis, bronchitis, or a history of mycobacterial infection [2, 7, 12], and inhalation of foreign bodies [13-14], have been described in previous studies. Improved oral hygiene was noted to decrease the incidence of pulmonary actinomycosis and lower the aggressiveness of this disease while patients are treated with antibiotics [10]. A few case reports indicated that pulmonary actinomycosis or lung abscess were likely related to a previous invasive dental procedure or oral lesions [15-17]. The greater possibility of alcoholic patients aspirating their oral secretion contributed to their higher risk of developing pulmonary actinomycosis [11]. In a previous study involving 94 patients with pulmonary actinomycosis, one-fifth of the patients had the issue of alcohol abuse [2]. Numerous case reports have revealed pulmonary actinomycosis related to the inhalation of foreign bodies [13-14], including the leaves of plants [18], animal bones from meals [19-20], and an obstruction due to bronchial dentures [21]; our patient had inhaled a piece of

animal bone. The patient had undergone HSCT, and his immunocompromised status should be considered as a risk factor for pulmonary actinomycosis. However, there was no strong evidence for a higher prevalence of pulmonary actinomycosis in patients infected with human immunodeficiency virus (HIV), or those treated with chemotherapy, taking oral steroids, or receiving an immunosuppressant for solid organ transplantation [1, 6, 10, 22]. Few case reports and studies have indicated pulmonary actinomycosis as a disease of concern in patients who have undergone HSCT, and there is no proof of an increased risk of such an infection in patients who have undergone bone marrow transplantation [23-24].

The diagnosis of pulmonary actinomycosis is crucial, but very difficult. Less than 7% of pulmonary actinomycosis patients were suspected to have had the disease on admission; it takes 6 months on average for physicians to confirm the diagnosis of pulmonary actinomycosis after the first presentation of symptoms [2, 25]. Chest pain was usually the most prominent symptom of pulmonary actinomycosis, while purulent cough was the most common symptom [1]. The laboratory examination was indefinite [2]. A mass-like lesion or consolidation of the lung parenchyma, sometimes with cavitation or pleural effusion, are common presentations of pulmonary actinomycosis on CXR [1, 26]. Under computerized tomography (CT) scan or magnetic resonance imaging (MRI), pulmonary lesions were noted mostly at the lower and peripheral parenchyma, and included multifocal nodules, consolidations, cavitation, and sometimes pleural thickening or effusion near the lesions [27-28]. However, the clinical presentations and radiology examination provide mostly non-specific results for confirmation of the di-

agnosis [1].

A vital step in the diagnosis of pulmonary actinomycosis almost always includes a certain form of biopsy and pathological study, using bronchoscopy, image-guided transthoracic biopsy, or surgical biopsy [2]. Bronchoalveolar lavage and culture could be inadequate to distinguish between colonization of actinomycosis and true infection [1], and the high false negative rate for anaerobic specimens exposed to air during the procedure also sets up obstacles for the diagnosis [29]. The usefulness of TBLB is controversial: some studies have suggested an unsuccessful result for TBLB [1, 8], possibly related to the granulation tissue surrounding the pathogen [30], and another study suggested a much better diagnostic rate, with 24.5% of patients diagnosed via TBLB and 25.5% diagnosed via protected transbronchial needle aspiration [2]. TBLB could be more helpful in the diagnosis when the actinomycosis shows endobronchial involvement, with occasional granular thickening and nodules in the submucosal region [31]. Removal of the infectious foreign bodies might affect the course of treatment and symptoms, with some patients recovering quickly after the foreign objects were removed [21]. Transthoracic biopsy, assisted by sonography or CT scan, was also used for pathology diagnosis. Although described as an effective and safe examination [1], image-guided biopsy could provide a non-diagnostic result [32]. Other methods involved surgical intervention, such as wedge resection or even lobectomy, which were often carried out under an initial concern for lung malignancies [33]. In a previous study, 18% of patients still required the use of a surgical method for the final diagnosis of pulmonary actinomycosis [2].

Treatment for pulmonary actinomycosis with antibiotics is effective, yet time-consuming. The suggested treatment was usually intravenous antibiotic for 2-6 weeks, followed by oral antibiotic treatment for 6 to 12 months. Penicillin G, amoxicillin, doxycycline, ceftriaxone, clindamycin, and ampicillin were all applicable for therapy [3]. However, there are case reports suggesting a shorter treatment course, with successful recovery from thoracic actinomycosis [3]. The duration could be as short as 3 days to 1 week in less bulky actinomycosis cases [3]. In patients who develop hemoptysis, the condition might be very severe and require surgical treatment or embolization to prevent further respiratory failure [31, 34]. Surgical treatment for thoracic actinomycosis might also be needed for necrotic tissue debridement or bulky abscess removal, in addition to antibiotics [6, 22]. Most studies have suggested that treatment for immunocompetent patients is adequate for treating those who are immunocompromised [22, 35]. Our patient used oral antibiotics for 3 weeks, which were stopped due to poor compliance. However, the patient's symptoms and CXR showed no marked deterioration. Possible reasons for the good recovery under an inadequate treatment duration could be the already removed infectious foreign body, the limited involvement of actinomycosis in endobronchial mucosa and lung parenchyma, and the variation in the effective treatment course from case to case.

There are limitations in our case report. Although pulmonary actinomycosis is strongly related to aspiration, and multiple cases of pulmonary actinomycosis associated with foreign body inhalation have been reported, further clinical study or case series might be required to prove the relationship between foreign body inhalation and actinomycosis infection. Other

details of these patients, such as suggested antibiotic duration, the effects of different inhaled objects, and if empiric treatment is needed before diagnosis, need further survey. Second, the efficacy of using non-surgical methods for the biopsy of pulmonary actinomycosis remains controversial. These methods, including bronchoscopy and image-guided transthoracic biopsy, might require standardization in terms of procedure details, as well as large-scale prospective or retrospective studies to determine if these invasive examinations are helpful. Third, the management of pulmonary actinomycosis, especially the treatment course of antibiotics, varies in different patients. It is also difficult for the physician to follow up simple markers or images to decide whether the treatment course is adequate or not. The treatment of, and recovery from pulmonary actinomycosis thus require close observation and careful evaluation of a patient's clinical condition.

Conclusion

We reported a 67-year-old man who presented with the symptoms of dyspnea, fever, and cough with purulent yellow sputum, initially treated as CAP. He was later found to have pulmonary actinomycosis, which had an aspiration-related pathogenesis; the patient was also found to have inhaled a piece of animal bone into his right main bronchus. Being a disease that is difficult to diagnose, pulmonary actinomycosis requires an imaging study such as a CT scan and a bronchoscopy-assisted invasive procedure for identification, before referring the patient for surgical pathological proof. Although the treatment duration for actinomycosis is usually long, the recovery condition varies among different patients, and could be influenced by

the severity of the disease or the removal of the infectious foreign body.

References

1. Mabeza GF, Macfarlane J. Pulmonary actinomycosis. Eur Respir J 2003;21(3): 545-51.
2. Kim SR, Jung LY, Oh I-J, *et al.* Pulmonary actinomycosis during the first decade of 21st century: cases of 94 patients. BMC Infect Dis 2013;13(1): 216.
3. Choi J, Koh WJ, Kim TS, *et al.* Optimal duration of IV and oral antibiotics in the treatment of thoracic actinomycosis. Chest 2005;128(4): 2211-7.
4. Sullivan DC, Chapman SW. Bacteria that masquerade as fungi: actinomycosis/nocardia. Proc Am Thorac Soc 2010;7(3): 216-21.
5. Ferry T, Valour F, Karsenty J, *et al.* Actinomycosis: etiology, clinical features, diagnosis, treatment, and management. Infect Drug Resist 2014:183.
6. Bennhoff DF. Actinomycosis: diagnostic and therapeutic considerations and a review of 32 cases. Laryngoscope 1984;94(9): 1198-217.
7. Heffner JE. Pleuropulmonary manifestations of actinomycosis and nocardiosis. Semin Respir Infect 1988;3(4): 352-61.
8. Kinnear WJ, MacFarlane JT. A survey of thoracic actinomycosis. Respir Med 1990;84(1): 57-9.
9. Brown JR. Human actinomycosis. A study of 181 subjects. Hum Pathol 1973;4(3): 319-30.
10. Russo TA. Actinomycosis. In: Jameson JL, Fauci AS, Kasper DL, *et al*, editors. Harrison's Principles of Internal Medicine, 20e. New York, NY: McGraw-Hill Education; 2018.
11. Apotheloz C, Regamey C. Disseminated infection due to *Actinomyces* meyeri: case report and review. Clin Infect Dis 1996;22(4): 621-5.
12. Schaal KP, Lee H-J. Actinomycete infections in humans — a review. Gene 1992;115(1): 201-11.
13. Umeki S, Nakajima M, Tsukiyama K, *et al.* Foreign body-induced bronchial actinomycosis with severe stenosis that must be distinguished from lung cancer. Nihon Kyobu Shikkan Gakkai Zasshi 1990;28(3): 481-6.
14. Kim YS, Suh JH, Kwak SM, *et al.* Foreign body-induced actinomycosis mimicking bronchogenic carcinoma. Korean J Intern Med 2002;17(3): 207-10.

15. Endo S, Mishima E, Takeuchi Y, *et al*. Periodontitis-associated septic pulmonary embolism caused by *Actinomyces* species identified by anaerobic culture of bronchoalveolar lavage fluid: a case report. BMC Infect Dis 2015; 15(1).

16. Takiguchi Y, Terano T, Hirai A. Lung abscess caused by *Actinomyces* odontolyticus. Intern Med 2003;42(8): 723-5.

17. Suzuki JB, Delisle AL. Pulmonary actinomycosis of periodontal origin. J Periodontol 1984;55(10): 581-4.

18. Sobajima T, Asano F, Tsuzuku A, *et al*. A case of pulmonary actinomycosis associated with aspiration of cedar leaves. J Bronchology Interv Pulmonol 2015;22(3): 259-62.

19. Ocal Z, Ozdogan S, Caglayan B, *et al*. Endobronchial actinomycosis caused by occult foreign body aspiration. Ann Saudi Med 2004;24(3): 210-2.

20. Ling Hsu AA, Pena Takano AM, Wai Chan AK. Beyond removal of endobronchial foreign body. Am J Respir Crit Care Med 2014;189(8): 996-7.

21. Murray MA, Rogan MP, Morgan RK, *et al*. Bronchial dentures as a cause of airway actinomycosis. Case Rep 2014;2014(aug22 1): bcr2014204109-b.

22. Chaudhry SI, Greenspan JS. Actinomycosis in HIV infection: a review of a rare complication. Int J STD AIDS 2000;11(6): 349-55.

23. Barraco F, Labussière-Wallet H, Valour F, *et al*. Actinomycosis after allogeneic hematopoietic stem cell transplantation despite penicillin prophylaxis. Transpl Infect Dis 2016;18(4): 595-600.

24. Kapadia M, Shapiro TW. Pulmonary Complications Associated with HSCT. Springer International Publishing; 2018. p. 301-25.

25. Weese WC, Smith IM. A study of 57 cases of actinomycosis over a 36-year period: a diagnostic 'failure' with good prognosis after treatment. Arch Intern Med 1975;135(12): 1562-8.

26. Flynn MW, Felson B. The roentgen manifestations of thoracic actinomycosis. Am J Roentgenol 1970;110(4): 707-16.

27. Kwong JS, Müller NL, Godwin JD, *et al*. Thoracic actinomycosis: CT findings in eight patients. Radiology 1992;183(1): 189-92.

28. Wand A, Gilbert HM, Litvack B, *et al*. MRI of thoracic actinomycosis. J Comput Assist Tomogr 1996;20(5): 770-2.

29. Smego JRA, Foglia G. Actinomycosis. Clin Infect Dis 1998;26(6): 1255-61.

30. Nakamura S, Kusunose M, Satou A, *et al*. A case of pulmonary actinomycosis diagnosed by transbronchial lung biopsy. Respir Med Case Rep 2017;21: 118-20. Epub 20170413.

31. Lu M-S, Liu H-P, Yeh C-H, *et al*. The role of surgery in hemoptysis caused by thoracic actinomycosis; a forgotten disease. Eur J Cardiothorac Surg 2003;24(5): 694-8.

32. Fahim A, Teoh R, Kastelik J, *et al*. Case series of thoracic actinomycosis presenting as a diagnostic challenge. Respir Med CME 2009;2(1): 47-50.

33. Moore WR, Scannell JG. Pulmonary actinomycosis simulating cancer of the lung. J Thorac Cardiovasc Surg 1968;55(2): 193-5.

34. Hamer DH, Schwab LE, Gray R. Massive hemoptysis from thoracic actinomycosis successfully treated by embolization. Chest 1992;101(5): 1442-3.

35. Wong VK, Turmezei TD, Weston VC. Actinomycosis. BMJ 2011;343: d6099.

Subglottic Lobular Capillary Hemangioma-Associated Extra-Thoracic airway Obstruction: A Case Report

En-Chi Hsu[1], Cheng-Hao Chuang[1,2]

Lobular capillary hemangioma, sometimes known as pyogenic granuloma, is a vascular proliferation of the skin and oral cavity that mimics granulation tissue grossly, but hemangioma microscopically. Most airway lobular capillary hemangiomas are located in the oral and nasopharyngeal mucosa. Here, we reported the case of a college student who presented to our clinics with dyspnea for 1 month. He had visited a local medical doctor, but the symptoms progressed despite medication treatment. Loud stridor during both inspiration and expiration was noted at the outpatient department. Tracing back his history, he was involved in a traffic accident with traumatic brain injury with a 2-week-long intubation period about 5 months ago, and aspiration pneumonia with a 1-week intubation 2 months before this presentation. The lung function test showed a flattened curve during inspiration, indicating upper airway obstruction. The chest film did not disclose an active pulmonary lesion, but a small protruding mass just below the vocal cords was found by bronchoscopic examination. The patient underwent surgical treatment, and recovered well. Our case highlights the role of a lung function test in providing an initial impression and indicating further diagnostic approaches that can be taken by the physician. *(Thorac Med 2023; 38: 236-240)*

Key words: pyogenic granuloma, complication of intubation, stridor, dyspnea, lung function test

Introduction

Lobular capillary hemangioma (LCH) is a vascular proliferative disease that mostly occurs in the oral and nasal cavities. It also affects the lower respiratory tract, though rarely. In previous case reports, it was usually confirmed by radiography, and no pulmonary function tests were performed before diagnosis. Herein, we present the case of an 18-year-old man with subglottic LCH with an extra-thoracic obstruction, who had suffered from dyspnea for 1 month with a poor treatment response.

[1]Division of Pulmonary and Critical Care Medicine, Kaohsiung Medical University Hospital, [2]Graduate Institute of Medicine, College of Medicine, Kaohsiung Medical University, Kaohsiung, Taiwan
Address reprint requests to: Dr. Cheng-Hao Chuang, Division of Pulmonary and Critical Care Medicine, Department of Internal Medicine, Kaohsiung Medical University Hospital, Kaohsiung Medical University No.100, Tzyou 1st Road, Kaohsiung 807, Taiwan

Case Presentation

This 18-year-old young man visited our clinics due to progressive shortness of breath for 3 days. He complained of intermittent difficulty in taking a deep breath and severe dyspnea on exertion during the past month. He had visited a local medical department, but his condition was scarcely improved after taking medication. Marked stridor on auscultation during both the inspiration and the expiration phase was noticed in the physical examination. The patient had a traffic accident history with a traumatic brain injury 5 months previous, and a 2-week intubation during hospitalization. Furthermore, aspiration pneumonia and acute respiratory failure with intubation for 1 week occurred 2 months previous to this visit. Chest radiograph found no active pulmonary lesion (Fig 1). A pulmonary function test was arranged and showed a significant inspiratory plateau, a severe obstructive ventilator defect, and marked
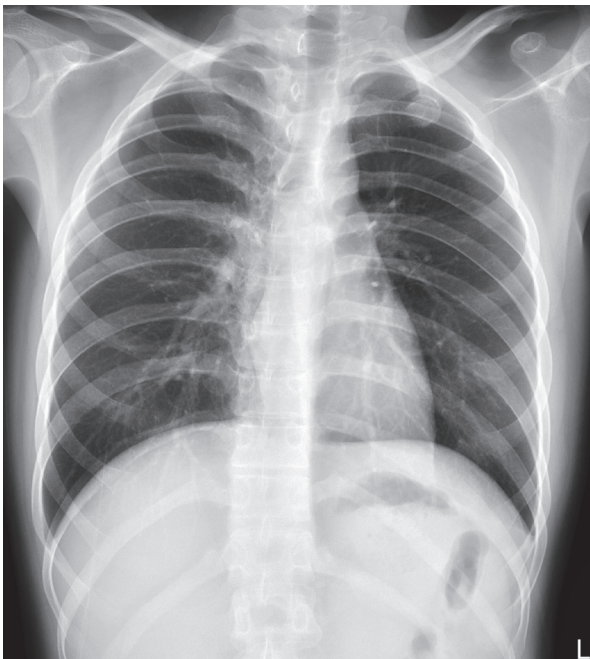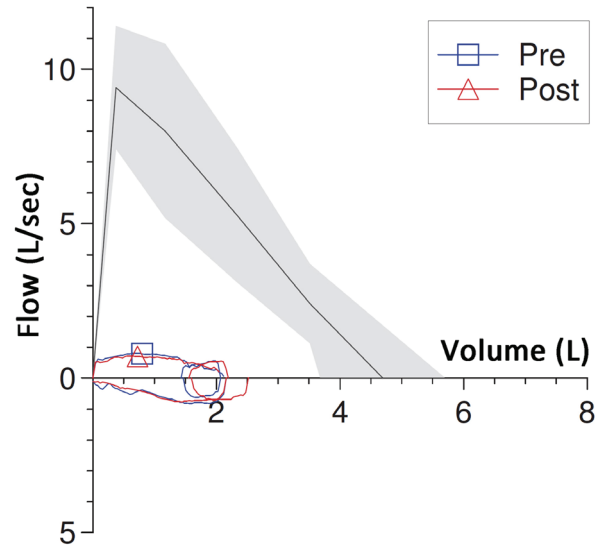

Fig. 2. Pulmonary function test showed a significant inspiratory plateau.

air-trapping presenting with an increased ratio of residual volume (RV) to total lung capacity (TLC) (Fig 2).

Under the impression of extra-thoracic airway obstruction, bronchoscopy was arranged immediately, and all pre-procedure laboratory results were within normal range. During the bronchoscopic evaluation, 1 whitish, smooth-surfaced mass-like lesion was found right below the vocal cords, and nearly total obstruction of the upper airway was presented (Fig 3). We did not pass the bronchoscope through the vocal cords because of a concern about total airway obstruction during the advancement of the bronchoscope. Due to a high risk of airway compromise, the patient was transferred to the emergency room right after the procedure, and chest computed tomography (CT) was arranged soon after. A tiny nodular lesion, 0.65 centimeters in size, stemming from the posterior tracheal wall right below the vocal cords, was found (Fig 4 A,B).

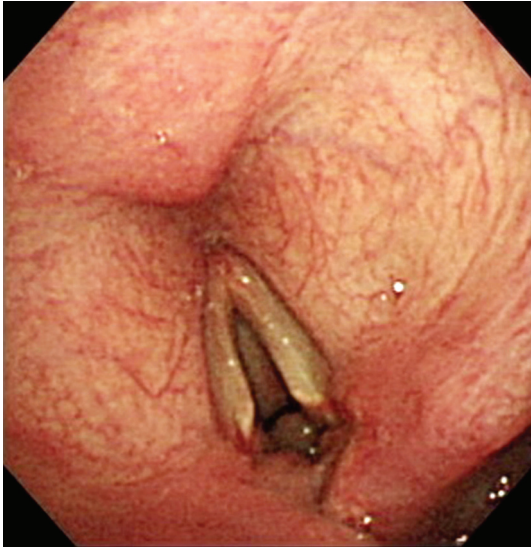Post-intubation granulation tissue growth

Fig. 1. Chest radiographs revealed no obvious air-space lesion.

Fig. 3. Bronchoscopy found a small protruding mass just below the vocal cords, with nearly total obstruction of the airway.

with extra-thoracic airway compromise was suspected, and surgical treatment was indicated after comprehensive evaluation. After discussion with the patient and his family, surgical excision of the subglottic nodular lesion with pre-excision tracheostomy creation was performed by the otolaryngologist. The operation was successful, and the patient was free from dyspnea after intervention. Tracheostomy tube decannulation also was performed without complication. Surprisingly, the microscopic finding revealed lobular proliferation of the capillaries and poorly-canalized vascular tufts within the inflammatory stroma, covered by focally ulcerated epithelium (Fig 5 A,B). Rather than simply
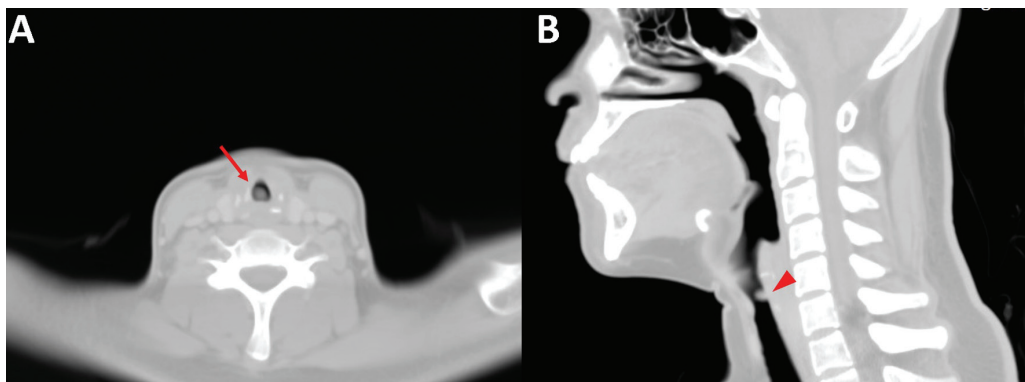

Fig. 4. Computed tomography (CT) of the chest with contrast enhancement disclosed a tiny nodular lesion, stemming from the posterior tracheal wall right below the vocal cords (A, arrow). Sagittal view (B, arrowhead).
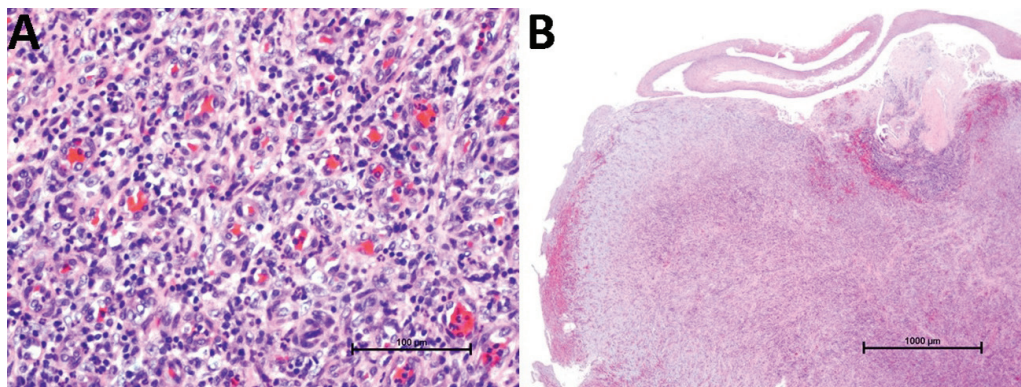

Fig. 5. The microscopic picture showed lobular proliferation of capillaries and poorly-canalized vascular tufts within inflammatory stroma (A) covered by focally ulcerated epithelium (B).

post-intubation granuloma, the final pathologic diagnosis was pyogenic granuloma, also known as LCH.

Discussion

Tracheal tumors comprise only about 2% of all airway tumors, and most of them are malignant in adults [1]. LCH, also known as pyogenic granuloma, is a benign vascular proliferative lesion that is usually found on the skin and mucosa. LCHs are mostly located in the oral and nasal cavities; those within the trachea are extremely rare. Since the first case presented in 2003, only 24 cases of tracheal LCHs have been reported in the literature so far [1].

Clinical discussion

Airway LCHs are usually painless, and often present with cough, hemoptysis, and sometimes, dyspnea due to airway obstruction [2]. Even when they are located in a major airway, tracheal LCHs rarely cause respiratory failure. However, our patient suffered from a tracheal LCH that was located at a critical anatomical site right below the vocal cords, with nearly total obstruction. The typical flow-volume curve of the extra-thoracic airway obstruction helped in reaching an immediate diagnosis and in providing timely treatment for the patient.

Although the pathophysiology of LCH remains unclear, several possible risk factors have been reported in previous cases, including trauma, local irritation or hormone changes [3]. LCH occurs more often in young people than in the elderly, and is predominant in females of reproductive age, which may be related to hormone changes during pregnancy and associated angiogenesis [4]. Connective tissue growth factor, vascular endothelial growth factor, basic

fibroblast growth factor and nitric oxide synthase may also play an important role in LCH [5]. The possible precipitating factor in our case was the 2 previous intubation episodes.

CT and bronchoscopy are both helpful in the diagnosis of tracheal LCH. CT helps to identify and locate the lesion, and a bronchoscope is required to perform tissue biopsy to make a definite pathological diagnosis and differentiate other etiologies such as granulation tissue, angioendothelioma, angiosarcoma, hemangioma, intravascular angiomatosis, and Kaposi sarcoma [6].

There are several treatment choices, including endoscopic excisional biopsy, snare electrocautery, cryotherapy, laser therapy, and surgical resection [7]. Treatment depends on patient symptoms, tumor size, comorbidities, and other contributing clinical conditions. Bronchoscopic treatment was chosen in almost all previous cases in the literature, although 1 chose embolization, and another chose spontaneous regression [1]. Only 2 of the 23 cases had recurrence. Surgical resection was suggested in our case due to both the symptomatic lesions causing nearly total airway compromise and to the critical location, which would have rendered bronchoscopic intervention relatively difficult.

Radiologic discussion

There are no typical characteristics of tracheal LCH, although they are usually small in size, ranging from 2 mm~20 mm, and rarely exceed 3 cm in diameter in previous case reports [3]. However, 1 case had a multifocal lesion, and the others presented with 1 solitary nodule, as did our case.

The chest plain film generally discloses no gross lesions in the LCH patient, and CT is needed to reveal the occult lesions. The lesion

can be homogenously or heterogeneously enhanced after contrast injection, and the average density is more than 100 HU in most cases [3]. Most previous low respiratory tract LCH were located in the trachea, except for 2 cases -- 1 at the left main bronchus, and the other at the truncus intermedius [1].

Pathologic discussion

Lobular capillary hemangioma is also known as pyogenic granuloma, but it is neither related to bacterial infection nor is it a granulation. It is a benign capillary proliferation tissue with a lobular pattern, separated by fibrous stroma, pathologically similar to granulation tissue [8]. LCH and granulation tissue each have different characteristics. First, the main structure of LCH is the proliferation of capillaries, while granuloma has a proliferation of epithelial cells. Second, LCH usually grows rapidly, with frequent recurrence, compared to simple granulation tissue. Sometimes the surface of the LCH might be ulcerative and infiltrated by inflammation cells, and then form a granulation [6].

Conclusion

Tracheal LCH is rarely reported in the literature. Here, we presented the first case of tracheal LCH located right below the vocal cords, that caused typical extra-thoracic airway obstruction in both symptoms and flow-volume curve. Timely recognition of upper airway compromise is crucial in patient management, and comprehensive history-taking, physical examination, and correct interpretation of images and pulmonary function test results are fundamental.

References

1. Maturu VN, Vaddepally CR, Narahari NK, *et al*. Lobular capillary hemangioma of the trachea - A rare cause of stridor in elderly: a case report with review of literature. Asian Cardiovasc Thorac Ann 2021; 29(5): 424-7.
2. Wang RY, Quintanilla NM, Chumpitazi BP, *et al*. Pediatric tracheal lobular capillary hemangioma: a case report and review of the literature. Laryngoscope 2021; 131(8): 1729-31.
3. Xu Q, Yin X, Sutedjo J, *et al*. Lobular capillary hemangioma of the trachea. Arch Iran Med 2015; 18(2): 127-9.
4. Acharya MN, Kotidis K, Loubani M. Tracheal lobular capillary haemangioma: a rare benign cause of recurrent haemoptysis. Case Rep Surg 2016; 2016: 6290424.
5. Jafarzadeh H, Sanatkhani M, Mohtasham N. Oral pyogenic granuloma: a review. J Oral Sci 2006; 48(4): 167-75.
6. Qiu X, Dong Z, Zhang J, *et al*. Lobular capillary hemangioma of the tracheobronchial tree: a case report and literature review. Medicine (Baltimore) 2016; 95(48): e5499.
7. Ruenwilai P, Liwsrisakun C, Limsukon A, *et al*. Tracheal capillary hemangioma successfully treated with combined bronchoscopic cryotherapy and argon-plasma coagulation. Cureus 2021; 13(10): e18547.
8. Kalanjeri S, Kumar A, Mukhopadhyay S, *et al*. Lobular capillary hemangioma ("pyogenic granuloma") of the trachea. Am J Respir Crit Care Med 2016; 193(12): 1429-30.

Ideopathic Pleuroparenchymal Fibroelastosis Treated with Lung Transplantation: First Case Report in Taiwan and Review of the Literature

Pin-Li Chou[1], His Chieh-Ning[2], Han-Chung Hu[3], Wei-hsun Chen[1]

Pleuroparenchymal fibroelastosis (PPFE) is a rare subtype of interstitial lung disease, and presents with upper pulmonary lobe fibrosis and bilateral subpleural dense consolidation. There is no certain etiology for idiopathic PPFE, which progresses slowly but with rapid clinical deterioration. Surgical biopsy for pathological diagnosis was the gold standard in the past, but may result in pneumothorax, which is dangerous for these fragile lungs. Modified diagnostic criteria, including chest tomography imaging and clinical presentation, were adopted for our patient. There is not much evidence for medical treatment so far, so lung transplantation is the ultimate treatment for idiopathic PPFE, though reports on postoperative long-term follow-up are still scarce. We reported the case of a 41-year-old male patient diagnosed with idiopathic PPFE, who suffered from progressive dyspnea for 3 years and recurrent bilateral pneumothorax. He is the first patient in Taiwan to undergo bilateral lung transplantation, and had a smooth postoperative recovery and uneventful?? follow-up for 1.5 years. *(Thorac Med 2023; 38: 241-249)*

Key words: pleuroparenchymal fibroelastosis (PPFE), end-stage lung disease, lung transplantation

Introduction

Pleuroparenchymal fibroelastosis (PPFE) is a rare subtype of interstitial lung disease (ILD) first noted for-with?? upper pulmonary lobe fibrosis in 1992 [1]. The term was coined by Frankel *et al*. in 2004 [2]. It has been listed as a classification of idiopathic interstitial pneumonias (IIPs) by the American Thoracic Society and European Respiratory Society since 2013 [3].

Most PPFE patients are slender with a flattened thoracic cage [4], and have suffered from progressive dyspnea for months to years. There is not enough reported evidence of medical therapy for progressive PPFE, so lung transplantation is the ultimate viable curative treatment option [5, 6]. Spontaneous recurrent pneumothorax occurs in 56.6% patients, and they have poorer survival outcomes [7]. Fur-

[1]Division of Thoracic Surgery, Chang Gung Memorial Hospital-Linkou, Taoyuan, Taiwan, [2]Department pf Surgery, Taipei Veterans General Hospital, Taipei, Taiwan, [3]Department of Chest Medicine, Chang Gung University, Taoyuan, Taiwan
Address reprint requests to: Dr. Wei-Hsun Chen, Division of Thoracic and Cardiovascular Surgery, Chang Gung Memorial Hospital, 5 Fu-Hsing Street, Kweishan, Taoyuan, Taiwan

thermore, lung biopsy for tissue proof can often result in pneumothorax and acute exacerbation [8]. So it is important that idiopathic PPFE is diagnosed based on clinical presentation and modified criteria for typical image patterns (i.e., bilateral subpleural dense consolidation with predominantly upper lobe pleural thickening) without pathological proof [9-11], after excluding other identifiable etiologies.

We present the case of 41-year-old male patient diagnosed with idiopathic PPFE, who suffered from progressive dyspnea for 3 years and recurrent bilateral pneumothorax. He was clinically diagnosed by chest high resolution computed tomography (HRCT) and physiological characteristics, then underwent bilateral lung transplantation with the final pathological result of PPFE.

Case Presentation

This 41-year-old male patient, with no cigarette or asbestos exposure history, presented with progressive dyspnea and chronic productive cough for 3 years. He had no contributing family medical history. Physical examination revealed cachexia (body mass index (BMI): 14.7 kg/m^2) and platythorax. There was no clubbing of the fingers or pedal edema. In addition, bilateral upper lung inspiratory crackles on auscultation were noted. Laboratory tests showed normocytic anemia (hemoglobin: 12.2 mg/dl, MCV: 89%). Biochemical tests were all within normal limits. No evidence of autoimmune disease was reported.

The pulmonary function test revealed severe restrictive lung disease, with forced vital capacity (FVC) of 1.05 L (27% predicted), forced expiratory volume in 1 second (FEV1) of 1.00 L (30% predicted), and a FEV1/FVC ra-

tio of 95.2%. The patient had impaired exercise performance, with a 6-minute walking distance of 360 meters (53.8% predicted). HRCT of the lung showed progressive subpleural change in interstitial fibrosis and bronchiectasis traction for the last 2 years without signs of bronchial obliterative syndrome. There was also a lung volume decrease of the bilateral upper lobes with left-side predominant. Surgical lung biopsy was not performed in case of further lung injury and because of recurrent bilateral spontaneous pneumothorax. Based on the modified diagnostic criteria, the patient was diagnosed clinically by serial chest CT scans and physiological characteristics as having idiopathic PPFE (Figure 1, Figure 2), after excluding other identifiable lung diseases.
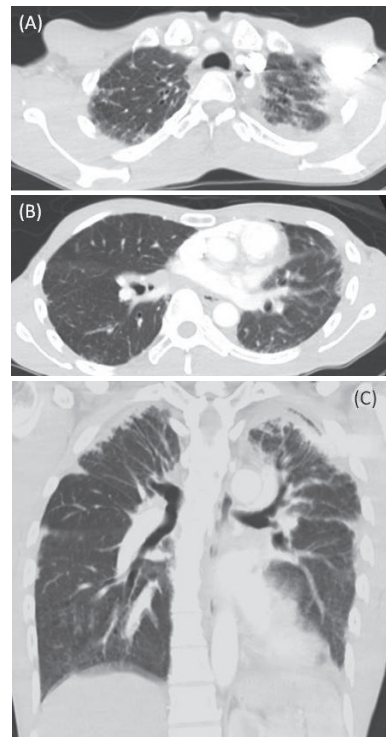

Fig. 1. Pre-transplant High-resolution CT
(A)(B) Axial cuts show bilateral upper lobes subpleural interstitial fibrosis and lung volume volume, left side predominantly for this patient. (C) Coronal view demonstrates bilateral upper lobes pleural thickening.
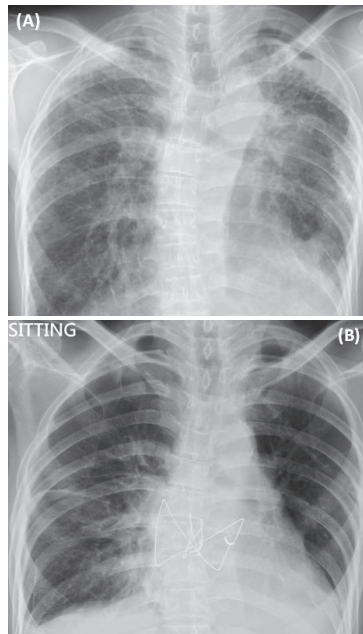
Fig. 2. Pre- and post-transplant Chest X-ray. (A) 1 month before lung transplants: bilateral pleural thickening and fibrosis, bilateral upper lobes most markedly; volume reduction of the left lug. (B) 11 months after bilateral lung transplants.

Fig. 3. Histopathological stains. (A)、(B) H & E stain: pleural thickening (red stars) and subpleural parenchymal fibrosis (blue star). (C)、(D) Elastical Van Gieson stain: abundant elastic tissue deposition (yellow star). Lung parenchymal far away from pleura is relative unaffected (green star).

The patient required long-term oxygenation therapy due to his deteriorated lung function. Nintedanib was prescribed for the patient to treat lung parenchyma fibrosis initially, without specific effect. Given his worsening symptoms, complicated with recurrent pneumothorax, bilateral lung transplantation was suggested and performed successfully. Due to the long-term lung fibrosis and chest wall deformity, with his left chest volume decreased, a donor left lower lung lobectomy was performed for chest wound closure. Histopathology revealed an upper lung-predominant distribution of pleural and subpleural lung parenchymal fibrosis. Elastic fiber stain showed marked septal elastosis (Figure 3). The patient was extubated smoothly on postoperative day 2 and discharged on postoperative day 40. Post-transplantation bilateral pleural effusion with left lower pleural thickening was noted as a suspected result of the previous left
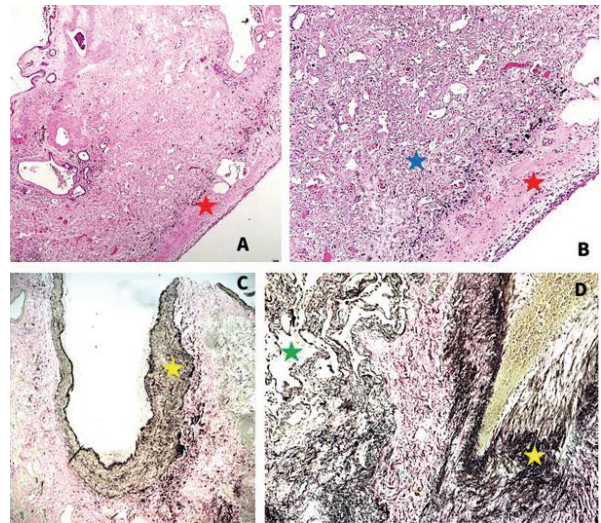

Fig. 4. Post-transplant high-resolution CT. High-resolution chest CT 1 month after bilateral lung transplants shows increased lung volume especially the bilateral upper lobes.
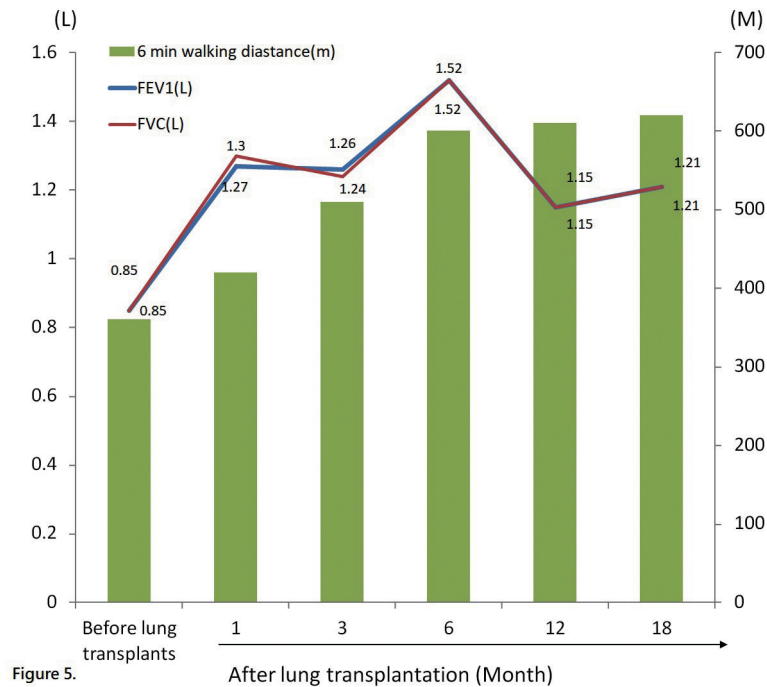
Fig. 5. Post-transplantation serial pulmonary function and 6-minute walking test were arranged regularly 1 month after surgery and then every 3 months for most of our recipients. In the figure—6-min walking distance (m), FEV1 (L), FVC (L), After lung transplantation (month), Before lung transplantation.

lower lung lobectomy. Transbronchial lung biopsy was performed 1 month later, and at the 3rd and 6th month, and revealed no acute rejection. Chest CT showed widening of the thoracic inlet 4 weeks after transplantation (Figure 4), and further widening at 1.5 years post-operation. A pulmonary function test was arranged at postoperative 1 month and every 3 months after transplantation, to monitor the postoperative pulmonary condition. Peak FEV1 and FVC values of 1.2 L (46%) were noted 6 months after bilateral lung transplantation, without the requirement of oxygen therapy (Figure 5).

Discussion

Pleuroparenchymal fibroelastosis (PPFE) is a rare clinicopathological entity of ILD characterized by pleural thickening with fibrosis and elastosis deposited in the subpleural lung parenchyma, predominantly located at the bilateral upper lobes [5-6, 12]. There are 2 distinct forms recognized [6] as idiopathic or primary PPFE, and secondary PPFE, often related to graft-versus-host disease after stem cell transplantation, and chronic rejection after lung transplantation due to restrictive allograft syndrome, autoimmune disease, chemotherapy or recurrent infections [24].

The most common clinical presentations of PPFE are dyspnea, chronic cough, chest pain, weight loss, pneumothorax and thoracic cage deformity [12-14]. Physical examination typically reveals inspiratory coarse crackles in bilateral lungs with the absence of finger clubbing (differing from idiopathic pulmonary fibrosis (IPF)) [5]. Radiological features on HRCT are bilateral irregular pleuroparenchymal thicken-

ing, located predominantly in the upper lobes, with an associated subpleural reticular pattern consistent with fibrosis [5, 6, 9]. Traction bronchiectasis and honeycombing patterns are also common.

Taishi *et al*. reported a small observational study of the long-standing fibrosis process to examine whether the flat chest became more pronounced during disease progression. They collected axial chest CT examinations of 8 patients to evaluate the anteroposterior diameter of the thoracic cage (APDT)/transverse diameter of the thoracic cage (TDT) ratio at the 6th vertebral level, which significantly decreased during follow-up of from 1.87 to 5.27 years, accompanied with FVC impairment [15].

Histopathological features of patients with PPFE are subpleural zonal dense fibrosis consisting of collapsed and collagen-filled alveoli with septal elastosis and collagenous thickening of visceral pleura [16-17]. Distribution is mainly concentrated in the upper lung lobes, while the lower lobes become involved as the disease progresses, but the pathology often reports a non-PPFE pattern in the lower lobes.

Reddy *et al*. proposed PPFE diagnosis criteria in 2012 based on the imaging-pathology correlation after surgical lung biopsy [18]. Five years later, modified criteria proposed by Enomoto *et al*. required no pathologic confirmation, and were as follows: (1) radiologic PPFE pattern of multiple subpleural foci of air space consolidation with traction bronchiectasis located predominantly in the bilateral upper lobes on HRCT scans, with or without pleural thickening; (2) radiologic proof of disease progression: increase consolidation in the upper lobes and/or a decrease in upper lobe volume on series of images; (3) exclusion of other lung diseases with similar etiologies, including connective tissue disease-

related ILD, pulmonary sarcoidosis, pneumoconiosis, chronic hypersensitivity pneumonitis, and active pulmonary infection [11]. Wantanabe *et al*. further took physiologic characteristics into consideration in 2019 [8] along with 2 other factors, and only 1 of each is required for diagnosis: (1) residual volume/total lung capacity ratio (RV/TLC %pred.) $\geq 115\%$, or (2) BMI: $\leq 20 \, kg/m^2$ plus RV/TLC %pred. $\geq 80\%$.

No medical therapy for PPFE patients has confirmed efficacy, and treatment options are limited. Miyahara *et al*. retrospectively investigated 56 IIP patients, and 11 of them who had idiopathic PPFE received anti-fibrinolytic??? agents before lung transplantation. Those who took anti-fibrotic??? agents had a lower mortality rate, lower risk of pneumothorax and a longer 6-minute-walk distance than patients without therapy [17]. Delanote *et al*. retrospectively assessed 9 patients with IPF receiving anti-fibrotic treatment. FVC seemed to be stabilized after 12 weeks in most patients [18]. However, our patient had a poor response to nintedanib after ??? weeks of treatment.

Idiopathic PPFE is associated with a worse prognosis than secondary PPFE [19, 20, 21]. Idiopathic PPFE progresses slowly, but with rapid clinical deterioration. The onset age is highly heterogeneous, ranging from 13 to 87 years, with bimodal peaks occurring during the patient's 30s and 60s. No association with gender or cigarette exposure has been established, so far [12]. Familial forms are more frequent in young female patients. The pathogenesis of primary PPFE is still unclear. Contributions from auto-immune mechanisms and genetic predisposition have been proposed in several studies [22]. At present, bilateral lung transplantation is considered the definitive treatment. Survival outcome of lung transplantation for idiopathic

PPFE was similar to that for IPF. However, the flat chest, low BMI, and associated restrictive impairment of FVC (about 20% lower than IPF recipients) persisted after lung transplantation in a published report [23], and was also observed in our patient.

Sekine *et al.* described a young woman with idiopathic PPFE that deteriorated rapidly during pregnancy. Cesarean section was performed at 28 weeks of gestation. She underwent living-donor lung transplantation on postpartum day 26, and survived nearly 2 years after transplantation [25]. Rasciti *et al.* reported the case of a patient with idiopathic PPFE who underwent bilateral lung transplantation, but the disease relapsed 8 months later, so the patient underwent another lung transplantation. This may suggest the contribution of an underlying process accelerating the development of PPFE in the transplanted lung [26]. Ali *et al* presented the case of a 26-year-old female with symptoms of chronic dyspnea since she was 15 years old, who came to the pulmonary clinic due to platythorax with an abnormal chest X-ray. She underwent video-assisted thoracic surgery for diagnostic tissue proof, and pathology revealed idiopathic PPFE. The complication of hydropneumothorax requiring prolonged chest tube drainage occurred after surgical lung biopsy, with worsening symptoms. Bilateral lung transplantation was performed and the patient survived for 4 years [27]. Yanagiya *et al.* reported a young woman with idiopathic PPFE and pectus excavatum who underwent bilateral living lobar donor lung transplantation without thoracic cage correction. Her flat chest wall had reversed gradually by 6 months after transplantation, with much improvement in pulmonary function [28]. Some patients had a Ravitch procedure for pectus excavatum correction before lung transplantation, but there was still disease progression due to a fibrosis process (Table 1).

Table 1. Ideopathic PPFE

Authors (Year/Country)	Age/ Sex	Pre-op diagnosis method	Surgical method	Follow-up duration	Post-op complications	Outcome
Sekine *et al.* (2020/Japan)	29/F	Images	LDLLT	2 years	Acute rejection Pneumonia	Alive
Shiiya *et al.* (2020/Japan)	40/F	Images and physiological characteristics	Left single LT	1.5 years	Right heart failure Acute rejection	Deceased
Righi *et al.* (2019/Italy)	42/M	Surgical lung biopsy	Bilateral LT	5 years	Chronic rejection	Alive
Ali *et al.* (2019/USA)	26/F	Surgical lung biopsy	Bilateral LT	4 years	Chylothorax Hydropneumothorax	Alive
Rasciti *et al.* (2019/Italy)	48/M	Surgical lung biopsy	Bilateral LT	8 months	Relapse of PPFE Re-transplant	Re-transplant
Aljefri *et al.* (2018/Saudi Arabia)	27/M	Surgical lung biopsy	Bilateral LT	45 days	Vocal cord paralysis Pneumonia Bilateral bronchomalacia	Alive
Huang *et al.* (2017/China)	34/M	Surgical lung biopsy	Bilateral LT	6 months	Uneventful	Alive
Yanagiya *et al.* (2016/Japan)	27/F	Surgical lung biopsy	LDLLT	6 months	Uneventful	Alive

PPFE: pleuroparenchymal fibroelastosis; LT: lung transplantation; LDLLT: living-donor lobar lung transplantation; LDSLT: living-donor segmental lung transplantation; M: male; F: female; SLB: surgical lung biopsy; NA: not available.

Table 2. Secondary PPFE

Underlying causes	Authors (Year/Country)	Age/ Sex	Pre-op diagnosis method	Surgical method	Follow-up duration	Post-op complication	Outcome
Liver transplantation	Goondi *et al.* (2021/Canada)	69/M	Images	Bilateral LT	NA	NA	Alive
C/T	Tsubosaka *et al.* (2019/Japan)	19/M	Images	LDSLT	NA	NA	Alive
HSCT	Shimada *et al.* (2018/Japan)	21/F	SLB	LDLLT	1 year	Malnutrition Decubitus	Alive
C/T	Hata *et al.* (2016/Japan)	19/M	Images	LDLLT	6 weeks	Uneventful	Alive
Castleman's disease	Portillo *et al.* (2015/Spain)	25/M	SLB	Bilateral LT	2 years	Uneventful	Alive
C/T	Chen *et al.* (2014/Japan)	14/M	Images	Left single LT	4 months	Uneventful	Alive

PPFE: pleuroparenchymal fibroelastosis; LT: lung transplantation; LDLLT: living-donor lobar lung transplantation; LDSLT: living-donor segmental lung transplantation; M: male; F: female; SLB: surgical lung biopsy. C/T: chemotherapy; HSCT: hematopoietic stem cell transplantation; NA: not available.

Goondi *et al.* first presented the case of a patient with secondary PPFE 3 years after liver transplantation [29]. Shimada *et al.* reported a patient with secondary PPFE that developed 10 years after hematopoietic stem cell transplantation. She underwent extracorporeal membrane oxygenation-bridged living-donor transplantation and was doing well at the 1-year follow-up [30]. Righi *et al.* presented a patient with idiopathic PPFE who survived 5 years, which is the longest post-transplantation follow-up interval [31] (Table 2).

Our patient had clinically diagnosed idiopathic PPFE before bilateral lung transplantation, with modified criteria of progressive change on the HRCT scan and physiologic characteristics. He had improved quality of life post-surgery, with his best pulmonary FVC and FEV1 function at 6 months post-transplantation. The patient's exercise activity was enhanced, and he had an improved 6-minute walking distance that was sustained for about 2 years during follow-up.

Conclusion

PPFE is a rare and progressive form of diffused pulmonary fibrosis, characterized by upper lobe-predominant pleural thickening and elastosis in the subpleural lung parenchyma. Its pathogenesis is still poorly understood, but there is disease progression, especially for idiopathic PPFE. Lung transplantation is a valid treatment choice for patients with end-stage idiopathic PPFE without response to medical treatment. Short-term outcomes after transplantation have been good, with an improving respiratory pattern, pulmonary function and level of daily activities.

References

1. Amitani R, Niimi A, Kuse F. Idiopathic pulmonary upper lobe fibrosis. Kokyu 1992; 11: 693-9.

2. Frankel SK, Cool CD, Lynch DA. Idiopathic pleuroparenchymal fibroelastosis: description of a novel clinicopathologic entity. Chest 2004; 126(6): 2007-13.

3. Travis WD, Blasi F, Kraft M, *et al*. An official American Thoracic Society/European Respiratory Society statement: update of the international multidisciplinary classification of the idiopathic interstitial pneumonias. Am J Respir Crit Care Med 2013; 188(6): 733-48.

4. Harada T, Yoshida Y, Kitasato Y, *et al*. The thoracic cage becomes flattened in the progression of pleuroparenchymal fibroelastosis. Eur Respir Rev 2014; 23: 263-66.

5. Cheng SK, Chuah KL. Pleuroparenchymal fibroelastosis of the lung: a review. Arch Pathol Lab Med 2016; 140(8): 849-53.

6. Chua F, Desai SR, Nicholson AG, *et al*. Pleuroparenchymal fibroelastosis. A review of clinical, radiological, and pathological characteristics. Ann Am Thorac Soc 2019; 16(11): 1351-59.

7. Kono M, Nakamura Y, Enomoto Y, *et al*. Pneumothorax in patients with idiopathic pleuroparenchymal fibroelastosis: incidence, clinical features, and risk factors. Respiration 2021; 100(1): 19-26.

8. Hurtado EJS, González MLA, Soto MdelM, *et al*. Idiopathic pleuroparenchymal fibroelastosis, a new idiopathic interstitial pneumonia: a case report. Chron Respir Dis 2016; 13(3): 312-6.

9. Tanizawa K, Handa T, Kubo T, *et al*. Clinical significance of radiological pleuroparenchymal fibroelastosis pattern in interstitial lung disease patients registered for lung transplantation: a retrospective cohort study. Respir Res 2018; 19(1): 162.

10. Watanabe K, Ishii H, Kiyomi F, *et al*. Criteria for the diagnosis of idiopathic pleuroparenchymal fibroelastosis: a proposal. Respir Investig 2019; 57(4): 312-320.

11. Enomoto Y, Nakamura Y, Satake Y, *et al*. Clinical diagnosis of idiopathic pleuroparenchymal fibroelastosis: A retrospective multicenter study. Respir Med 2017; 133:1-5.

12. Bonifazi M, Montero MA, Renzoni EA. Idiopathic pleuroparenchymal fibroelastosis. Curr Pulmonol Rep 2017; 6(1): 9-15.

13. Watanabe K. Pleuroparenchymal fibroelastosis -- its clinical characteristics. Curr Respir Med Rev 2013; 9: 229-37.

14. Shiiya H, Tian D, Sato M, *et al*. Differences between patients with idiopathic pleuroparenchymal fibroelastosis and those with other types of idiopathic interstitial pneumonia in candidates for lung transplants. Transplant Proc 2019; 51(6): 2014-21.

15. Tsubosaka A, Matsushima J, Ota M, *et al*. Whole-lung pathology of pleuroparenchymal fibroelastosis (PPFE) in an explanted lung: significance of elastic fiber-rich, non-specific interstitial pneumonia-like change in chemotherapy-related PPFE. Pathol Int 2019; 69(9): 547-55.

16. Shimada A, Terada J, Tsushima K, *et al*. Veno-venous extracorporeal membrane oxygenation bridged living-donor lung transplantation for rapid progressive respiratory failure with pleuroparenchymal fibroelastosis after allogeneic hematopoietic stem cell transplantation. Respir Investig 2018; 56(3): 258-262.

17. Miyahara S, Waseda R, Tokuishi K, *et al*. Elucidation of prognostic factors and the effect of anti-fibrotic therapy on waitlist mortality in lung transplant candidates with idiopathic interstitial pneumonias. Respir Investig 2021; 59(4): 428-435.

18. Delanote I, Wuyts WA, Yserbyt J, *et al*. Safety and efficacy of bridging to lung transplantation with antifibrotic drugs in idiopathic pulmonary fibrosis: a case series. BMC Pulm Med 2016; 16(1): 156.

19. Pakhale SS, Hadjiliadis D, Howell DN, *et al*. Upper lobe fibrosis: a novel manifestation of chronic allograft dysfunction in lung transplantation. J Heart Lung Transplant 2005; 24(9): 1260-8.

20. von der Thüsen JH, Hansell DM, Tominaga M, *et al*. Pleuroparenchymal fibroelastosis in patients with pulmonary disease secondary to bone marrow transplantation. Mod Pathol 2011; 24(12): 1633-9.

21. Reddy TL, Tominaga M, Hansell DM, *et al*. Pleuroparenchymal fibroelastosis: a spectrum of histopathological and imaging phenotypes. Eur Respir J 2012; 40(2): 377-85.

22. Konen E, Weisbrod G L, Pakhale S, *et al*. Fibrosis of the upper lobes -- a newly identified late-onset complication

after lung transplantation. AJR Am J Roentgenol 2003; 181: 1539-1543.

23. Shiiya H, Nakajima J, Date H, *et al*. Outcomes of lung transplantation for idiopathic pleuroparenchymal fibroelastosis. Surg Today 2021 Aug; 51(8): 1276-1284. doi: 10.1007/s00595-021-02232-6.

24. Delanote I, Wuyts WA, Yserbyt J, *et al*. Safety and efficacy of bridging to lung transplantation with antifibrotic drugs in idiopathic pulmonary fibrosis: a case series. BMC Pulm Med 2016; 16(1): 156.

25. Sekine A, Seo K, Matsukura S, *et al*. A case report of idiopathic pleuroparenchymal fibroelastosis with severe respiratory failure in pregnancy. BMC Pulm Med 2020; 20(1): 264.

26. Rasciti E, Cancellieri A, Romagnoli M, *et al*. Suspected pleuroparenchymal fibroelastosis relapse after lung transplantation: a case report and literature review. BJR Case Rep 2019; 5(4): 20190040.

27. Ali MS, Ramalingam VS, Haasler G, *et al*. Pleuroparenchymal fibroelastosis (PPFE) treated with lung transplantation and review of the literature. BMJ Case Rep 2019 Apr 20; 12(4): e229402. doi: 10.1136/bcr-2019-229402. PMID: 31005872; PMCID: PMC6506043.

28. Yanagiya M, Sato M, Kawashima S, *et al*. Flat chest of pleuroparenchymal fibroelastosis reversed by lung transplantation. Ann Thorac Surg 2016; 102(4): e347-9.

29. Goondi D, Franko A, Johannson KA. Pleuroparenchymal fibroelastosis after liver transplantation. Am J Respir Crit Care Med 2021 Jul 15; 204(2): 222-3. doi: 10.1164/rccm.202009-3432IM. PMID: 33662223.

30. Shimada A, Terada J, Tsushima K, *et al*. Veno-venous extracorporeal membrane oxygenation bridged living-donor lung transplantation for rapid progressive respiratory failure with pleuroparenchymal fibroelastosis after allogeneic hematopoietic stem cell transplantation. Respir Investig 2018; 56(3): 258-62.

31. Righi I, Morlacchi L, Rossetti V, *et al*. Lung transplantation as successful treatment of end-stage idiopathic pleuroparenchymal fibroelastosis: a case report. Transplant Proc 2019; 51(1): 235-38.

Salivary Bypass Stent and Intercostal Muscle Flap for Treatment of Cervical Esophageal Conduit Ischemia and Perforation

Yu-Hsiang Wang[1], Cheau-Feng Lin[1,2]

A 57-year-old man with esophageal squamous cell carcinoma in the middle to lower thoracic region underwent thoracoscopic esophagectomy and gastric tube reconstruction with mediastinal node dissection, and on the 7th day post-operation, developed cervical esophageal conduit ischemia and perforation. After decortication, intercostal muscle flap repair and adequate sepsis control, a salivary bypass tube (Boston Montgomery®) was emplaced to bypass the fistula and exclude the salivary alimentary stream. Few studies have reviewed the use of salivary bypass tubes for the management of cervical esophageal conduit ischemia. Herein, we reported a successful case of salvage salivary bypass stent placement for esophageal conduit ischemia and perforation. *(Thorac Med 2023; 38: 250-254)*

Key words: Esophageal tumor, Squamous cell carcinoma, Anastomosis leakage Introduction

Introduction

Esophageal conduit ischemia and necrosis are severe complications and remain some of the most challenging issues after esophagectomy due to their high morbidity and mortality rates [1-2]. Because of the lack of a standardized definition, the incidence of esophageal conduit ischemia has varied from 0.5% to 10% in different studies [3-4]. Several studies have reported on the management of conduit ischemia and perforation, but there is still no gold standard for these complications. Anastomosis and pullback of the gastric tube are always required [5]. In this report, we present the case of a 57-year-old man diagnosed with middle to lower esophageal squamous cell carcinoma post-thoracoscopic esophagectomy and gastric stent reconstruction, who developed gastric conduit ischemic changes and perforation 7 days post-operation. He successfully recovered after a salivary bypass stent and intercostal muscle flap procedure.

Case Presentiont

A 57-year-old man was diagnosed with esophageal squamous cell carcinoma, mod-

[1]Department of Thoracic Surgery, Chung Shan Medical University Hospital, [2]School of Medicine, Chung Shan Medical University
Address reprint requests to: Dr. Cheau-Feng Lin, Department of Thoracic Surgery, Chung Shan Medical University Hospital, Taichung 40201, Taiwan

erately differentiated, cT1N0M0, stage I, in the middle to lower thoracic region following dysphagia for 6 months. After discussion with the patient, he agreed to undergo thoracoscopic esophagectomy, gastric tube reconstruction, mediastinal node dissection and feeding jejunostomy. No regional cancer invasion or lymphadenopathy was noted during the surgery. The whole gastric conduit was pulled up from the posterior mediastinal route, and a side-to-side anastomosis was performed with an Endo-GIA stapler. The final pathological report revealed pT1bN0M0, stage IB cancer. However, on postoperative day (POD) 7, the follow-up chest film revealed haziness and infiltration at the right lung field (Fig. 1). Leukocytosis with sepsis had also developed. Chest computed tomography (CT) revealed several air bubbles at the cervical anastomosis site and massive pleural effusion with right lung atelectasis, which was highly suspected to be due to gastric conduit rupture and empyema (Fig. 2A and 2B).

Thoracoscopic surgery was performed, and a 1×1-cm defect with tip area necrosis was noted at the gastric conduit. After debridement
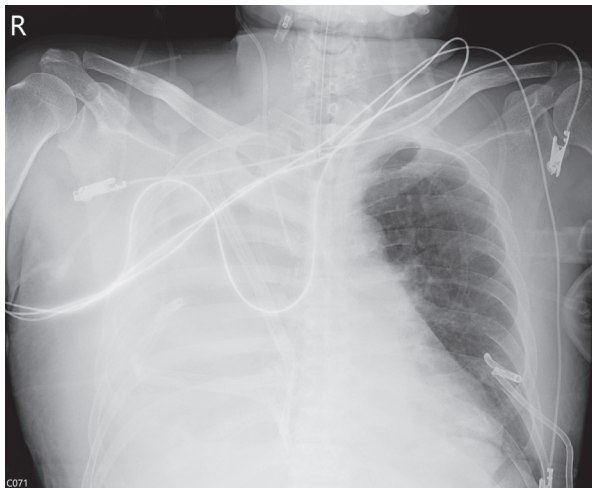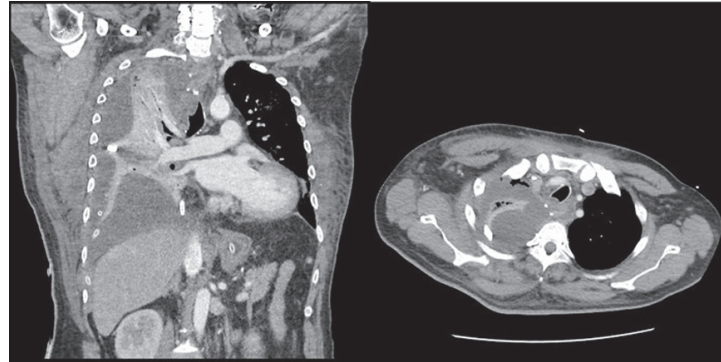

Fig. 2. Contrast-enhanced computed tomography revealed free air at the cervical anastomosis site and massive lobulation effusion, compatible with gastric conduit necrosis and empyema thoracis.
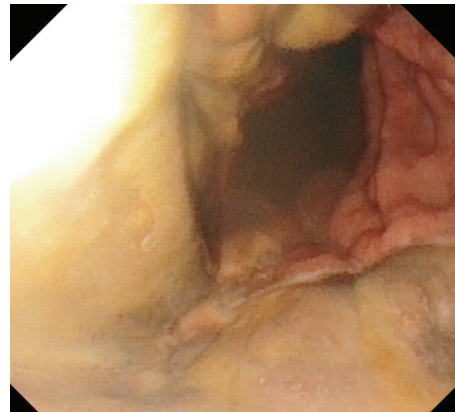

Fig. 3. Esophagoscope, POD 14, revealed non-healing mucosa at the gastric conduit with pus formation.

Fig. 1. Plain film, POD 7: Massive right-side pleural effusion despite chest tube drainage.

of the necrotic area and primary repair of the defect with 4-0 VICRYL® (Ethicon, Inc., Polyglactin-910), an intercostal muscle flap was emplaced, with 3×3-cm coverage of the defect for reinforcement. After surgery, the patient's sepsis and lung consolidation improved. Therefore, on POD 14, after esophagoscopy examination of the perforation site (Fig. 3), a 14-mm salivary bypass stent (Boston Montgomery® 322140R) was emplaced through a rigid esophagoscope. The salivary bypass stent was passed over a bougie, advanced into the esophagus, passed through the esophageal perforation site,

and distally sutured with another nasogastric tube. Then, with another intra-thoracic pigtail and chest tubes emplaced during decortication, the entire irrigation-drainage system was established to bridge the fistulous tract (Fig 4). The irrigation amount was monitored daily, and the distal nasogastric tube was adjusted to reach the desired stent position, generating an ideal environment for the fistula healing process. Follow-up chest film on POD 30 revealed improved right lung infiltration due to adequate drainage after salivary bypass drain emplacement (Fig. 5).

The patient underwent extubation on POD 37, and tolerated room air well. We also arranged for water trials after bypass stent removal on POD 55. His follow-up panendoscopy revealed fistula formation at the previous necrosis site, and the chest tube was also visible
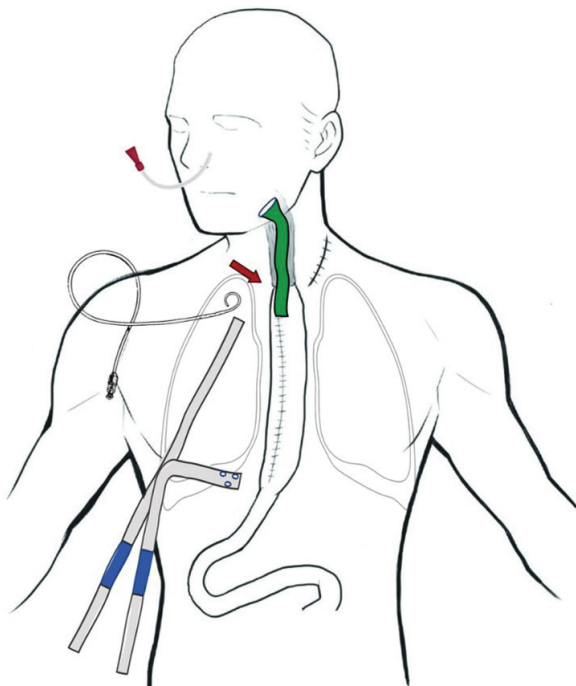

Fig. 5. Plain film on POD 30 revealed that with the irrigation system, the right empyema thoracis and consolidation showed improvement.

Fig. 6. Esophagoscope, POD 55, revealed healing mucosa with 1 fistula formation at the gastric conduit. The chest tube was visible during the examination. Esophagoscope, POD 95, revealed healing mucosa with no fistula formation, but some stricture at the previous fistula side.

Fig. 4. The entire irrigation system: The stent (red arrow) bypassed the oral alimentary stream from the esophageal perforation site and was sutured with the nasogastric tube. The leakage from the alimentary stream that escaped our bypass stent was drained by another intra-thoracic pigtail and chest tube.
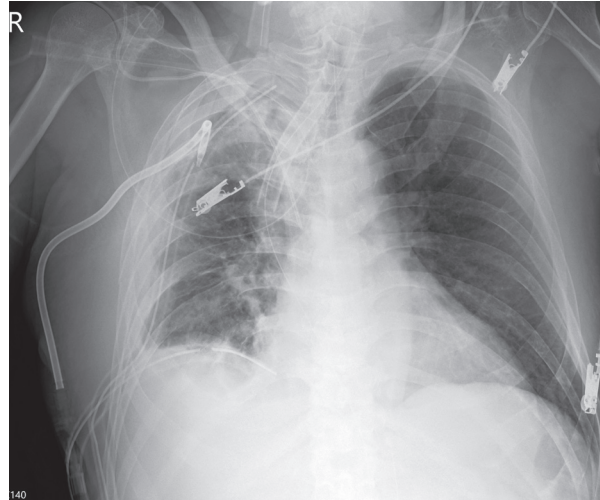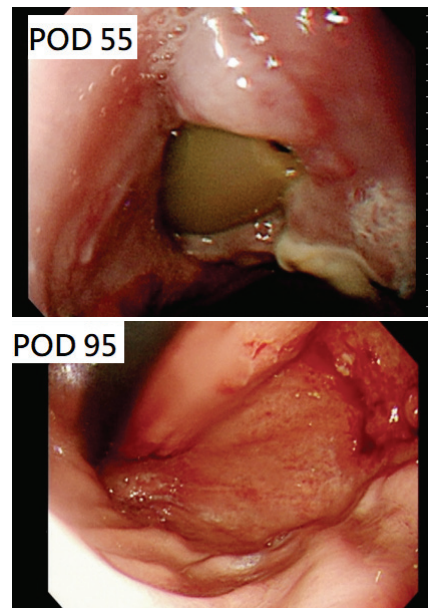
through the hole (Fig. 6-1). His stent drainage amounts decreased gradually, and the bypass drain was removed on POD 66. Chest CT and panendoscopy confirmed that the entire gastric

conduit was intact, and only a mild anastomotic stricture was noted during outpatient department follow-up (Fig. 6-2). He was followed up by our chest surgeon for 1 year, with solid food.

Discussion

Despite progress in surgical techniques, esophageal conduit ischemia, necrosis, and intra-thoracic anastomosis leakage remain some of the most challenging and costly complications. According to Agzariano et al., conduit failure may require at least 73 days of hospitalization and an additional USD68,296 in hospitalization costs [6]. Several non-surgical and surgical management strategies have been proposed to salvage the conduit, with good responses [7]. For a high-risk patient who has recently undergone major surgery, surgical intervention may lead to higher mortality and morbidity than more conservative treatments. In a literature review, endoscopic stent placement had a reported success rate of 72% and a mortality rate of 3.3% [8]. Several stents, including self-expanding metal stents, self-expanding plastic stents, and Montgomery salivary bypass tubes, have been proposed for clinical use in these cases, with good results [9].

The salivary bypass stent (Boston Montgomery® 322140R) was first described in 1955 by William W. Montgomery (Boston, Massachusetts) as a bridging gap between pharyngostomy and esophagostomy following laryngoesophagectomy [10]. Since its introduction, several additional indications had been proposed, including fistula management, palliation of dysphagia caused by malignancy, esophageal stricture, and reconstruction of the cervical esophagus [11, 12]. Kim *et al*. demonstrated its use in a series of 17 patients with esophageal

complications, including esophageal disruptions (13 patients) and chronic fistula (3 patients), with 6% mortality (1 patient) [13]. The salivary bypass stent serves as a bypass route, excluding the oral alimentary stream, and provides an optimal environment for fistula healing. However, migration was the most common complication in several studies, and occurred in more than 35% of cases in which an external stent without suture fixation in the conduit was used [14]. In addition, long-term placement of the salivary bypass stent may also cause colonization of antibiotic-resistant Gram-negative pathogens, especially *Klebsiella pneumoniae*, which may lead to further opportunistic infections [15]. There were also some case reports and series reporting serious complications due to failure of stenting, in which esophageal erosion eventually occurred in the great vessels [16].

Although several studies have demonstrated the successful use of endoscopic stenting for the management of esophageal conduit ischemia, necrosis, and anastomotic leak, these were all small and limited case studies with heterogeneous clinical situations. In our case, another nasogastric tube fixation was emplaced with the salivary bypass stent beforehand, and this could reset the stent to the optimal position. The length of time from the initial surgery to the bypass stent emplacement was 52 days, which was similar to that reported by Kim et al. There has been no literature review regarding the timing of salivary stent removal because of its rarity and due to disease complexities. In our case, we successfully combined a muscle flap with a salivary bypass stent for the management of gastric conduit necrosis. Further studies should focus on preventing stent migration and determining the optimal timing of stent removal.

Conclusion

Salivary bypass stents with primary repair served as an effective way of salvaging esophageal conduit ischemia and necrosis in our case. The stent with an irrigation-drainage system helps avoid salivary leakage into the pleural cavity and provides optimal conditions for preventing sepsis progress. Despite the existence of only a few case series regarding the use of a salivary bypass stent in esophageal conduit ischemia and different manipulations, our case provides an effective example of combined salivary bypass stent and muscle flap repair.

References

1. Wormuth JK, Heitmiller RF. Esophageal conduit necrosis. Thorac Surg Clin 2006; 16(1): 11-22.

2. Fumagalli U, Baiocchi GL, Celotti A, *et al*. Incidence and treatment of mediastinal leakage after esophagectomy: insights from the multicenter study on mediastinal leaks. World J Gastroenterol 2019; 25(3): 356-66.

3. Briel JW, Tamhankar AP, Hagen JA, *et al*. Prevalence and risk factors for ischemia, leak, and stricture of esophageal anastomosis: gastric pull-up versus colon interposition. J Am Coll Surg 2004; 198(4): 536-41.

4. Luketich JD, Pennathur A, Awais O, *et al*. Outcomes after minimally invasive esophagectomy: review of over 1000 patients. Ann Surg 2012; 256(1): 95-103.

5. Athanasiou, A., Hennessy M, Spartalis E, *et al*. Conduit necrosis following esophagectomy: an up-to-date literature review. World J Gastrointest Surg 2019; 11(3): 155-68.

6. Agzarian J, Visscher SL, Knight AW, *et al*. The cost burden of clinically significant esophageal anastomotic leaks—a steep price to pay. J Thorac Cardiovasc Surg 2019; 157(5): 2086-92.

7. Famiglietti A, Lazar JF, Henderson H, *et al*. Management of anastomotic leaks after esophagectomy and gastric pull-up. J Thorac Dis 2020; 12(3): 1022-1030.

8. Schaheen L, Blackmon SH, Nason KS. Optimal approach to the management of intrathoracic esophageal leak following esophagectomy: a systematic review. Am J Surg 2014; 208(4): 536-43.

9. van Boeckel PGA, Sijbring A, Vleggaar FP, *et al*. Systematic review: temporary stent placement for benign rupture or anastomotic leak of the oesophagus. Aliment Pharmacol Ther 2011; 33(12): 1292-1301.

10. Montgomery WW. Current modifications of the salivary bypass tube and tracheal T-tube. Ann Otol Rhinol Laryngol 1986; 95(2): 121-5.

11. Minni A, Ralli M, Di Cianni S, *et al*. Montgomery salivary bypass tube in head and neck cancer: the experience of our otolaryngology clinic. Ear Nose Throat J 2020; (101)7: 463-7.

12. Tirelli G.R, Baruca R, Nata FB. Salivary bypass tube placement in esophageal stricture: A technical note and report of three cases. Auris Nasus Larynx 2017; 44(6): 758-61.

13. Kim AW, Liptay MJ, Snow N, *et al*. Utility of silicone esophageal bypass stents in the management of delayed complex esophageal disruptions. Ann Thorac Surg 2008; 85(6): 1962-7.

14. Warren WH, Smith C, Faber LP. Clinical experience with Montgomery salivary bypass stents in the esophagus. Ann Thorac Surg 1994; 57(5): 1102-7.

15. Grasl S, Janik S, Grasl MC, *et al*. Bacterial colonization of Montgomery salivary bypass tubes after hypopharyngeal reconstruction in head and neck cancer patients. Eur Arch Otorhinolaryngol 2020; 277(4): 1149-54.

16. D'Cunha J, Rueth NM, Groth SS, *et al*. Esophageal stents for anastomotic leaks and perforations. J Thorac Cardiovasc Surg 2011; 142(1): 39-46.e1.

Successful Treatment of Leptomeningeal Metastasis Using Intrathecal Chemotherapy in a Patient Harboring an Epidermal Growth Factor Receptor L858R Mutation: A Case Report

Geng-Ning Hu[1], Meng-Rui Lee[1], Chao-Chi Ho[1]

Leptomeningeal metastasis (LM) is a poor prognostic factor for lung cancer, and its incidence is increasing in non–small cell lung cancer (NSCLC) patients. The treatment effect of systemic chemotherapy and radiotherapy is not good. In patients with oncogenic drivers, the treatment of choice is tyrosine kinase inhibitors (TKIs), which have a high central nervous system (CNS) penetration ability. Here, we reported the case of 47-year-old female NSCLC patient with an epidermal growth factor receptor (EGFR) L858R mutation who was diagnosed as having LM via magnetic resonance imaging and cerebrospinal fluid cytology after treatment with TKIs, immunotherapy, chemotherapy, and anti-EGFR monoclonal antibody. Salvage whole brain radiotherapy was administered. Owing to the progression of CNS symptoms and intolerance of the side-effects of systemic anti-cancer therapy, osimertinib and bevacizumab combined intrathecal chemotherapy with pemetrexed (IP) were initiated. The patient achieved remission of neurologic symptoms, stable brain metastases and long-term survival without notable adverse events. IP, when combined with tailored systemic anti-cancer therapy, provides a potential therapeutic option for patients with EGFR-mutant LM who have failed TKIs treatment. *(Thorac Med 2023; 38: 255-260)*

Key words: intrathecal chemotherapy, leptomeningeal metastasis, lung cancer

Introduction

Up to 5% of patients with non-small cell lung cancer (NSCLC) will develop leptomeningeal metastasis (LM) at the time of initial diagnosis or during treatment, and this is more common among adenocarcinoma patients [1,2]. Furthermore, the incidence of LM is higher in patients with epidermal growth factor receptor tyrosine kinase inhibitor (EGFR-TKI)-targetable mutations, because of the prolonged survival achieved by molecular targeted therapy [3].

LM can cause damage to the cerebral hemisphere, cranial nerves and spinal cord, and

[1]Division of Pulmonary and Critical Care Medicine, Department of Internal Medicine, National Taiwan University Hospital, Taipei, Taiwan
Address reprint requests to: Dr. Geng-Ning Hu, Division of Pulmonary and Critical Care Medicine, Department of Internal Medicine, National Taiwan University Hospital, No.7, Chung Shan S. Rd., Zhongzheng Dist., Taipei City 100225, Taiwan (R.O.C.)

associated roots, resulting in a progressive decline in the functional status of the patient and rapid progression to mortality if left untreated. Because of the limited ability to penetrate the blood-brain barrier (BBB), traditional treatment methods are not ideal. Despite the continuous development of traditional treatments, such as EGFR-TKIs, systemic chemotherapy and whole-brain radiotherapy (WBRT), the prognosis for NSCLC patients with LM remains poor, and median survival time is only 3-11 months [2,4]. Limited data are available to establish treatment recommendations for the management of LM. Furthermore, no randomized trials have shown a survival benefit from a specific treatment, and the optimal strategy is still poorly defined [5].

Pemetrexed is an anti-folate antimetabolite. Compared with methotrexate, pemetrexed has a broader spectrum of anti-tumor effects through its targeting of 3 enzymes, including thymidylate synthase, dihydrofolate reductase, and glycinamide ribonucleotide formyl transferase [3]. Pemetrexed combined with platinum is considered to be 1 of the first-line treatment options for advanced NSCLC with or without brain metastases [6-7]. This implies that pemetrexed has the potential capacity to overcome central nervous system (CNS) involvement. Nevertheless, concentrations of pemetrexed in the cerebrospinal fluid (CSF) remained low using the intravenous route [8-9]. Intrathecal chemotherapy with pemetrexed (IP) may be a way to overcome the limited CSF penetration. The ChiCTR1800016615 study by Fan et al. found that intrathecal administration of 50 mg of pemetrexed resulted in few adverse events (AEs) and achieved a good response rate of 84.6% for patients with EGFR-mutant NSCLC-LM who had failed TKIs [10].

Here, we report the case of a patient with LM from EGFR mutation-positive NSCLC who achieved both clinical and CSF cytological responses to IP.

Case Report

A 47-year-old woman presented to our hospital in June 2018 with intermittent productive cough for months. She was a non-smoker and had childhood asthma. Serial image studies showed a left upper lung tumor with mediastinal lymphadenopathies, right iliac bone metastasis, and multiple brain metastases. Transbronchial biopsy was performed, and the pathology confirmed lung adenocarcinoma. EGFR testing revealed exon 21 L858R mutations. Systemic anti-cancer therapy was started with erlotinib 150 mg daily and the anti-angiogenic agent bevacizumab, which was shifted to osimertinib 80 mg daily in November 2018, due to its better CNS permeation. Remission of brain metastases was noticed in the follow-up images.

However, the brain MRI in April 2019 revealed progressive disease with enlarged brain metastases. WBRT was initiated, and a double dosage of osimertinib along with bevacizumab were administered.

In early 2021, facial palsy with mild blurred vision was noticed. Gait instability, hearing impairment, and occasional loss of consciousness were also recorded. LM was confirmed by brain MRI in April 2021, showing hyperintensity at the basal cistern and the fourth ventricle (Figure 1). The CSF analysis also revealed positivity of malignant cells, with L858R and TP53 mutations detected in the CSF next-generation sequencing study. Thus, osimertinib combined with immunotherapy, chemotherapy, and anti-EGFR monoclonal antibody were implemented,
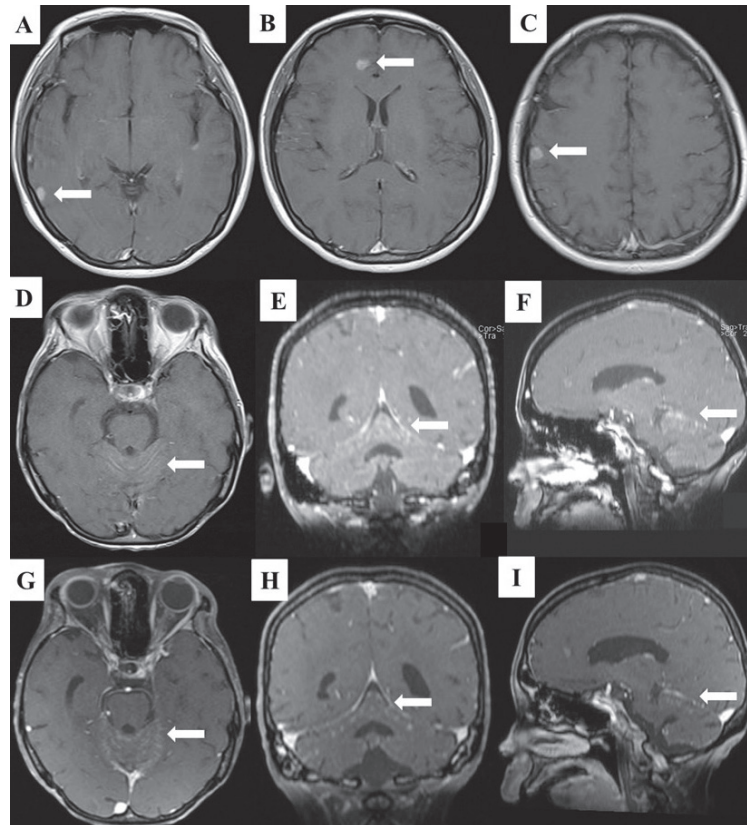
Fig. 1. The status of BM and LM lesions before and after IP. (A-C) Brain MRI with contrast on July 4, 2018, revealed multiple metastatic brain lesions located in the bilateral cerebral and cerebellar hemispheres (as indicated by the white arrows). (D-F) Brain MRI with contrast on September 13, 2021, showed the onset of LM (as indicated by the white arrows). (G-I) Brain MRI with contrast on August 12, 2022, showed stable LM lesions (as indicated by the white arrows) after 9 courses of IP. BM, brain metastases; LM, leptomeningeal metastasis; IP, intrathecal chemotherapy with pemetrexed; MRI, magnetic resonance imaging.

including 1 cycle of atezolizumab, carboplatin, and pemetrexed, and 1 cycle of cetuximab. Salvage WBRT was also initiated. Nevertheless, adverse effects including general malaise and severe mucositis were reported. Intermittent headache, hearing loss, and mild slurred speech occurred during this period.

Owing to the progression of CNS symptoms and intolerance to systemic therapy, IP was implemented on day 1 and 5 every 21 days, along with auxiliary betamethasone via lumbar drainage catheter. The dosage of pemetrexed was set at 30 mg during the first 3 cycles and titrated to 50 mg for the later cycles. The patient also continued to take high dose osimer-

tinib (160 mg daily) and bevacizumab. This combined treatment relieved the neurological defects and led to improvement in MRI images of the lesions (Figure 1) and in CSF cytology. Grade 2 neutropenia as an adverse effect was recorded, with no significant complications. Her condition related to LM remained stable for the following 15 months. The whole course of diagnosis and treatment has been organized as a timeline (Figure 2).

Discussion

Most patients with NSCLC-LM are in a critical, life-threatening condition. Patients with
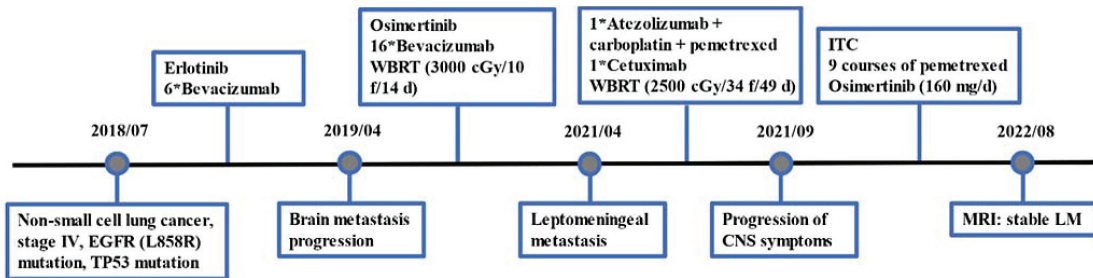
Fig. 2. Timeline for the diagnosis, treatment, and outcome of this patient. WBRT, whole brain radiotherapy; CNS, central nervous system; ITC, intrathecal chemotherapy; MRI, magnetic resonance imaging; LM, leptomeningeal metastasis.

EGFR-mutated lung cancer have a higher incidence of LM than their EGFR wild-type counterparts (9.4% vs. 1.7%) [4].

There is currently no consensus or standard guidelines for the treatment of LM associated with advanced NSCLC [4]. The third-generation TKI osimertinib has standout antineoplastic activity and several-fold higher ability to permeate the BBB than other EGFR-TKIs [11]. Osimertinib has impressive efficacy in controlling both systemic and CNS diseases. Thus, it is the preferred choice for patients with LM from EGFR-mutant NSCLC [12]. NSCLC patients with LM treated with osimertinib experienced an LM objective response rate of 55% to 62%, and median progression-free survival (PFS) of 8 to 11 months [13-15]. Based on the above-mentioned evidence, we chose osimertinib for this patient. The BLOOM study reported that high-dose osimertinib (160 mg daily) had a significant treatment effect on patients with EGFR-mutant NSCLC with LM and a manageable safety profile [13]. The median investigator-assessed PFS was 8.6 months (95% CI: 5.4–13.7 months). Thus, current evidence supports the use of high-dose osimertinib in EGFR-mutated LM patients when standard-dose TKIs are ineffective.

Pemetrexed is a compound currently approved both in combination with platinum in a first-line setting and as a single agent in a maintenance or second-line setting for the treatment of non-squamous NSCLC, especially for patients with an adenocarcinoma histology [5]. Pemetrexed demonstrated consistent activity against brain metastases from NSCLC with an intracranial response rate of about 40% [6,16]. A previous study indicated that IP was an effective therapeutic approach against LM from NSCLC [17], and that this approach can achieve higher and more stable concentrations in the CNS [18-19]. In the ChiCTR1800016615 study, the recommended dose of pemetrexed observed in the phase 1 study was 50 mg [10]. Grade 3-4 myelosuppression, physical pain, or headache was observed in this study, in spite of supplementation with vitamin B12 and folic acid. However, our case only had grade 2 myelosuppression. Whether an increased dose of pemetrexed will increase the incidence of AEs requires more evidence. However, the application of a novel intrathecal drug like pemetrexed, combined with appropriate systemic treatment, could be considered for the treatment of LM patients with NSCLC.

Bevacizumab is a recombinant humanized monoclonal antibody that targets vascular endothelial growth factor. The BRAIN study

reported the encouraging efficacy of bevacizumab with first-line paclitaxel and carboplatin in patients with asymptomatic, untreated brain metastases with NSCLC [20]. The response rate of brain metastases in this study was as high as 61.2% [21].

Radiotherapy can be effective for isolated lesions in the brain, whereas whole brain and craniospinal radiotherapy are not effective for LM diffuse lesions; these approaches are controversial due to severe marrow suppression and increased mortality [22]. There is currently no consensus about the role of WBRT in LM [3].

With respect to gene testing, the EGFR mutation types in the CSF were highly concordant with those in the primary tumor, suggesting that gene testing of the CSF could guide clinical management. Liquid biopsy of CSF is a reliable method for identifying the genetic characteristics of LM. This is because circulating tumor DNA from CSF more accurately represents genomic alterations in CNS lesions than circulating tumor DNA from plasma [23]. A previous study compared the different genetic profiles of CSF to peripheral plasma and found that CSF as a liquid biopsy specimen could facilitate translational research programs and help personalize follow-up care [24].

In summary, IP showed controllable toxicity and good efficacy, prolonged survival time and improved quality of life when combined with tailored systemic antitumor therapy in lung cancer patients with LM. Further prospective studies are needed to explore the optimal dose, frequency of administration, and optimal treatment duration of IP.

Conclusion

In this article, we presented the case of a patient with NSCLC-LM harboring an EGFR exon 21 L858R mutation, who responded well to IP. This case provides a practicable option for such patients. Furthermore, 50 mg of pemetrexed is an appropriate dose with few adverse effects and a promising response during the following 15 months.

References

1. Reckamp KL. Targeted therapy for patients with metastatic non-small cell lung cancer. J Natl Compr Canc Netw 2018; 16: 601-4.
2. Remon J, Le Rhun E, Besse B. Leptomeningeal carcinomatosis in non-small cell lung cancer patients: a continuing challenge in the personalized treatment era. Cancer Treat Rev 2017; 53: 128-37.
3. Cheng H, Perez-Soler R. Leptomeningeal metastases in non-small-cell lung cancer. Lancet Oncol 2018; 19: e43-55.
4. Li YS, Jiang BY, Yang JJ, *et al*. Leptomeningeal metastases in patients with NSCLC with EGFR mutations. J Thorac Oncol 2016; 11: 1962-9.
5. Turkaj A, Morelli AM, Vavalà T, *et al*. Management of leptomeningeal metastases in non-oncogene addicted non-small cell lung cancer. Front Oncol 2018; 8: 278.
6. Barlesi F, Gervais R, Lena H, *et al*. Pemetrexed and cisplatin as first-line chemotherapy for advanced non-small-cell lung cancer (NSCLC) with asymptomatic inoperable brain metastases: a multicenter phase II trial (GFPC 07-01). Ann Oncol 2011; 22: 2466-70.
7. Scagliotti GV, Parikh P, von Pawel J, *et al*. Phase III study comparing cisplatin plus gemcitabine with cisplatin plus pemetrexed in chemotherapy-naive patients with advanced-stage non-small-cell lung cancer. J Clin Oncol 2008; 26: 3543-51.
8. Stapleton SL, Reid JM, Thompson PA, *et al*. Plasma and cerebrospinal fluid pharmacokinetics of pemetrexed after intravenous administration in non-human primates. Cancer Chemother Pharmacol 2007; 59: 461-6.
9. Dai H, Chen Y, Elmquist WF. Distribution of the novel antifolate pemetrexed to the brain. J Pharmacol Exp Ther 2005; 315: 222-9.
10. Fan C, Zhao Q, Li L, *et al*. Efficacy and safety of

intrathecal pemetrexed combined with dexamethasone for treating tyrosine kinase inhibitor-failed leptomeningeal metastases from EGFR-mutant NSCLC-a prospective, open-label, single-arm phase 1/2 clinical trial (unique identifier: chiCTR1800016615). J Thorac Oncol 2021; 16: 1359-68.

11. Ballard P, Yates JW, Yang Z, *et al*. Preclinical comparison of osimertinib with other EGFR-TKIs in EGFR-mutant NSCLC brain metastases models, and early evidence of clinical brain metastases activity. Clin Cancer Res 2016; 22: 5130-40.

12. Ettinger DS, Wood DE, Aisner DL, *et al*. NCCN Guidelines Insights: non-small cell lung cancer, version 2.2021. J Natl Compr Canc Netw 2021; 19: 254-266.

13. Yang JCH, Kim SW, Kim DW, *et al*. Osimertinib in patients with epidermal growth factor receptor mutation-positive non-small-cell lung cancer and leptomeningeal metastases: the BLOOM study. J Clin Oncol 2020; 38: 538-47.

14. Lee J, Choi Y, Han J, *et al*. Osimertinib improves overall survival in patients with EGFR-mutated NSCLC with leptomeningeal metastases regardless of T790M mutational status. J Thorac Oncol 2020; 15: 1758-66.

15. Ahn MJ, Chiu CH, Cheng Y, *et al*. Osimertinib for patients with leptomeningeal metastases associated with EGFR T790M-positive advanced NSCLC: the AURA leptomeningeal metastases analysis. J Thorac Oncol 2020; 15: 637-48.

16. Bailon O, Chouahnia K, Augier A, *et al*. Upfront association of carboplatin plus pemetrexed in patients with brain metastases of lung adenocarcinoma. Neuro Oncol 2012; 14: 491-5.

17. Li H, Lin Y, Yu T, *et al*. Treatment response to intrathecal chemotherapy with pemetrexed via an Ommaya reservoir in EGFR-mutated leptomeningeal metastases from non-small cell lung cancer: a case report. Ann Palliat Med 2020; 9: 2341-6.

18. Sun JM, Nam MH, Chung JY, *et al*. Safety and pharmacokinetics of intrathecal administration of pemetrexed in rats. Cancer Chemother Pharmacol 2011; 68: 531-8.

19. Pan Z, Yang G, Cui J, *et al*. A pilot phase 1 study of intrathecal pemetrexed for refractory leptomeningeal metastases from non-small-cell lung cancer. Front Oncol 2019; 9: 838.

20. Besse B, Le Moulec S, Mazières J, *et al*. Bevacizumab in patients with nonsquamous non-small cell lung cancer and asymptomatic, untreated brain metastases (BRAIN): a nonrandomized, phase II study. Clin Cancer Res 2015; 21: 1896-1903.

21. Brower JV, Saha S, Rosenberg SA, *et al*. Management of leptomeningeal metastases: prognostic factors and associated outcomes. J Clin Neurosci 2016; 27: 130-7.

22. Chamberlain MC. Leptomeningeal metastasis. Curr Opin Oncol 2010; 22: 627-35.

23. De Mattos-Arruda L, Mayor R, Ng CKY, *et al*. Cerebrospinal fluid-derived circulating tumour DNA better represents the genomic alterations of brain tumours than plasma. Nat Commun 2015; 6: 8839.

24. Li YS, Jiang BY, Yang JJ, *et al*. Unique genetic profiles from cerebrospinal fluid cell-free DNA in leptomeningeal metastases of EGFR-mutant non-small-cell lung cancer: a new medium of liquid biopsy. Ann Oncol 2018; 29: 945-52.

Hyperbaric Oxygen Therapy to Treat Iatrogenic Air Embolism Following CT-guided Lung Biopsy: Case Reports

Chuan-Yen Sun[1], Yen-Wen Chen[1,2], Kuang-Yao Yang[1,2]

Computed tomography (CT)-guided biopsy is a well-established technique to obtain lung tissue for evaluation of a pulmonary lesion. Several complications after transthoracic biopsy have been documented, but seldom led to a catastrophic outcome. Air embolism is a rare but fatal complication of CT-guided lung biopsy and can result in morbidity and mortality. Hyperbaric oxygen therapy (HBOT) is defined as treatment with 100% oxygen in air pressure higher than 1.4 atmosphere absolute (ATA). It plays a crucial role in treating systemic air embolism and may reduce neurological sequelae. *(Thorac Med 2023; 38: 261-266)*

Key words: air embolism, percutaneous lung biopsy, hyperbaric oxygen therapy

Introduction

Percutaneous CT-guided lung biopsy remains a widely used method in diagnosing a pulmonary nodule or mass [1]. Pneumothorax and lung parenchymal hemorrhage are common complications after the procedure, but seldom lead to morbidity and mortality. Air embolism is extremely rare, with an estimated incidence of 0.01 to 0.4%, but this incidence could be underestimated due to misdiagnosing cases without symptoms [2]. Air embolism is caused by the entry of air into systemic circulation, and may lead to tissue or organ ischemia, such as coronary infarction, stroke or spinal infarction.

Air bubbles in the systemic circulation may block blood flow and cause tissue inflammation and ischemia [3]. Urgent management of air embolism is important to prevent further tissue damage and reduce cardiac or neurological sequelae.

Hyperbaric oxygen therapy (HBOT) remains the critical treatment for systemic air embolism. HBOT can exchange nitrogen in air bubbles with oxygen and induce bubble absorption, and, eventually, decrease bubble volume [4]. A previous study reported that HBOT could also lead to cerebral vasoconstriction, lower intracranial pressure, and a better neurological outcome [5].

[1]Department of Chest Medicine, Taipei Veterans General Hospital, Taipei, Taiwan, [2]School of Medicine, National Yang Ming Chiao Tung University, Taipei, Taiwan
Address reprint requests to: Dr. Yen-Wen Chen, Department of Chest Medicine, Taipei Veterans General Hospital 201, Section 2, Shih-Pai Road, Taipei, 112, Taiwan

We report below 2 cases of systemic air embolism followed by percutaneous lung biopsy treated with HBOT.

Case Report

Case 1

This 61-year-old male was an ex-smoker with past medical histories of schizophrenia under olanzapine treatment, chronic obstructive pulmonary disease, hypertension, and hyperlip-idemia, who presented with an isolated pulmonary nodular lesion, measuring 2.0 cm, at his right lower lobe (RLL) (Figure 1A). Therefore, CT-guided lung biopsy was performed. Before the procedure, there was no obvious abnormal finding in his blood test. During his CT-guided biopsy, the patient had sudden vigorous coughing. Right after the coughing, the radiologist found free air within the aorta and pneumome-diastinum, with right-sided pneumothorax during the procedure (Figure 1B) (Figure 1C). Fortunately, his vital signs remained stable, and no
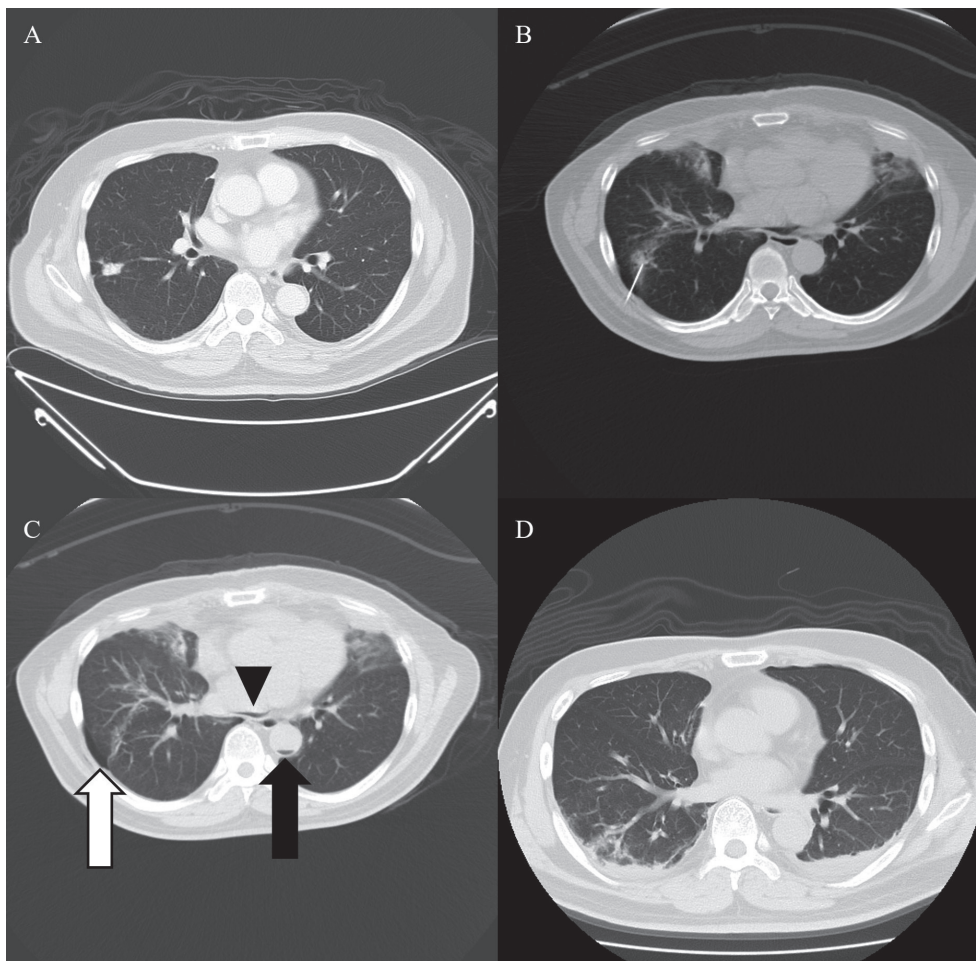

Fig. 1. (A) A 2.0 cm nodule is noted at the right lower lobe (RLL) of the lung, with pleural traction. (B) Computed tomography (CT)-guided percutaneous lung biopsy for the RLL lesion. (C) Free air accumulation in the aorta (arrow) and pneumomediastinum (arrowhead) with right-side pneumothorax (white arrow). (D) CT scan after hyperbaric oxygen therapy (HBOT), and there was no residual free air in the cardiovascular system.

neurological deficit was noted. The patient was put in a Trendelenburg position immediately. A 12 French pig-tail drainage was inserted with a negative pressure of 15 cm H2O for the right-side pneumothorax. After the drain was placed, the patient underwent a course of HBOT (2.5 ATA) for 2 hours in a multi-place chamber (HAUX-IIFE SUPPORT, Germany). We repeated the whole-body CT scan 30 minutes after HBOT, and it showed no residual free air (Figure 1D). He was found to have mild troponemia (high-sensitive cardiac troponin T (hs-cTnT) of 151.0 ng /L) about 6 hours after the event (normal reference: 3.0-14.0 ng /L). The patient was sent to the intensive care unit for further monitoring. The decline in his hs-cTnT level was checked (57.5 ng /L). Subsequent observation of the patient was uneventful and no neurological deficit was noted during his follow-up.

Case 2

This 66-year-old man was a heavy smoker and had the underlying disease of left renal cell carcinoma status post-left open radical nephrectomy. During the follow-up of his renal cell carcinoma at the outpatient genitourinary department, a chest CT was arranged and an 8 mm-sized nodular lesion was seen at the RLL (Figure 2A). Observation at the outpatient chest surgery department was suggested for the abnormal RLL lesion. Another chest CT followed about 75 days later, and a slight increase in the size of the RLL subsolid lesion, compared with the previous image, was seen. Moreover, another newly formed 5 mm lesion located at the RLL was noted (Figure 2B and 2C).

Due to a high degree of suspicion of lung metastasis, he was suggested to be admitted for pre-operative CT-guided localization, and for subsequent video-assisted thoracic surgery (VATS) wedge resection of both of his RLL lesions. Prior to CT-guided localization of the 2 lesions, the blood test showed no contraindications to the procedure. According to the medical record, the patient denied any neurologic discomfort, except that mildly blurred vision was mentioned. Therefore, he received CT-guided localization of his pulmonary lesions. After deployment of the hook-wire to the first lesion under CT guidance (Figure 3A), another hook-wire cannula was advanced to the second lesion. However, the patient had sudden vigorous coughing and kept moving his body. The procedure was discontinued immediately, and a
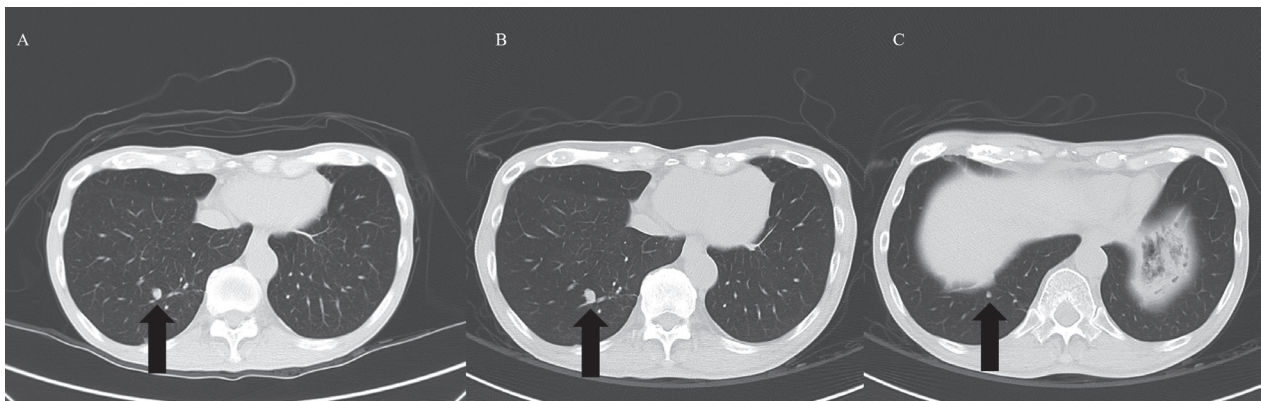

Fig. 2. (A) 8-mm nodular lesions at the RLL at the initial presentation (arrow). (B) Slight increase in the size of the previous RLL lesion during follow-up (arrow). (C) Another new pulmonary lesion at the RLL seen in the following chest CT (arrow).
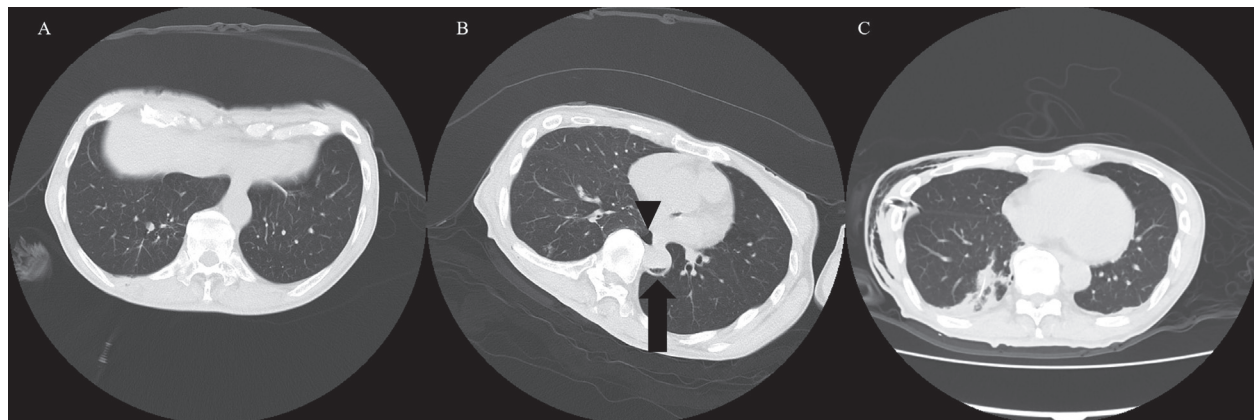
Fig. 3. (A) A hook-wire was deployed at the RLL lesion under CT scan guidance. (B) Free air accumulation within the thoracic aorta (arrow) and right-side minimal pneumothorax (arrowhead). (C) CT scan revealed no free air within the cardiovascular system after HBOT. Chest tube insertion for right-side pneumothorax and a hook-wire at the RLL lesion.

whole lung CT scan was conducted right after the event. The CT scan revealed minimal pneumothorax and free air located in the thoracic aorta (Figure 3B). The cannula for the second lesion was removed. A chest tube was emplaced for the right-side pneumothorax, and pure oxygen was given.

The patient's vital signs remained stable during and after the event, and he was referred for HBOT. Two hours of HBOT (2.5 ATA) was performed and a whole-body CT scan followed. No obvious air accumulation in the cardiovascular system was observed (Figure 3C). The patient underwent VATS wedge resection of his pulmonary lesions 1 hour after confirming that there was no residual free air. However, a new neurologic sign, with eye deviation to the right side, developed in the postoperative room. Urgent magnetic resonance imaging (MRI) of the brain was performed. The MRI showed gyriform restricted diffusion at the bilateral occipital lobes, more at the left side and predominant on the cortex, compatible with acute stroke (Figure 4). There was no significant MR angiography evidence of a visible filling defect within the bilateral internal carotid arteries,
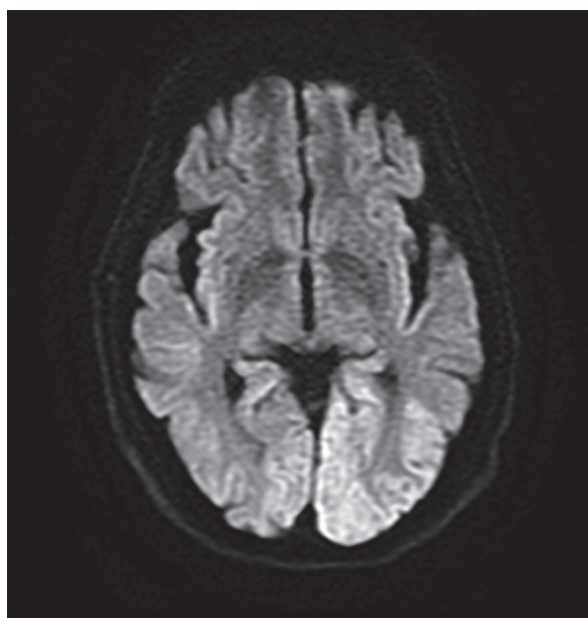

Fig. 4. Gyriform restricted diffusion at the bilateral occipital lobes, more to the left side and predominant on the cortex, compatible with acute stroke.

bilateral middle cerebral arteries, bilateral anterior cerebral arteries, basilar artery, or bilateral vertebral arteries. After consulting the neurologist, administration of anti-convulsive agents was suggested. Furthermore, an ophthalmologist was consulted for the patient's blurred vision, which was compatible with acute stroke in

the bilateral occipital lobes with cortical blindness. His blurred vision and limited extraocular motion improved gradually after treatment and, eventually, the patient was discharged under relatively stable condition.

Discussion

Air embolism is a rare, but potentially fatal complication after percutaneous CT-guided lung biopsy. Air or gas embolism is a condition in which air bubbles in the blood cause blood flow obstruction, followed by tissue hypoperfusion and cell death. A possible mechanism is gas entering the pulmonary veins or arteries of the systemic circulation. Another potential cause is the formation of fistula between the pulmonary veins and alveoli or bronchi caused by a biopsy needle [6]. The risk factors related to systemic air embolism include a lesion located at the lower lobes of the lung, a lesion above the level of the left atrium, use of a coaxial biopsy device, longer distance between the ventilated lung and the biopsy needle, number of biopsies, coughing during the procedure, being under positive pressure ventilation, and a lesion with cavitation [7].

In the treatment of systemic air embolism, HBOT plays an important role in reducing morbidity. HBOT has 2 major mechanisms: hyperoxygenation and shrinkage of the air bubble. According to Henry's law, a pressure of 3 ATA may lead to 6 ml of O_2 dissolved in the plasma and eventually increase oxygenation [8]. In an application of Boyle's law, a 6-fold increase in the atmospheric pressure will shrink the air bubble volume and diameter to 16.6% and 55% of its original size and length, respectively, and achieve decompression of the air bubble [9].

Cerebral air embolism is a serious and le-thal complication of systemic air embolism. Regarding this, some studies have reported that HBOT may have some neuroprotective effects, in addition to its previously mentioned benefits. In some animal studies, the potential recovery of cortical somatosensory ability was 50-fold more in HBOT-treated animals than in a control group [10]. Another animal study found that after middle cerebral artery occlusion, HBOT reduced striatal dopamine secretion and decreased focal brain injury [11]. Moreover, cerebral edema was improved by vasoconstriction due to hyperoxygenation, and this led to better neurological outcomes [12].

In previous experience, managing acute gas embolism followed by percutaneous lung biopsy required providing compression to 3 atmospheres for 90 minutes [13]. Both of our patients were diagnosed with iatrogenic air embolism caused by CT-guided percutaneous lung biopsy and were referred to HBOT for 2 hours under 2.5 ATA right after the event. Neither patient had significant neurologic sequelae, and were then discharged. Our experience with these 2 cases suggests that early consultation with an HBOT expert in treating systemic air embolism is crucial. Further research is needed to investigate the potential mechanism of how neurologic outcomes are improved with HBOT.

References

1. Li GC, Fu YF, Cao W, *et al*. Computed tomography-guided percutaneous cutting needle biopsy for small (</= 20 mm) lung nodules. Medicine (Baltimore) 2017; 96(46): e8703.
2. Ibukuro K, Tenaka R, Takeguchi T, *et al*. Air embolism and needle track implantation complicating CT-guided percutaneous thoracic biopsy: single-institution experience. AJR Am J Roentgenol 2009; 193(5): W430-6.

3. Ramaswamy R, Narsinh KH, Tuan A, *et al*. Systemic air embolism following percutaneous lung biopsy. Semin Intervent Radiol 2014; 31(4): 375-7.

4. Trent JS, Hodgson JK, Ackermann B, *et al*. Hyperbaric oxygen therapy for vascular air embolism from iatrogenic intravenous infusion of air in a patient with atrial septal defect: a case report. Cureus 2020; 12(8): e9554.

5. Huang L, Obenaus A. Hyperbaric oxygen therapy for traumatic brain injury. Med Gas Res 2011; 1(1): 21.

6. Franke M, Reinhardt HC, von Bergwelt-Baildon M, *et al*. Massive air embolism after lung biopsy. Circulation 2014; 129(9): 1046-7.

7. Rott G, Boecker F. Influenceable and avoidable risk factors for systemic air embolism due to percutaneous CT-guided lung biopsy: patient positioning and coaxial biopsy technique-case report, systematic literature review, and a technical note. Radiol Res Pract 2014; 2014: 349062.

8. Bhutani S, Vishwanath G. Hyperbaric oxygen and wound healing. Indian J Plast Surg 2012; 45(2): 316-24.

9. Ziser A, Adir Y, Lavon H, *et al*. Hyperbaric oxygen therapy for massive arterial air embolism during cardiac operations. J Thorac Cardiovasc Surg 1999; 117(4): 818-21.

10. Ahmadi F, Khalatbary AR. A review on the neuroprotective effects of hyperbaric oxygen therapy. Med Gas Res 2021; 11(2): 72-82.

11. Yang ZJ, Camporesi C, Yang X, *et al*. Hyperbaric oxygenation mitigates focal cerebral injury and reduces striatal dopamine release in a rat model of transient middle cerebral artery occlusion. Eur J Appl Physiol 2002; 87(2): 101-7.

12. Murphy BP, Harford FJ, Cramer FS. Cerebral air embolism resulting from invasive medical procedures. Treatment with hyperbaric oxygen. Ann Surg 1985; 201(2): 242-5.

13. Hellinger L, Keppler AM, Schoeppenthau H, *et al*. Hyperbaric oxygen therapy for iatrogenic arterial gas embolism after CT-guided lung biopsy : A case report. Anaesthesist 2019; 68(7): 456-60.

Iatrogenic Tracheal Diverticulum with Spontaneous Recovery: A Case Report

Yun-Tse Chou[1], Sheng-Huan Wei[1], Chang-Wen Chen[1,2]

Tracheal diverticulum is a consequence of focal weakness of the trachea wall. Tracheal diverticula can be due to either congenital or acquired causes. Patients with tracheal diverticulum are usually asymptomatic and the condition is self-limited, but may develop serious infectious complications. We report the case of a 36-year-old female with iatrogenic tracheal diverticulum diagnosed by thoracic CT scan and bronchoscopy, who had a spontaneous recovery. *(Thorac Med 2023; 38: 267-270)*

Key words: Tracheal diverticulum, tracheal wall, iatrogenic, bronchoscopy

Background

Iatrogenic tracheal diverticulum is a potential complication after airway intervention. Management depends on the clinical symptoms. However, there are limited reports describing the disease course of iatrogenic tracheal diverticulum, especially in a critically ill patient. We reported here a case of iatrogenic tracheal diverticulum and provide a review of the literature.

Case Presentation

A 36-year-old female patient had a medical history of systemic lupus erythematosus. One month before admission, she underwent pulse steroid therapy for class III lupus nephritis. Afterward, the patient had progressive dyspnea for 1 week, associated with low-grade fever and dry cough. Computed tomography (CT) of the chest demonstrated bilateral ground-glass opacities. Hypoxemic respiratory failure developed, and she was intubated for acute respiratory distress syndrome (ARDS). The bronchoalveolar lavage studies showed an infection of *Pneumocystis* pneumonia, which was further managed by trimethoprim/sulfamethoxazole. Due to anticipated prolonged mechanical ventilation (MV), a surgical tracheostomy with a non-fenestrated, size 7 tracheostomy tube was performed on day 12 of MV.

However, subcutaneous emphysema developed soon after the operation. The chest radiograph revealed no pneumothorax. Bronchoscopic examination revealed a posterior tracheal wall laceration located at the tip of the tracheostomy tube, with false lumen formation. There was no evident tracheoesophageal fistula, and the morphological classification was level II, as proposed by Cardillo *et al*. [1] However, CT of the chest revealed a newly developed diverticulum in the right posterolateral tracheal wall. The volume of the diverticulum was around 15 x 7 x 16 mm. There was no evidence of mediastinal infection. Therefore, an iatrogenic tracheal laceration leading to diverticulum formation was diagnosed. Since the patient required only minimal MV, and there was no progression of pneumomediastinum or subcutaneous emphysema, conservative treatment was concluded by agreement in the multidisciplinary consensus meeting. We changed to a size 7 non-kinking tracheostomy tube and bypassed the diverticulum under bronchoscopic guidance. Minimal airway pressure and low tidal volume were also applied.

Following treatment, the patient recovered well from *Pneumocystis* pneumonia and was smoothly weaned off ventilator support on day 34. Moreover, she corked well 1 month after discharge, and the tracheostomy tube was removed. The patient had regular follow-up at the rheumatologist's clinic during the following 2 years. She had no respiratory complaints during the period, and refused further bronchoscopic interval exams. A follow-up CT of the chest showed an absence of tracheal diverticulum at the posterolateral wall. The iatrogenic tracheal diverticulum had totally resolved spontaneously.

Fig. 1. Chest radiography after tracheostomy creation showed extensive subcutaneous emphysema.

Discussion

Here, we reported a 36-year-old woman who suffered an unintended tracheal laceration during surgical tracheostomy, that was complicated with tracheal diverticulum. The diverticulum diminished spontaneously following conservative treatment for 2 years. Acquired tracheal diverticula can result from tracheomalacia or sequelae of airway procedures, including bronchoscopy, endotracheal intubation, and surgery [2]. Unlike congenital tracheal diverticula, acquired tracheal diverticula are pseudodiverticula and are usually self-limited, because the lesion involves respiratory epithelium.

The clinical presentation of tracheal diverticula is often asymptomatic. Cough, dyspnea, stridor, or recurrent upper airway infection may be observed. The differential diagnosis of tra-
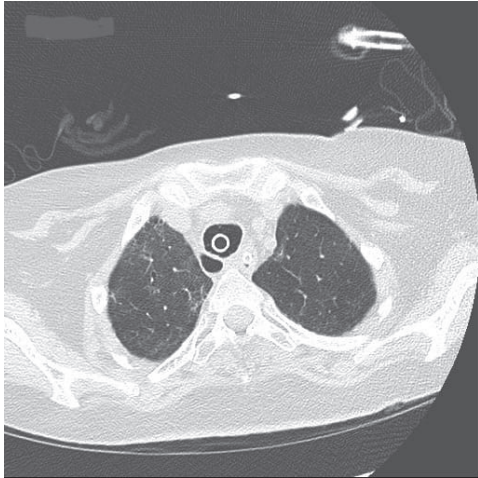
Fig. 2. CT of the chest after tracheostomy creation revealed tracheal diverticulum.
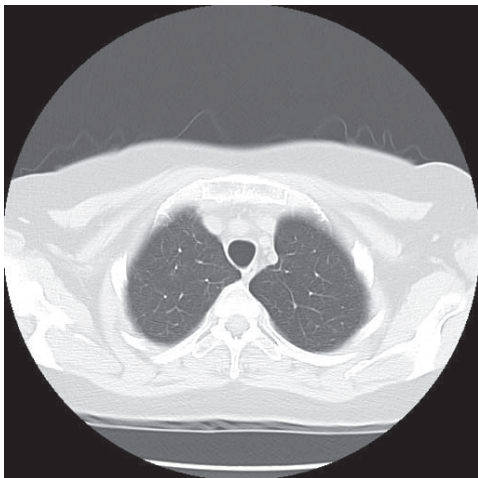

Fig. 3. CT of the chest after 2 years showed resolution of the tracheal diverticulum.

cheal diverticulum includes Zenker's trachea diverticulum, epical lung herniation, epical lung blebs, laryngocele and pharyngocele. Once suspected, bronchoscopy and advanced image study, such as CT, are indicated. Flexible bronchoscopy is recommended for a suspected tracheal laceration or diverticula in a ventilated patient, and should be carried out through the endotracheal tube while pulling the tube back

to the level of the vocal cords. In patients ventilated via tracheostomy, bronchoscopy via the larynx while slowly pulling the tracheostomy tube out is recommended, since the lesion may be above the tube entry. Aside from bronchoscopy, CT remains a good method to identify the diverticulum. In addition to the characteristics of the tracheal diverticulum, CT scan can reveal the narrow orifice of the diverticulum, which might be difficult to detect by bronchoscopic exam, and possible infection of the diverticulum.

There are a limited number of reports that describe the disease course of acquired tracheal diverticulum, especially in a critically ill ventilated patient. It is unclear whether the diverticulum would resolve and how much time it would take to recover. The patient we reported had more complex conditions because of her immunocompromised status due to glucocorticoid use and *Pneumocystis* pneumonia, leading to ARDS with positive MV. Sharma *et al*. [3] reported a 34-year-old female with opioid abuse that was admitted for acute pancreatitis and was intubated for methicillin-resistant Staphylococcus aureus pneumonia. Her endotracheal tube was misplaced at the right main bronchus for 8 hours in the emergency department. CT of the chest revealed a defect in the posterior-lateral wall of the trachea, with pneumomediastinum. Bronchoscopy showed an outpouching, 2 x 4 cm in size, located at 0.5 cm above the carina. They assumed that the tracheal diverticulum was related to single lung intubation, increased cuff pressure, and critical illness weakening the tracheal wall. They chose conservative treatment with close monitoring. Follow-up CT and bronchoscopy 3 days later showed a stationary diverticulum without infectious sequelae. The patient was extubated on day 5. One month

later, a repeat bronchoscopy showed complete resolution. The patient in our report also underwent conservative treatment successfully. The CT scan after 2 years revealed total resolution, which might indicate that the diverticulum takes months to years to recover.

Management of acquired tracheal diverticulum depends on its symptoms. Conservative treatment, including antitussive medication and prophylactic antibiotics if the infectious episode is concerning are reasonable for asymptomatic patients [4]. Clinicians should closely monitor the development of an infected diverticulum, paratracheal abscess, or even empyema. In ventilated patients, the tube should be positioned under bronchoscopic guidance to make the cuff contact the healthy mucosa and bypass the lesion. Cuff pressure should be as low as possible. Furthermore, protective lung ventilation should be used to avoid barotrauma and volutrauma. Surgical resection is reserved for selected young and symptomatic patients only. It should be emphasized that surgical resection carries the risk of injury to surrounding structures, such as the laryngeal nerve and esophagus.

In conclusion, clinicians should be aware of an iatrogenic tracheal diverticulum after invasive airway procedures. Subcutaneous emphysema or pneumomediastinum might precede the diagnosis. Although the tracheal diverticulum might resolve spontaneously, it might also lead to potential consequences such as an abscess. Early recognition and further image study arrangement are key to treating an iatrogenic tracheal diverticulum.
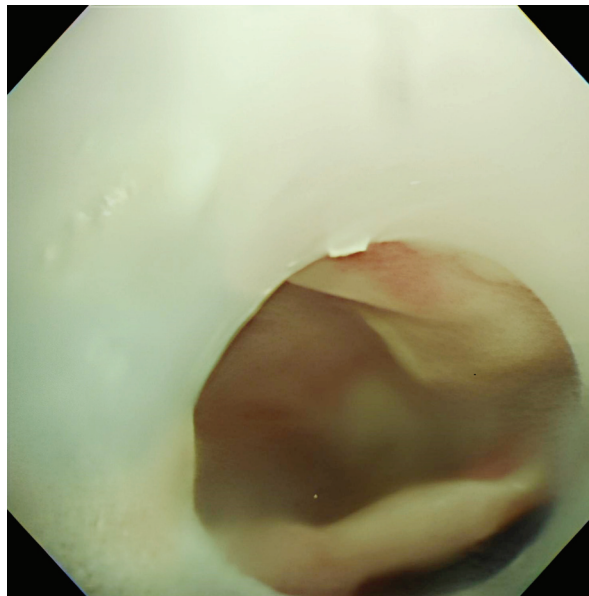

Fig. 4. Bronchoscopy revealed a false lumen of the tracheal diverticulum.

References

1. Cardillo G, Carbone L, Carleo F, *et al*. Tracheal lacerations after endotracheal intubation: a proposed morphological classification to guide non-surgical treatment. Eur J Cardiothorac Surg 2010; 37(3): 581-7.
2. Tanrivermis Sayit A, Elmali M, Saglam D, *et al*. The diseases of airway-tracheal diverticulum: a review of the literature. J Thorac Dis 2016; 8(10): E1163-7.
3. Sharma M, Bulathsinghala CP, Khan A, *et al*. An unusual case of iatrogenic tracheal diverticulum found in a mechanically ventilated patient: to treat or not to treat. Cureus 2019; 11(10).
4. Grewal HS, Dangayach NS, Ahmad U, *et al*. Treatment of tracheobronchial injuries: a contemporary review. Chest 2019; 155(3): 595-604.